MIXING CHEMICAL REACTIONS IN A MIXING ENVIRONMENT: BASIC CONSIDERATIONS

G. K. Patterson, University of Missouri-Rolla

ABSTRACT

There are two ways which have commonly been used to graphically represent the segregation of turbulently mixing chemical components which react with one another. These are the instantaneous concentration profile and the probability density function (pdf) of concentration occurances for each component. Both have been used for formulating closure approximations for modeling turbulent mixing of reacting species. Only the instantaneous profile representation will be extensively discussed in this paper because the pdf representation will be discussed in the following paper.

Experimental research has been done on both the reaction conversions and fluid mechanics (turbulent energy dissipation rates and length scales) for rapid second-order reactions in a tubular reactor.[2] That information has led to methods for modeling reaction rates between mixing components using finite rate kinetics and turbulence information. One method is an analytical closure approximation[3] and another is a random coalescence-dispersion (c-d) method.[12,9] Both the analytical closure approximation and the c-d method have subsequently been extended to stirred-tank[13,14] and mixing jet geometries.[5,10] The mixing jet geometry required the use of finite-difference modeling. Also, the mixing jet geometry involves large scale turbulent diffusion which gives rise to a segregation production term. Comparisons have been made between a total segregation transport model[5] and a segregation source term based on concentration gradient.[7] The model involving the total segregation transport equation has been tested against data for jet mixing of components which produce almost instantaneous reaction and results compared well with the experimental data.[5]

The important problem is the modeling of multiple reactions occurring in a mixing medium. This is a new area, so mostly untested methods have been proposed. A fluid-strand diffusion model;[15] a spherical eddy model;[16] and an interaction-with-the-mean (iem)[17] model have been proposed, but not really tested. The iem model can be shown to be equivalent to the c-d method, so it is not a unique method. The c-d method has been shown to properly model the yield of specific products in a multiple-species reaction[14] and can be used where large-scale diffusion exists.[10] Future work in this area will involve testing of analytical closure approximations which will allow use of the familiar finite-difference methods for multiple-species reactions. One such proposed model is the "paired-interaction" model.[18]

In this paper, some considerations of chemical reactions in the turbulent mixing and diffusing medium are presented. Some general concepts of mixing and segregation - mixedness - are presented as well as a picture of how the fluid field may look when mixing is occurring. Deductions about mixing and reaction without complications--temperature variations, density variations, large scale diffusion, and so on--will be made. This will be done by considering turbulent models of the reactor flows in which chemical reactions were carried out. Throughout the paper, distinction will be made between large scale diffusion (which is sometimes called mixing) and mixing which is occurring on a small scale, which, of course, is what leads to the capability of various species to react with one another. "Large scale diffusion" is used when mixing over a boundary layer or some large distance is meant. "Mixing" means on a small scale.

Finite difference modeling of species concentrations in jet flows has been done using a closure which was developed from flows that didn't involve large scale diffusion. The finite difference modeling used for the fluid mechanics was the two-equation k-ε approach. Also, random coalescence-dispersion (c-d) modeling and the inclusion of random coalescence dispersion methodology into the turbulent fluid mechanics for modeling complex chemistry has been developed. Complex chemistry is very hard to model. Coalescence-dispersion is one approach to effecting a solution to the problem of modeling the effects of complex chemistry in mixing situations. Formulation of a more analytical type of closure for closure for multi-species reactions is just being started.

Figure 1 is a representation of some unmixed blobs of two species of fluid.

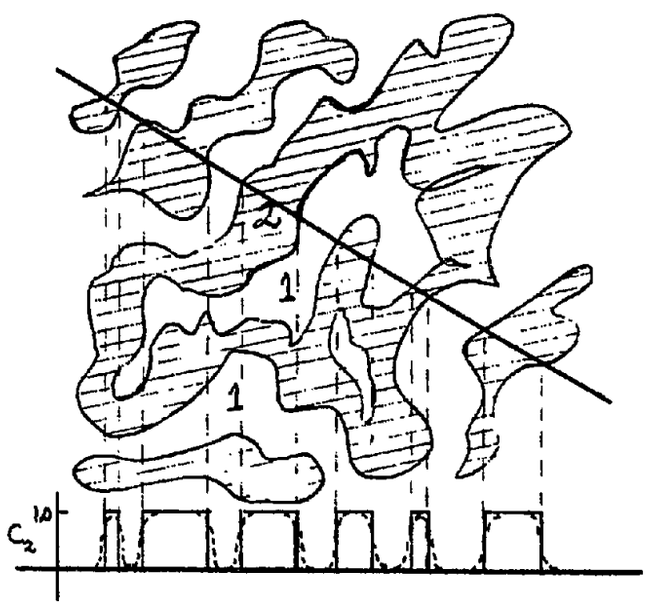

Fig. 1. Illustration of mixing process for two fluids.

There is a fluid one and fluid two, and some fluid one is even enclosed by some fluid two. That probably occasionally happens, even though one fluid is usually continuous and the other dispersed. If a line were projected across the fluid with some kind of a magic sensor, we might be able to measure the concentration profile along that line of fluid two. If there were total segregation, there would simply be rectangular features for fluid two. Of course, if diffusion occurs between the fluids, then, the concentration profile would be something like the dotted lines. Eventually, fluid two would fill-in and gradually develop a completely mixed system with fluid two and fluid one completely mixed. In a turbulent mixing environment, where fairly rapid reactions occur between the two fluids, the nearly segregated situation could possibly be maintained for quite some length of time. Such a possibility is used for a hypothesis for closure. There are details, such as build up of product fluid, which are neglected, but, of course, those are complications which one would have to incorporate in later and more complete models.

Figure 2 shows a more formalized drawing, where some overlap is shown as a rough way of representing the diffusion occurring between two species.

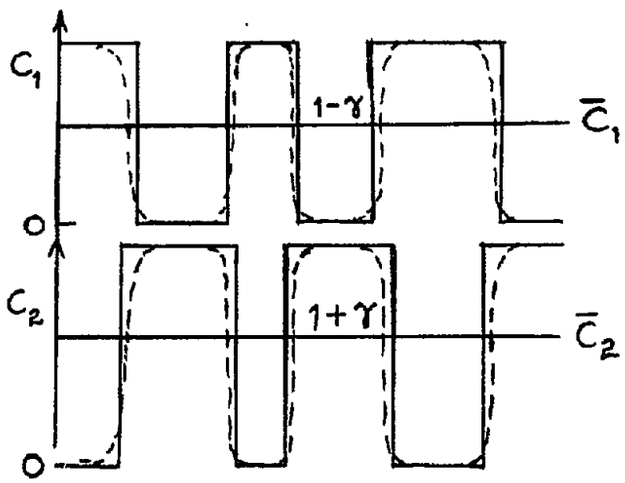

Interdiffusion of Reactants

—— ideal
--- real

Fig. 2. Idealization of reactant interdiffusion.

What actually happens, of course, is that the concentration profiles look more like the dotted lines. It turns out that, in doing the modeling, it isn't necessary to account for such details. The interdiffusion of the reacting components are assumed to be represented by an overlap scheme. It doesn't even preserve continuity, but it still works.

Many people think of this problem in terms of the probability density distribution (PDD) of the reacting species. Figure 2 represents an almost totally segregated PDD. That's one where you have a very high probability that, at a particular point, fluid two will occur at a concentration of one and fluid one will occur at a concentration of zero and vice versa as shown in Figure 3.

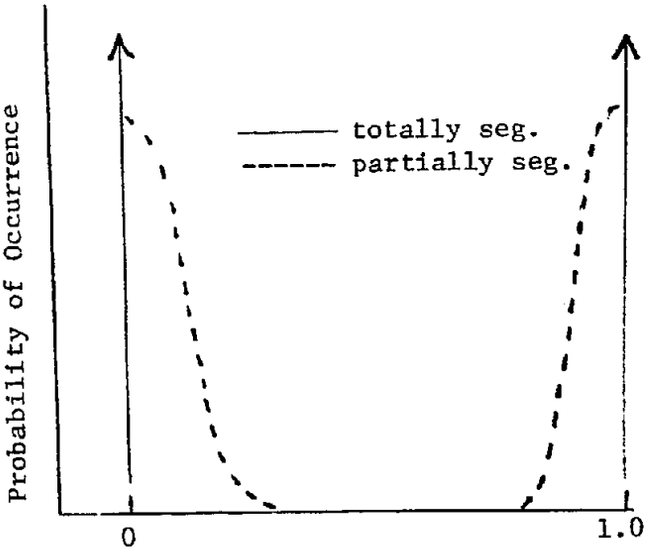

Figure 3. Probability density distribution for a segregated fluid (any component).

Various hypotheses for closure using PDD methods assume that there is some sort of filling in between these extremes with probabilities of intermediate concentrations for the species. This is the sort of thing that Ashok Varma describes in his paper "Mixing and Reaction in a Tubular Reactor--Simple Closure Approximation".

The simplest kind of closure which you can have for very rapid chemical reactions is one which was hypothesized and proven for extremely rapid chemical reactions by Toor and his students.[1] It simply states that, if you have stoichiometric feed of reactants with no large scale diffusion of ambient fluid into the reaction mixture, one minus the level of conversion of the reacting chemical component is equal to the square root of their normalized segregation (the ratio of their segregation to the initial segregation). This can form a closure approximation and modeling method if one has that simple kind of situation, but, of course, most situations are more complicated, that is, large scale turbulent diffusion is important. All the Toor hypothesis does is relate the level of conversion to the level of segregation. It is necessary to go a little further than that.

Figure 4 is an illustration of the fluid mechanics that existed in the reactor which Toor and his studients at Carnegie Mellon University used to measure rates of reaction in mixing systems. It turned out that the reactor wasn't quite as ideal as they thought.

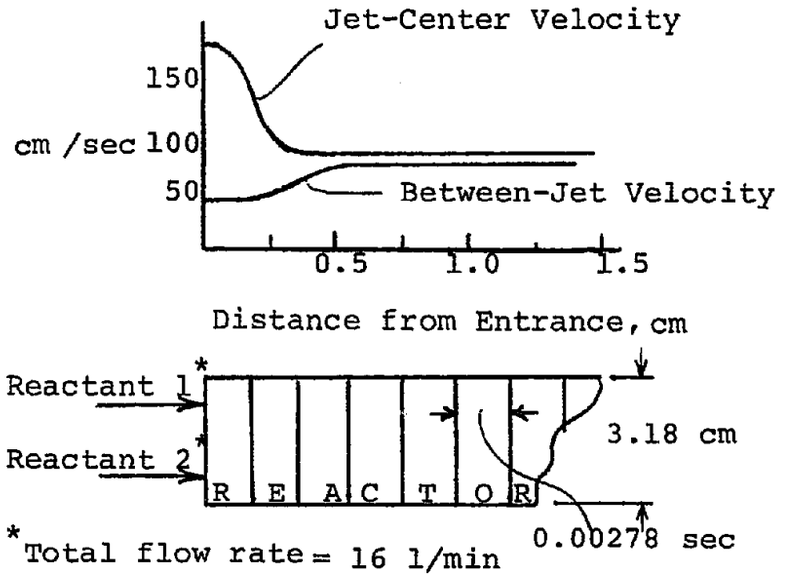

* Fig. 4. Axial velocities, flow rate, and segmentation for modeling of the Vassilatos and Toor tubular reactor.

They thought the velocity remained fairly constant for the length of the tube. That wasn't exactly true. The injection head was made up of 182 very closely packed injection nozzles. The idea was that by doing that, very little recirculation would occur and that high levels of turbulence would occur. However, it was found by Brodkey and coworkers[2] at Ohio State University that there was some recirculation very near the injection head. The resulting velocity variations are shown in Figure 4. It was possible to model around that problem, so the recirculation wasn't a serious effect.

Alternating reactions were fed in adjacent jets. In order to do modeling experiments to try to match this data, it was assumed that there was ideal plug flow with turbulent mixing. The reactor was divided into elements which were relatively short. With such simple fluid mechanics, the closure approximation for the reaction with mixing and its interaction with the segregation could be studied without other effects.

In order to do the modeling job, balance equations were written about each one of the conserved quantities.[3] The balance equations were for one of the reacting components (the concentration of the other one, of course, is simply the full concentration minus that).

The first balance, shown in Fig. 5, is the mass balance which is the time rate of change (zero for steady state) equal to the sum of what's coming in minus the sum of what's going out, plus a source term into which, of course, goes the reaction rate term.

$$\frac{\partial C_1}{\partial t} + U_K \frac{\partial C_1}{\partial x_k} = D\nabla^2 C_1 - k_2 C_1 C_2 \qquad (1)$$

$$\frac{\partial \bar{C}_1}{\partial t} + \underbrace{\bar{U}_k \frac{\partial \bar{C}_1}{\partial x_k} + \overline{u_k \frac{\partial c_1}{\partial x_k}}}_{\text{convec. + turb. diff.}} = D\nabla^2 \bar{C}_1 - k_2(\bar{C}_1\bar{C}_2 + \overline{c_1 c_2}) \qquad (2)$$

$$V_j \frac{\partial \bar{C}_1}{\partial t} - \underbrace{\sum_s Q_s \bar{C}_{1s} + \sum_m Q_m \bar{C}_{1m}}_{\text{conv. only}} \simeq V_j R_{1j}(\text{negl. diff.})$$

Fig. 5. Mass balance equations.

The same kind of balance is made for the segregation, which, of course, is the mean-square of the fluctuating concentration of the component of interest (see Fig. 6). The steady-state balance is the total rate of segregation coming in minus the total rate of segregation going out equals the volume times a source term for segregation. The whole modeling job is in the source terms.

Figure 7 shows what is involved in the source (closure) terms. If one has a perfectly mixed set of reactants, then the rate of reaction between them, if it's second-order, is simply a rate constant times the product of their concentrations. If they are not mixed and if one decomposes each of the instantaneous concentrations into an average plus the fluctuating quantity, multiplies them together for the second-order reaction rate and Reynold's averages the product, the results shown in Fig. 7 (first equation) are obtained, which is a product of the two average concentrations plus a correlation term. For the segregation rate term, there is a rate of segregation decay (or decrease) whether we have chemical reaction or not, and that's shown in the second equation. The terms occur in the segregation balance equation, which is generated by multiplying the mass balance equation for component one by the fluctuating concentration for component one and carrying out Reynolds averaging. The first term will be modeled by using the form of the isotropic mixer equation which, of course, was developed in the late 1950's by Corrsin.[4] That equation (shown last in Fig. 7) seems to be very successful for modeling mixing gases and liquids, even when the turbulence is not isotropic. The other terms are generated by the reaction term. In other words, they result from $k_2 C_1 C_2$ times c_1 after carrying out the Reynold's averaging.

Subtract (2) from (1):

$$\frac{\partial c_1}{\partial t} + u_k \frac{\partial \bar{C}_1}{\partial x_k} + \bar{U}_k \frac{\partial c_1}{\partial x_k} = D\nabla^2 c_1$$

$$- k_2(\bar{C}_1 c_2 + \bar{C}_2 c_1 + c_1 c_2 - \overline{c_1 c_2})$$

Multiply by c_1 and time-avg: $+ \overline{u_k \frac{c_1^2}{2}}$

$$\frac{1}{2}\frac{\partial \overline{c_1^2}}{\partial t} + \overline{u_k c_1}\frac{\partial \bar{C}_1}{\partial x_k} + \frac{\bar{U}_k}{2}\frac{\partial \overline{c_1^2}}{\partial x_k} = \frac{D}{2}\left(\nabla^2 \overline{c_1^2} - \overline{\left(\frac{\partial c_1}{\partial x_k}\right)^2}\right)$$

$$- k_2(\bar{C}_1 \overline{c_1 c_2} + \bar{C}_2 \overline{c_1^2} + \overline{c_1^2 c_2} - \overline{c_1 c_2})$$

$$V_j \frac{\partial \overline{c_1^2}}{\partial t} - \sum_s Q_s \overline{c_{1s}^2} + \sum_m Q_m \overline{c_{1m}^2} = V_j \, r_{1j}$$

Fig. 6. Segregation equations.

$$-R_1 = k_2 \, (\bar{C}_1 \bar{C}_2 + \overline{c_1 c_2})$$

$$-r_1 = D_1 \, \overline{(\partial c_1 / \partial x_k)^2} + 2k_2 \, (\bar{C}_2 \overline{c_1^2} + \bar{C}_1 \, \overline{c_1 c_2} + \overline{c_1^2 c_2})$$

$$\overline{c_1 c_2} \cong -\overline{c_1^2} \, (1-\gamma)/\beta(1+\gamma)$$

$$\overline{c_1^2 c_2} \cong 2(\overline{c_1^2})^{3/2} \, \gamma(1-\gamma)^{1/2} / \beta(1+\gamma)^{3/2}$$

where $\gamma = (\bar{C}_1 \bar{C}_2 - \overline{c_1^2}/\beta)/(\bar{C}_1 \bar{C}_2 + \overline{c_1^2}/\beta)$

$$D_1 \overline{(\gamma c_1 / \gamma x_k)^2} \cong 2\overline{c_1^2}/[4.1(L_s^2/\varepsilon)^{1/3} + (\mu/\rho\varepsilon)^{1/2} \ell n N_{Sc}]$$

Fig. 7. Closure relationships. Closure approximations for $\overline{C_1 C_2}$ and $C_1^2 C_2$, as well as the Corrsin equation for segregation decay.

If one can relate two correlation terms, $\overline{c_1 c_2}$ and $\overline{c_1^2 c_2}$, to the segregation term, c_1^2, for which there is a balance equation, then the set of equations will be closed, and solutions for each of the segments of the reactor model (see Fig. 4). By using the simple interdiffusion hypothesis for the mixing fluid, through simple geometric considerations, one can generate equations relating the correlations to the segregation as in the third and fourth equations in Fig. 6, where gamma represents the fractional degree of interdiffusion of the chemical components. Beta is the initial ratio of the two reactant concentrations (c_1 and c_2).

What must be done, then, is apply this closure hypothesis to the model with the hydrodynamic conditions that exist in the reactor, in other words, the level of turbulence, the velocity, the rate constants in the chemical reactions that were tested in experiment and see if the results match experimental data. The turbulence level is given by its rate of dissipation, ε, and by a length scale L_s. Those values are necessary for use of the Corrsin equation for the rate of segregation decay with or without reaction. There may be some interaction between the chemical reaction and segregation decay by mixing, but for now, we assume no effect. Generally, most aerodynamicists use only the length scale squared divided by the rate of turbulence energy dissipation for the rate of segregation decay. For fluids that have high Schmidt numbers, however, the term involving Schmidt number should be involved according to Corrsin's work. It does have some effect if the Schmidt number is high.

In order to use the model, one must know something about the rate of turbulence energy dissipation and length scale. Brodkey and his students measured profiles for the Toor tubular reactor as a function of distance downstream as shown in Fig. 8. Figure 8 reprinted with permission from CHEMICAL ENGINEERING SCIENCE, 32 1349 (1977). Copyright 1977, Pergamon Press, Ltd.

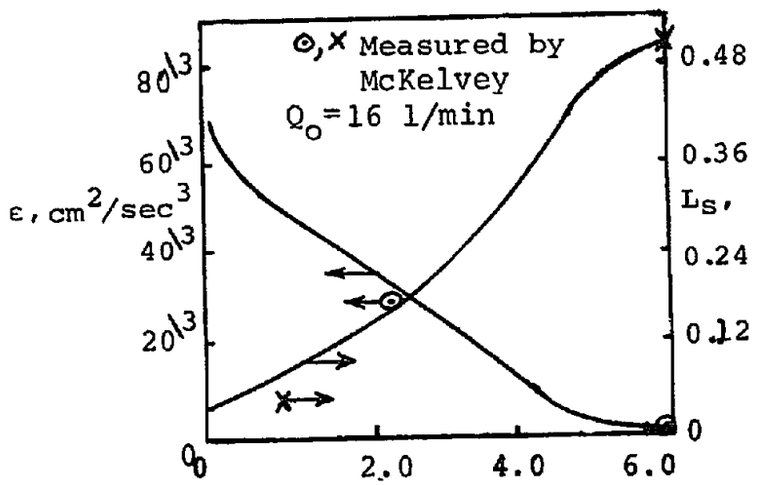

Fig. 8. Distribution lengthwise of energy dissipation rate and length scale for tubular reactor.

They were'nt as ideal as they wanted them to be. The rate of turbulence energy dissipation decreases downstream until it levels out. This presumably is about where the flow begins to become something like a fully developed pipe flow. The length scale, of course, gradually increases. The greatest rate of mixing is in a region where the turbulence energy dissipation is highest and the length scale is the smallest near the reactor entrance. The rate of the mixing decreases drastically downstream.

This is something one must keep in mind all the time, because if the process must have extremely high rates of mixing for almost perfect mixing with regard to chemical kinetics, then the rate of turbulence energy dissipation must be high and the length scale small.

In order for Corrsin to derive his equation for the rate of segregation decay, he hypothesized a spectrum which was easy to handle for the scalar component. He included all the possible scales of segregation that might occur. The length scale that occurred in his equation is a characteristic large scale that is in the spectrum that he hypothesized. As that characteristic large scale changes, the rate of mixing changes because it is a function of the characteristic scale. There is an ansatz involved here, which is not exactly right, but seems to work. That is, the turbulence scale is used in the Corrsin equation instead of the segregation scale. Apparently, the major scale of the segregation to some degree follows the scale of the turbulence itself. That may have something to do with the large scale structure that's involved in the turbulent flow.

Figure 9 shows a typical result of the use of the model for the tubular reactor used by Toor and his students.

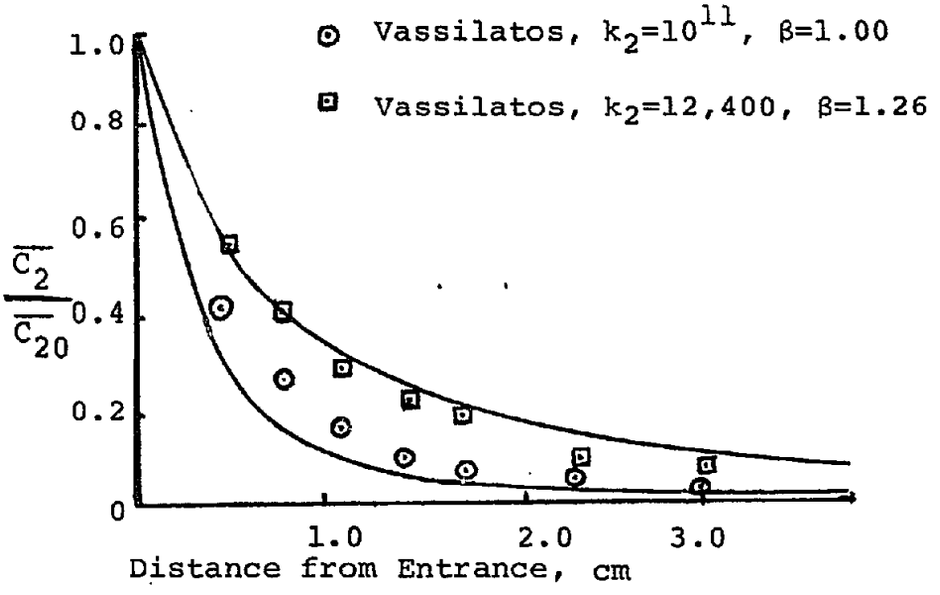

Fig. 9. Comparison of typical model and experimental results.

The points are data points for chemical reactions which were carried out. The extent of reaction was based on temperature measurements, since the reactions were all exothermic. They were acid-base chemical reactions, so they were relatively rapid, but they did have varying reaction rate constants. The one with a very high reaction rate constant can be thought of as being an instantaneous reaction. It's totally mixing (diffusion) controlled. The other reaction is somewhat less mixing controlled, but still one would call it a diffusion limited reaction. Good results were obtained in both of those. Such comparisons were made for about six different rates and several different ratios of chemical reactant in the feed. Overall, the trends are all good, so the simple closure hypothesis seems to be pretty good.

Mixing and Reaction with Large-Scale Diffusion

If one is fairly sure that the model works for a simple case where there isn't much of a fluid mechanics problem, then it's interesting to apply it to a case where the fluid mechanics are more complex. Finite difference modeling was done for a case with large scale turbulent diffusion, in this case, an annular mixing jet[5] (one fluid coming through an inside jet and another through an annulus). The fluids were mixing in a jet which also had some ambient fluid being entrained in the outside portions of the jet. A two-equation model (k-ε) for the hydrodynamics was used. The balance equation for ε was chosen because a rate of turbulent energy dissipation was needed in order to model the rate of decay of segregation. That lead to the use of the k-ε equation as formulated by Launder and Jones.[6]

Figure 10 shows the geometry of the experimental coaxial jet. It was a jet without contraction, a long tube with many small straightening tubes in both the annulus and the inside tube upstream of the exit. A quite different initial velocity profile results from this kind of jet than from a jet which is produced by a contraction. The equations which are used for modeling the annular jet flow and mixing are shown in Figs. 11 and 12.

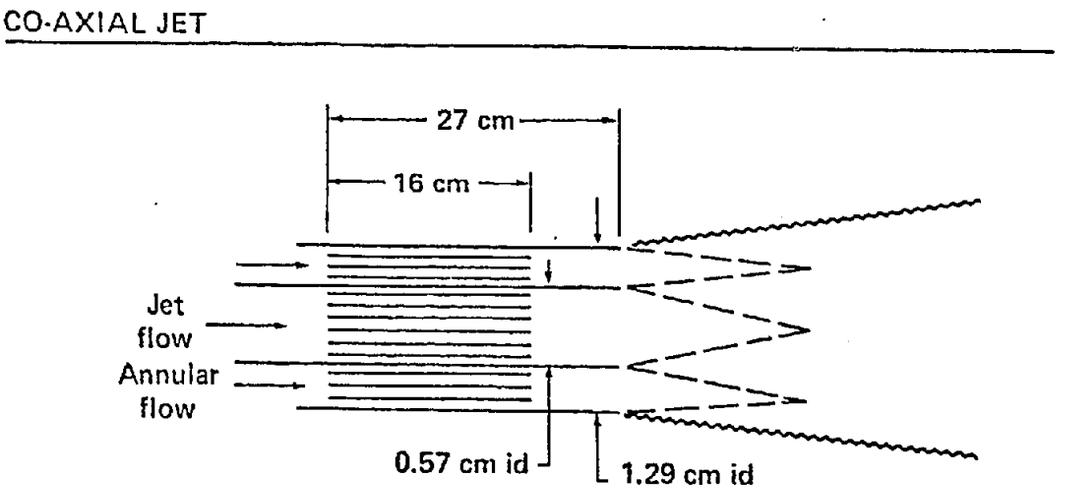

Fig. 10. Co-axial jet geometry.

Vorticity and Stream Function Eqns:

Vorticity

$$\frac{\partial}{\partial x_1}\left(\omega \frac{\partial \psi}{\partial x_2}\right) - \frac{\partial}{\partial x_2}\left(\omega \frac{\partial \psi}{\partial x_1}\right) =$$

$$\frac{1}{\rho} \frac{\partial}{\partial x_1}\left(\mu_t \frac{\partial \omega}{\partial x_1}\right) + \frac{1}{\rho} \frac{\partial}{\partial x_2}\left(\mu_t \frac{\partial \omega}{\partial x_2}\right)$$

Stream Function

$$0 = \frac{\partial^2 \psi}{\partial x_1^2} + \frac{\partial^2 \psi}{\partial x_2^2} + \omega/\rho$$

Turbulent Energy and Dissipation Balance Eqns:

Energy, $\overline{u^2}$

$$\frac{\partial}{\partial x_1}\left(\overline{u^2} \frac{\partial \psi}{\partial x_2}\right) - \frac{\partial}{\partial x_2}\left(\overline{u^2} \frac{\partial \psi}{\partial x_1}\right) = \frac{1}{\rho} \frac{\partial}{\partial x_1}\left(\frac{\mu_t}{\sigma_{u^2}} \frac{\partial \overline{u^2}}{\partial x_1}\right)$$

$$+ \frac{1}{\rho} \frac{\partial}{\partial x_2}\left(\frac{\mu_t}{\sigma_{u^2}} \frac{\partial \overline{u^2}}{\partial x_2}\right) + \frac{\mu_t}{\rho} \omega^2 - \varepsilon$$

Dissipation, ε

$$\frac{\partial}{\partial x_1}\left(\varepsilon \frac{\partial \psi}{\partial x_2}\right) - \frac{\partial}{\partial x_2}\left(\varepsilon \frac{\partial \psi}{\partial x_1}\right) = \frac{1}{\rho} \frac{\partial}{\partial x_1}\left(\frac{\mu_t}{\sigma_\varepsilon} \frac{\partial \varepsilon}{\partial x_1}\right)$$

$$+ \frac{1}{\rho} \frac{\partial}{\partial x_2}\left(\frac{\mu_t}{\sigma_\varepsilon} \frac{\partial \varepsilon}{\partial x_1}\right) + k_1 \frac{\mu_t \varepsilon \omega^2}{\overline{u^2} \rho} - k_2 \varepsilon^2/\overline{u^2}$$

Turbulent Viscosity and Constants:

$$\mu_t = k_\mu \rho (\overline{u^2})^2/\varepsilon$$

$k_\mu = 0.09$
$k_1 = 1.44$
$k_2 = 1.92$
$\sigma_{\overline{u^2}} = 2.0$
$\sigma_\varepsilon = 3.0$

} Spalding, et. al.

Fig. 11. Turbulence and flow model equations.

Steady State Balance Eqns:

Mass

$$\frac{\partial}{\partial x_1}\left(\bar{C}_1 \frac{\partial \psi}{\partial x_2}\right) - \frac{\partial}{\partial x_2}\left(\bar{C}_1 \frac{\partial \psi}{\partial x_1}\right) = \frac{1}{\rho}\frac{\partial}{\partial x_1}\left(\frac{\mu_t}{\sigma_{\bar{c}}}\frac{\partial \bar{C}_1}{\partial x_1}\right)$$

$$+ \frac{1}{\rho}\frac{\partial}{\partial x_2}\left(\frac{\mu_t}{\sigma_{\bar{c}}}\frac{\partial \bar{C}_1}{\partial x_2}\right) - k_2(\bar{C}_1\bar{C}_2 + \overline{c_1 c_2})$$

Segregation

$$\frac{\partial}{\partial x_1}\left(\overline{c_1^2}\frac{\partial \psi}{\partial x_2}\right) - \frac{\partial}{\partial x_2}\left(\overline{c_1^2}\frac{\partial \psi}{\partial x_1}\right) = \frac{1}{\rho}\frac{\partial}{\partial x_1}\left(\frac{\mu_t}{\sigma_{\overline{c^2}}}\frac{\partial \overline{c_1^2}}{\partial x_1}\right)$$

$$+ \frac{1}{\rho}\frac{\partial}{\partial x_2}\left(\frac{\mu_t}{\sigma_{\overline{c^2}}}\frac{\partial \overline{c_1^2}}{\partial x_2}\right) - 2\overline{\left(\frac{\partial c_1}{\partial x_k}\right)^2} - D_{Rx} + \text{Prod}_{\overline{c^2}}$$

Segregation for Mixing Streams:

$\overline{c_1^2} = \bar{C}_1\bar{C}_2$ for complete seg. in region

$= 0$ when only one component present

$$\text{Prod}_{\overline{c^2}} = \frac{\partial}{\partial x_1}\left(\bar{C}_1\bar{C}_2\frac{\partial \psi}{\partial x_2}\right) - \frac{\partial}{\partial x_2}\left(\bar{C}_1\bar{C}_2\frac{\partial \psi}{\partial x_1}\right)$$

$$D_{Rx} = 2k_2(\bar{C}_1\overline{c_1 c_2} + \bar{C}_2\overline{c_1^2} + \overline{c_1^2 c_2})$$

where

$$\overline{c_1 c_2} = -\overline{c_1^2}\,(1-\gamma)/(\beta(1+\gamma))$$

$$\gamma = (\bar{C}_1^2 - \beta\overline{c_1^2})/(\bar{C}_1^2 + \beta\overline{c_1^2})$$

Fig. 12. Mass and segregation balance equations.

The balance equations are not given in terms of primitive variables, but vorticity and stream function. The computer program used to solve the equations was written in terms of these variables. The closure terms for mass (concentration) and segregation are the same as for the simple tubular flow case, except for the segregation production term. For large scale diffusion of components which are being introduced separately into a flow situation, as they diffuse together due to the large scale turbulent motion, where there was initially no segregation between the components because there was only one pure component there, segregation is created because of the engulfing action and the large scale diffusion effect. The rate that segregation is created must be accounted for. A proposal by Spalding[7] involved a term for modeling this which is shown in Fig. 13. It assumes that segregation created by large scale diffusion is proportional to the square of the concentration gradient. In this work, it was assumed that what is diffused by the large scale of turbulence is a product of the two components concentrations. In order to explain what the basis is for this, a little background is needed. It was found through the work of Brodkey, Toor and some other people who

concerned themselves with the segregation problem that, if we have two totally segregated components, their segregation can be calculated simply as the product of their average concentrations. In other words, if one computes their concentration as if they were spread over the whole volume and multiplies them together, that would be the level of segregation for totally segregated components. So, here the rate of convection of that hypothetical total segregation is of concern. The balance equation is given in Fig. 12. The method seems to give very reasonable values of segregation creation in large scale diffusion. One advantage of the new method, which is based on a balance equation for $\overline{C_1}\,\overline{C_2}$ is that no empirical constant is necessary.

Spalding's Formulation for Scalar Turbulent Diffusion:

$$\rho \frac{D\overline{c_i^2}}{Dt} = \nabla\left[\frac{\mu e + \mu}{\sigma_{\overline{c^2}}} \nabla \overline{c_i^2}\right] + \underset{(P_{Di})}{Cg_1(\mu e + \mu)(\partial \overline{c_i}/\partial y)^2} - \underset{(D_{Ti})}{Cg_2 k^{1/2} \overline{c_i^2}}$$

Fig. 13. Spalding's segregation equation.

Figure 14 shows the major equipment used to obtain experimental data to test the modeling equations. Light scattering techniques were used to measure the concentration and segregation profiles in the jet flow using small particles. Velocities and turbulence were measured by a laser-Doppler anemometer. The character of this flow is what would be expected in a jet for velocity profiles at various distances downstream (see Fig. 15), where r_o is the outside radius of the annulus. These results are similar to what Durao and Whitelaw[8] got with an annular jet. The modeling of the velocity profiles was not exactly perfect. Results were not obtained close to the exit, but further downstream the modeling of the velocity profiles got better.

Figure 16 shows the square root of turbulence energy in the axial direction. Again, it's not perfect, but probably good enough to test the mixing model. Fig. 17 shows the concentration profiles at various distances downstream for mixing of the center jet fluid with the annular fluid with no reaction.

Figure 18 shows the root mean-square concentration fluctuation divided by the outlet concentration. Very close to the outlet where it's difficult to model, the comparison with the data is not perfect, but farther out the correspondence improves.

Comparisons of concentration profile results are shown in Fig. 19 for the model and experiment with chemical reaction. It's quite good; it actually turned out better than it did for the non-reacting case. The way the

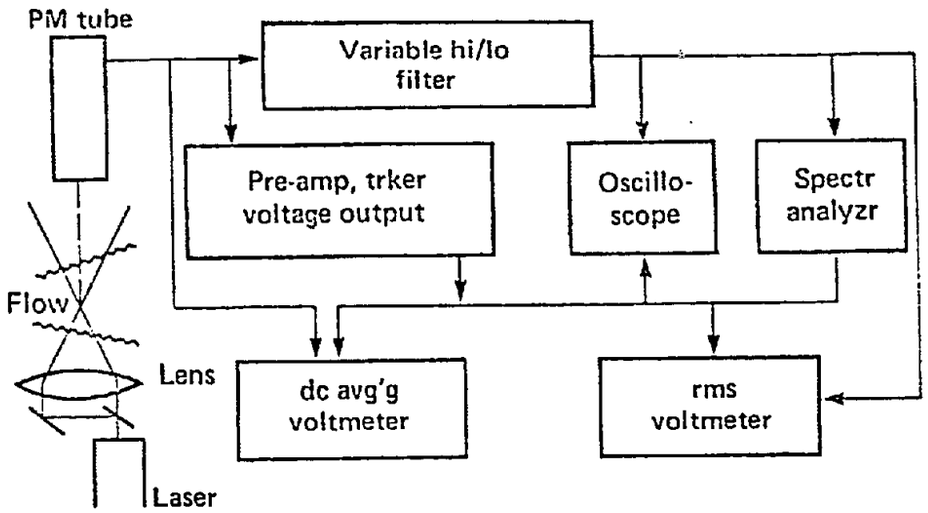

Fig. 14. Measuring system for co-axial jet.

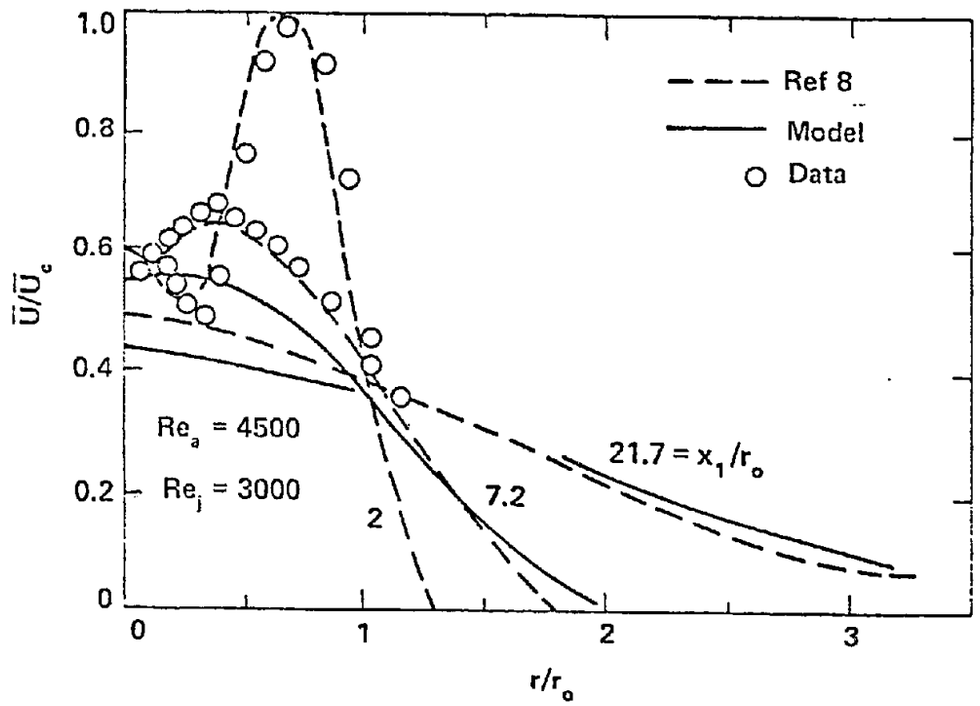

Fig. 15. Co-axial jet velocity profiles.

experimental data were produced for this was by injecting dilute concentrations of ammonia in the center jet and hydrogen chloride in the annular stream and allowing them to react to produce ammonium chloride. We measured the light scattering from the ammonium chloride. Downstream where the reaction was essentially complete, a normalizing variable was determined in order

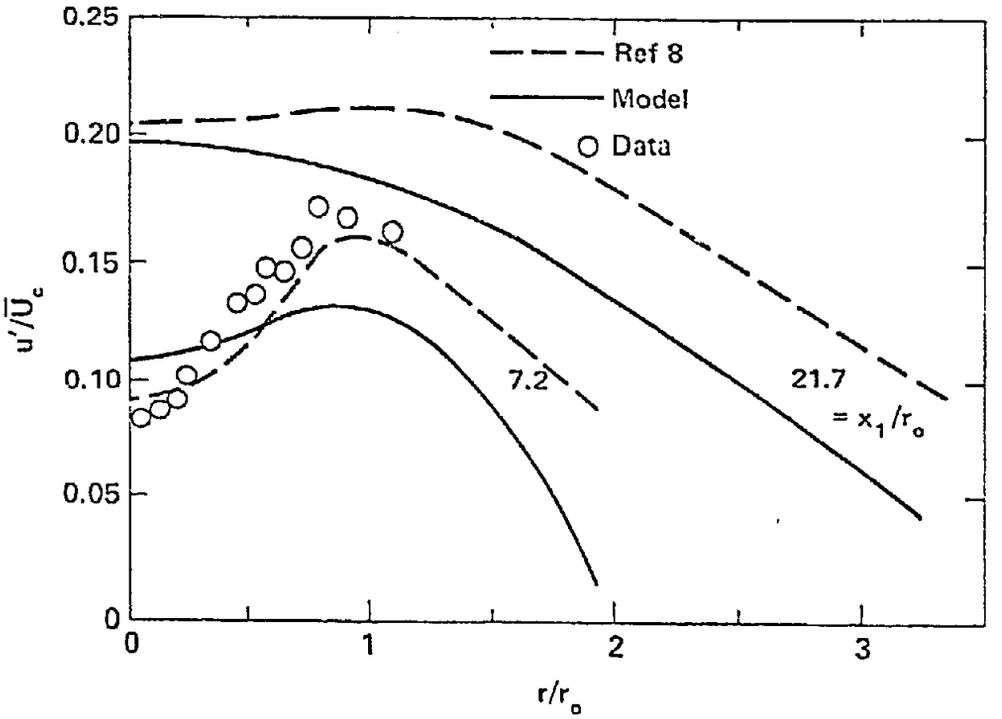

Fig. 16. Co-axial jet turbulence profiles.

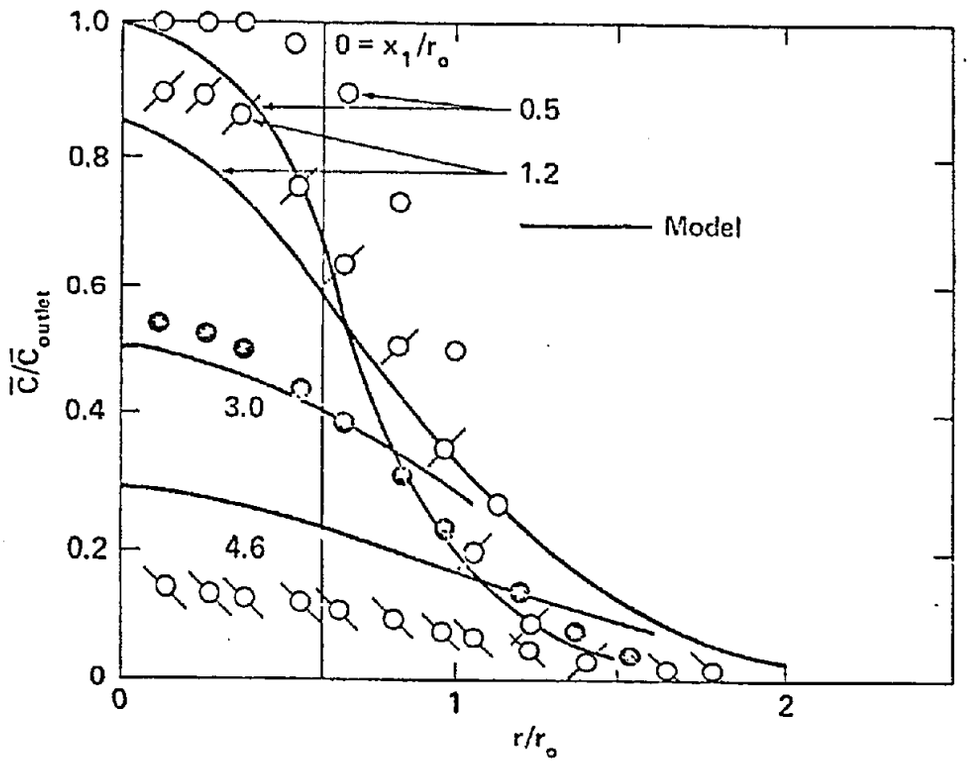

Fig. 17. Concentration profiles for co-axial jet for center fluid.

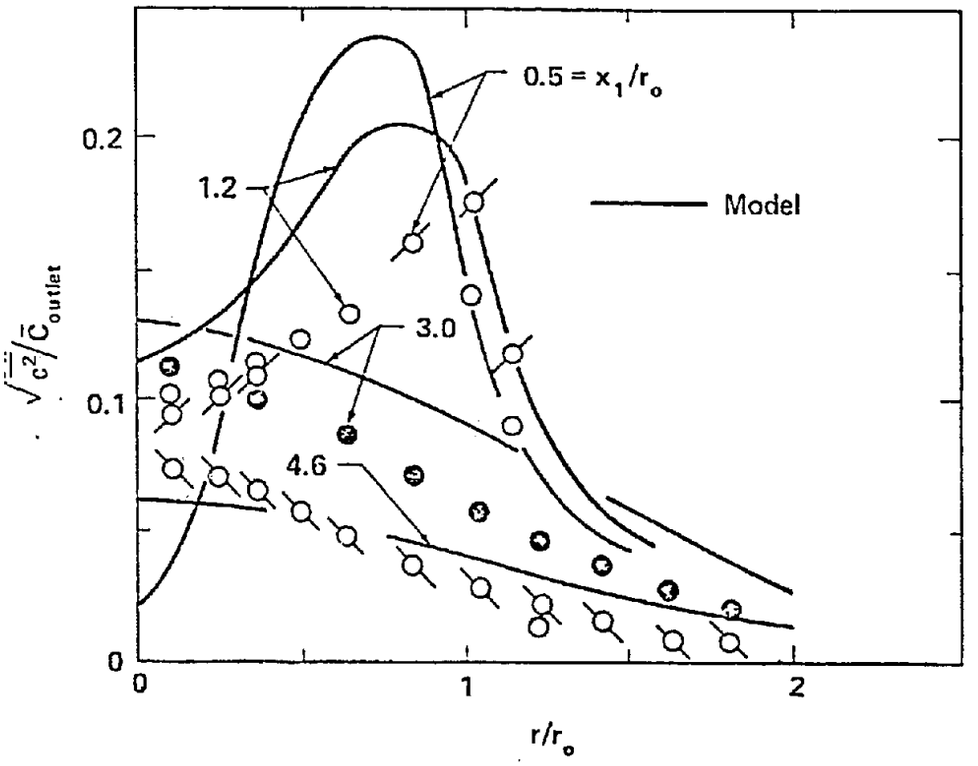

Fig. 18. Co-axial jet segregation profiles for center fluid.

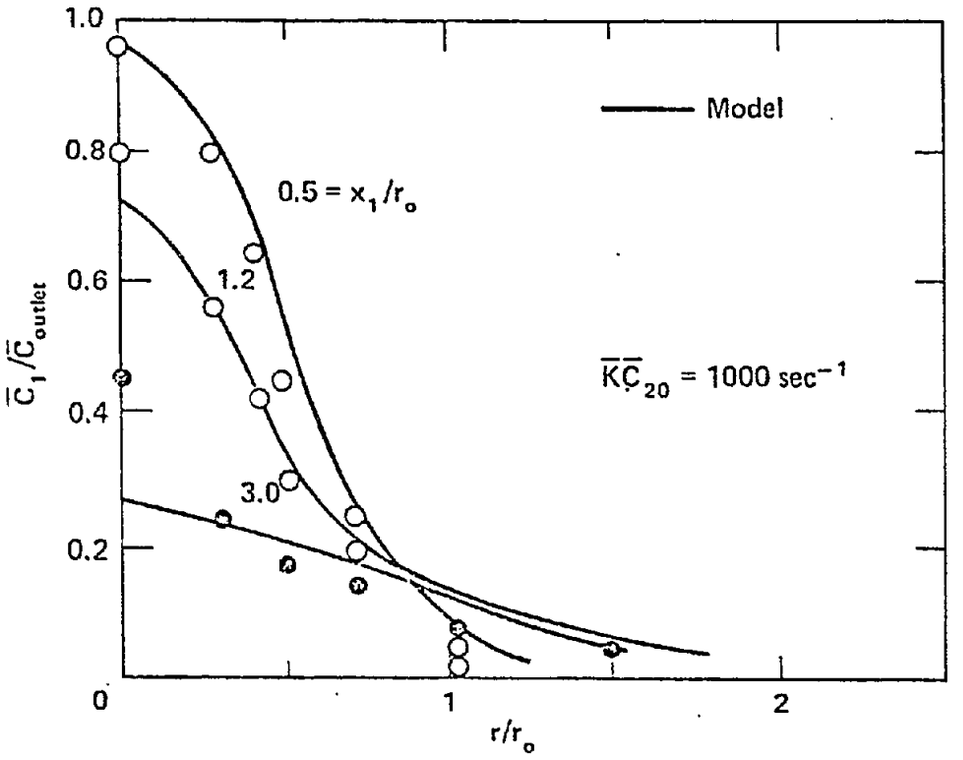

Fig. 19. Co-axial jet concentration profiles for reaction between center and annular fluids.

to determine the actual level conversion at each location. The reaction was essentially an instantaneous reaction between the ammonia and hydrogen chloride. The reaction rate constant of 1000 sec^{-1} represents a high enough rate constant for a nearly instantaneous reaction rate compared to the rate of mixing.

There is a bit of a problem in the finite rate kinetic modeling scheme when it is used for extremely high rate constants. As the rate constant goes up, in order to keep about the same rate of chemical reaction, the levels of segregation also have to increase. It gets to the point that the precision of the computation isn't great enough to account for extremely high rate constants. That is one serious limitation in using finite rate constant models.

Coalescence-Dispersion Modeling of Mixing

Coalescence-dispersion modeling of the trubulent mixing and hydrodynamics offers a way of simply handling very complex chemistry. Basically, what's involved in random coalescence-dispersion modeling is that one assumes that whole reactors can be represented by many sites where the mass that's in the reactor is coalesced into these sites. If one choses a particular site, the mass in that site may mix with the mass in another site (coalescence). One must have some rules regarding which other sites the original can mix with; adjacent sites or sites that are up to a certain distance away or whatever. Then, with those rules, one essentially formulates a mixing model.

In some work done in matching this kind of modeling effort with experimental data in a tubular reactor, coalescence was allowed only with adjacent sides (see Figure 20).

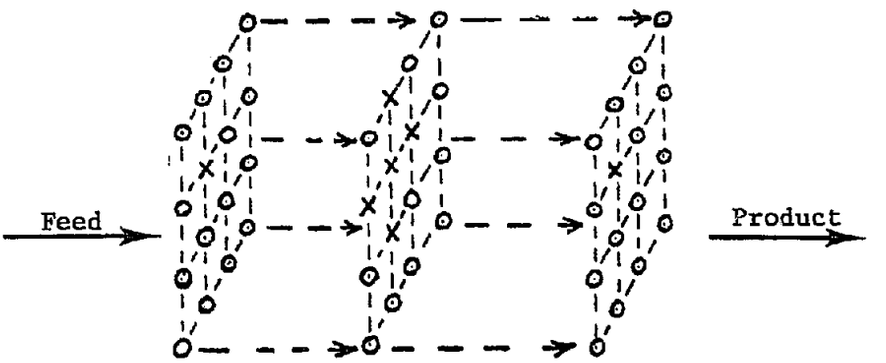

(1) IN $\Delta\bar{\tau}$ sites coalesce with an adj. site
(2) coalesced sites react for $\Delta\bar{\tau}$, then disperse
(3) between time increments each site moves toward exit

Fig. 20. Random coalescence-dispersion model scheme.

In that case, the scale to which these coalescences occur isn't important as long as there is a proper rate of coalescences occurring to cause mixing. There is a rate of coalescence dispersion "I" which is a commonly accepted variable for expressing that rate. "I" times the number of sites times the residence time in a particular volume element of the chemical reactor represents the actual number of sites which coalesce during a time increment in the chemical reactor.

Besides handling complex chemistry, one of the advantages of this method is that it's Lagrangian. The coalescent sides react for the time increment which is involved and then redisperse, in other words, they return to their original positions. Between these time increments, flow occurs, modeled by an instantaneous movement of sites from one place to another to simulate the flow which is occurring in the chemical reactor. The big problem, of course, in simulating complex flows with this kind of scheme is determining how the sites move around. If large scale diffusion occurs, simulating that kind of occurrence through the coalescence-dispersion mechanism is difficult.

In order to determine a relationship between turbulence level and coalescence-dispersion rate, the data from the Toor turbular reactor was used to determine how the rate of coalescence-dispersion corresponds to turbulence intensity.[9] An equation was developed which relates the coalescence-dispersion rate to the rate of turbulent energy dissipation and the scale in a turbulent mixing medium (see Fig. 21).

Effect of Turbulence on C-D

C-D rate:

$$I \cong 1333(\varepsilon/k)(\overline{\tau}/N)$$

C-D length scale:

$$L \cong 60(\mu e/\rho k^{1/2})(N/V)$$

Fig. 21. Model equations for mixing rate and length scale.

Figure 22 shows plots of I versus reactor length necessary to cause a good match of simulated reaction conversion to experimental data. Those values are proportional to (ε/L_s^2), a measure of turbulence level. Figure 23 shows comparisons of experimental and various model data for the tubular reactor.

If one wanted to use coalescence-dispersion for a case with large scale diffusion, another equation is necessary which has another empirical constant which relates the distance to which this coalescence can occur to the scale of the turbulent diffusion which is occurring in the mixing medium. That results in the second equation in Fig. 21. The constant obtained in matching coalescence-dispersion rate to the Toor data was 1333. It may be anywhere from a thousand to fifteen hundred, but that's the approximate order of magnitude that that number should be. For the constant in the turbulent

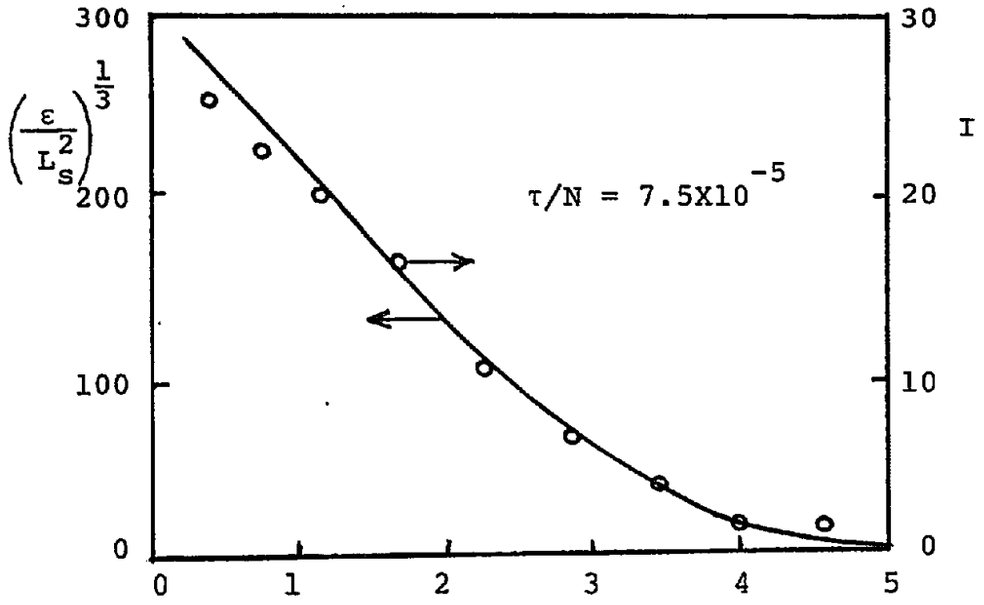

*Fig. 22. Plots of $(\varepsilon/L_s^2)^{1/3}$ and I for successful simulation of experimental tubular reactor results.

*Reprinted with permission from CHEMICAL ENGINEERING SCIENCE 32, 1349(1977). Copyright 1977, Pergamen Press, Ltd.

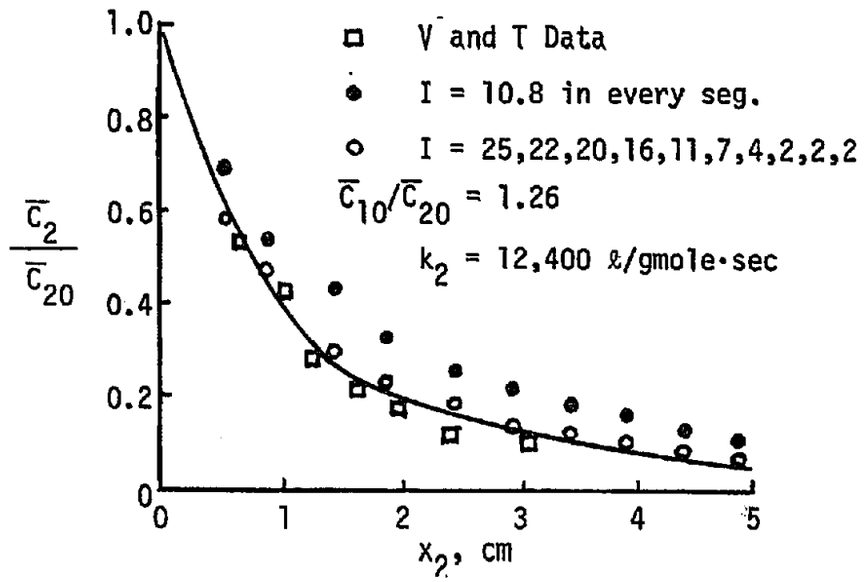

*Fig. 23. Comparisons of experimental data, C-D model, and numerical nodel results.

*See above footnote.

diffusion equation, which was determined by matching coalescence-dispersion results to finite-difference model results for mixing and diffusion in a jet, the constant was 60. It's only been tested with one experiment.[10]

In order to apply the coalescence-dispersion method to a jet shown in Fig. 24, it was divided into rather large regions (see Fig. 25).

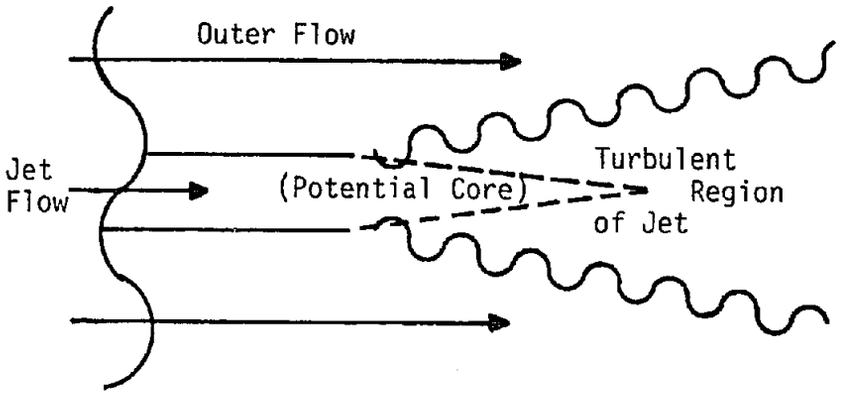

Fig. 24. Flow geometry of jet.

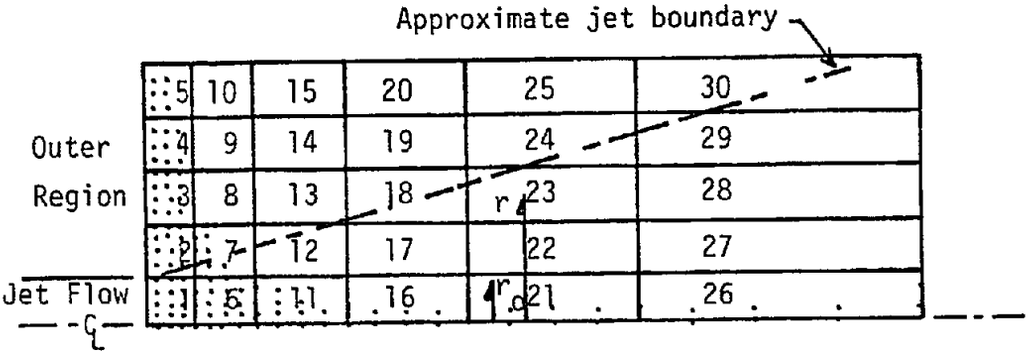

Fig. 25. Finite-Difference nodes and C-D segments in jet flow.

This is our jet flow and this is an outer region. The dots indicate where one might have the points for finite-difference calculation. But in order to do a coalescence-dispersion computation, one must divide the region into volume elements. The volume elements are rather large. It's a crude test of the method. Figure 26 shows the kind of velocity profile obtained for a single jet. A concentration profile is shown in Fig. 27 for the case of no chemical reaction. The correspondence between them was not bad. Of course, the modeling was done in such a way that we would get close correspondence for this kind of test. Figure 28 shows the segregations. With the volume

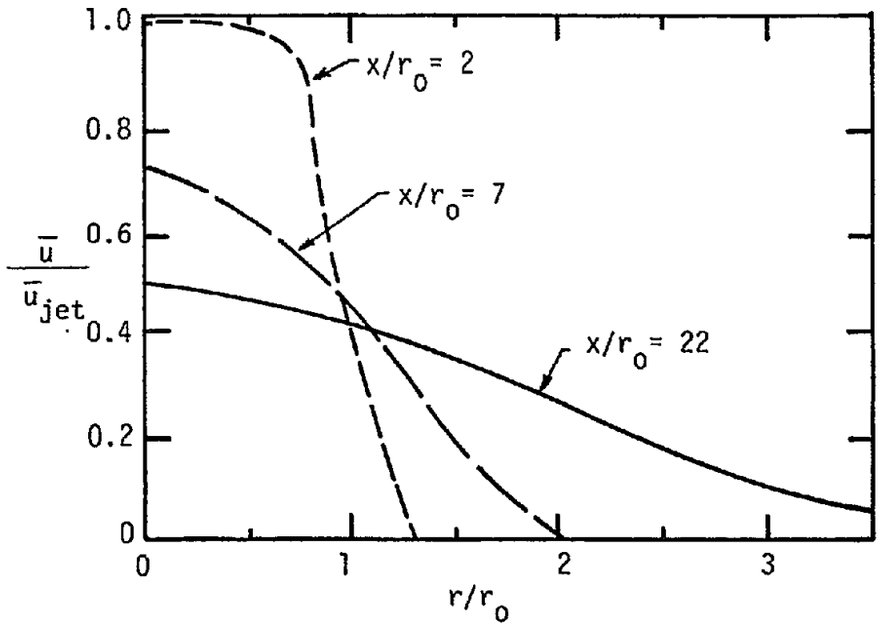

Fig. 26. Velocity profiles predicted by k-ε model.

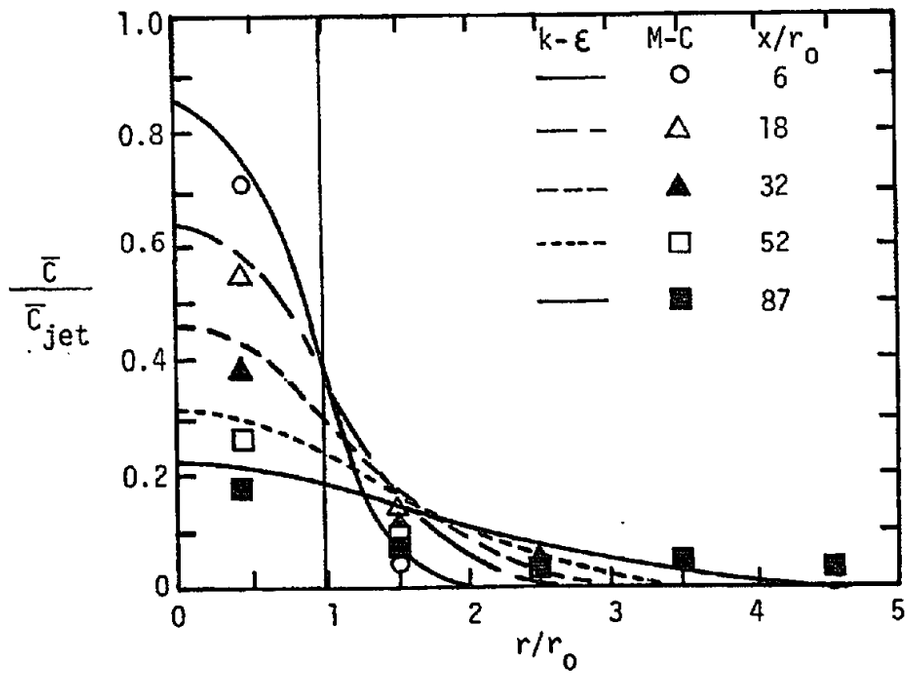

Fig. 27. Jet fluid concentration profiles with no reaction.

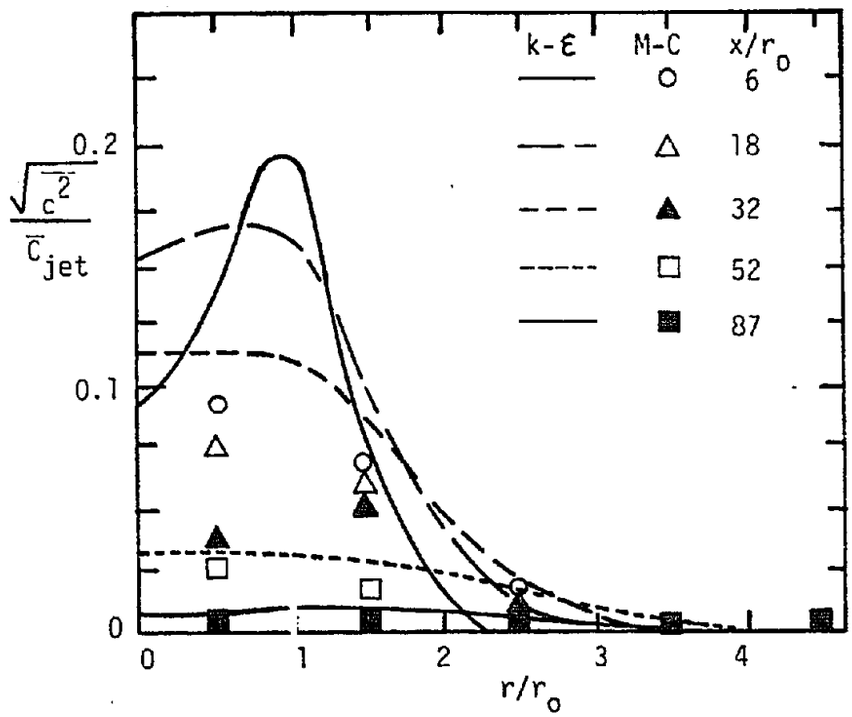

Fig. 28. Jet fluid segregation profiles for no reaction.

elements so large, the segregation results do not correspond very closely to the finite difference generated results.

One really wouldn't expect very good results for the segregation levels. The method turns out to work very well for calculating the extent of chemical reaction, because the rates of combination are not dependent on the results for segregation, but they are dependent on the correlation between the rate of coalescence-dispersion compared to real reaction rate.

Figure 29 shows simulations with and without chemical reaction for a jet mixing with a pipe flow. Figure 30 shows the same comparison for a jet with entrainment. The results without the chemical reaction are the circles, squares, and triangles without a line through them. Results with chemical reaction are shown as circles, squares and triangles with a line through them, to indicate how much change you get in the concentration profile if you have chemical reaction. Downstream there is a greater and greater effect of chemical reaction on the concentration profile. There is no comparison here between the random coalescence dispersion method and finite difference method. Both sets of results used the random coalescence dispersion scheme.

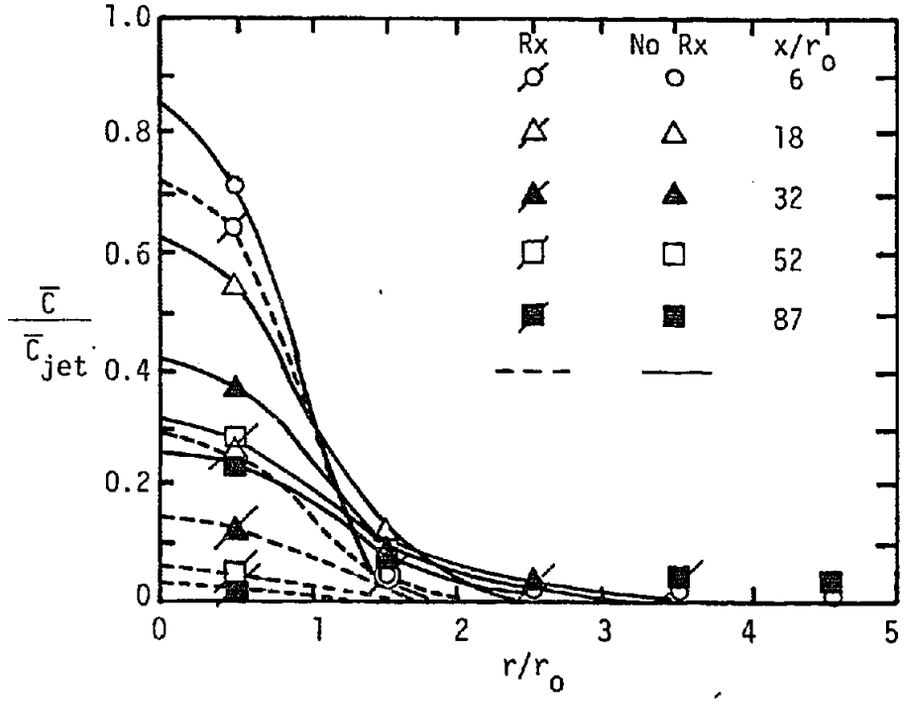

Fig. 29. Comparison of concentration profiles with and without reaction (isokinetic entrainment).

One simulation involved a complex reaction with two reactions where the product of one of the reactions reacted with one of the original reactants. This is the parallel-consecutive double reaction mechanism. The top graph in Fig. 31 is the yield of one of the products of the first reaction as a function of radial location far downstream (x/r_o = 37). The middle graph contains concentration profiles for that product normalized by the inlet concentration of one of the reactants, and the bottom graph shows the concentration ratio for that reactant to its initial value. It drops to zero quite fast.

Modeling Complex (Multi-Specie) Reactions

Some tests were made of the coalescence-dispersion method with some reaction data which were obtained in a stirred-tank reactor which was mixed by a standard turbine. This is a case where the hydrodynamics are not quite as complicated as in mixing jets, because large scale diffusion is a minor effect. The small-scale mixing is the predominant effect in mixing tanks of this type. Random coalescence-dispersion modeling was done by dividing the reactor into thirty regions, each with a large number of coalescence-dispersion sites. The minimum number used was a hundred (minimum number per region). Figure 32 shows an illustration of some of those regions. Region 0

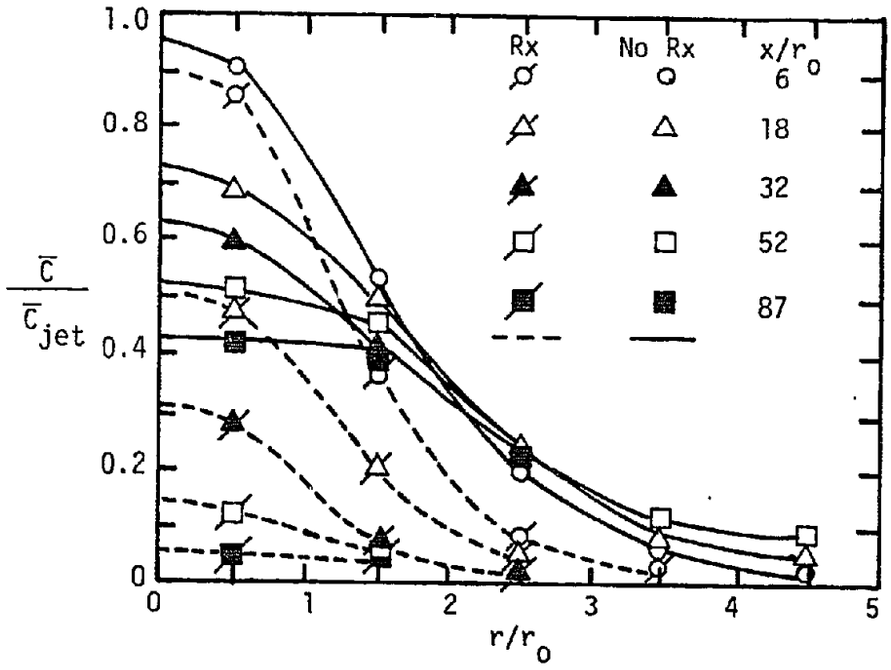

Fig. 30. Comparison of concentration profiles with and without reaction (inertial entrainment).

is a feed region necessary because coalescence-dispersion sites must have an origin to obtain the initial feed concentration. The whole reactor was filled with these regions. The level of conversion and yield of a product was computed for the same kind of reaction mentioned above (a consecutive-parallel reaction) for a case where good experimental data existed (data of Paul and Treball[11]).

Figure 33 snows some oi the results compared with experimental data for reactor outlet yield as a function of impeller rotation rate. It shows that as crude as coalescence-dispersion is, it seems to account very well for the effects on yield for various cases--feed at the top, feed to impeller center, and a double-size impeller. Recirculation, of course, occurs in the tank before the product comes out, so there are rather strong effects of where the feed is injected--near the intense turbulence of the impeller or far from it. The computer program was set up so that the turbulence properties and flow properties were modeled as a function of the impeller rotation rate. This simulation was for a tank which was one foot in diameter. To check scaling, a tank half that size was simulated also, and the results are shown in Fig. 34. Indications from comparisons of simulation and experimental data are that the coalescence-dispersion method is valuable for simulation and scaleup. There has always existed some question as to whether coalescence-dispersion really accounts for the complex effects existing when complex mixing and

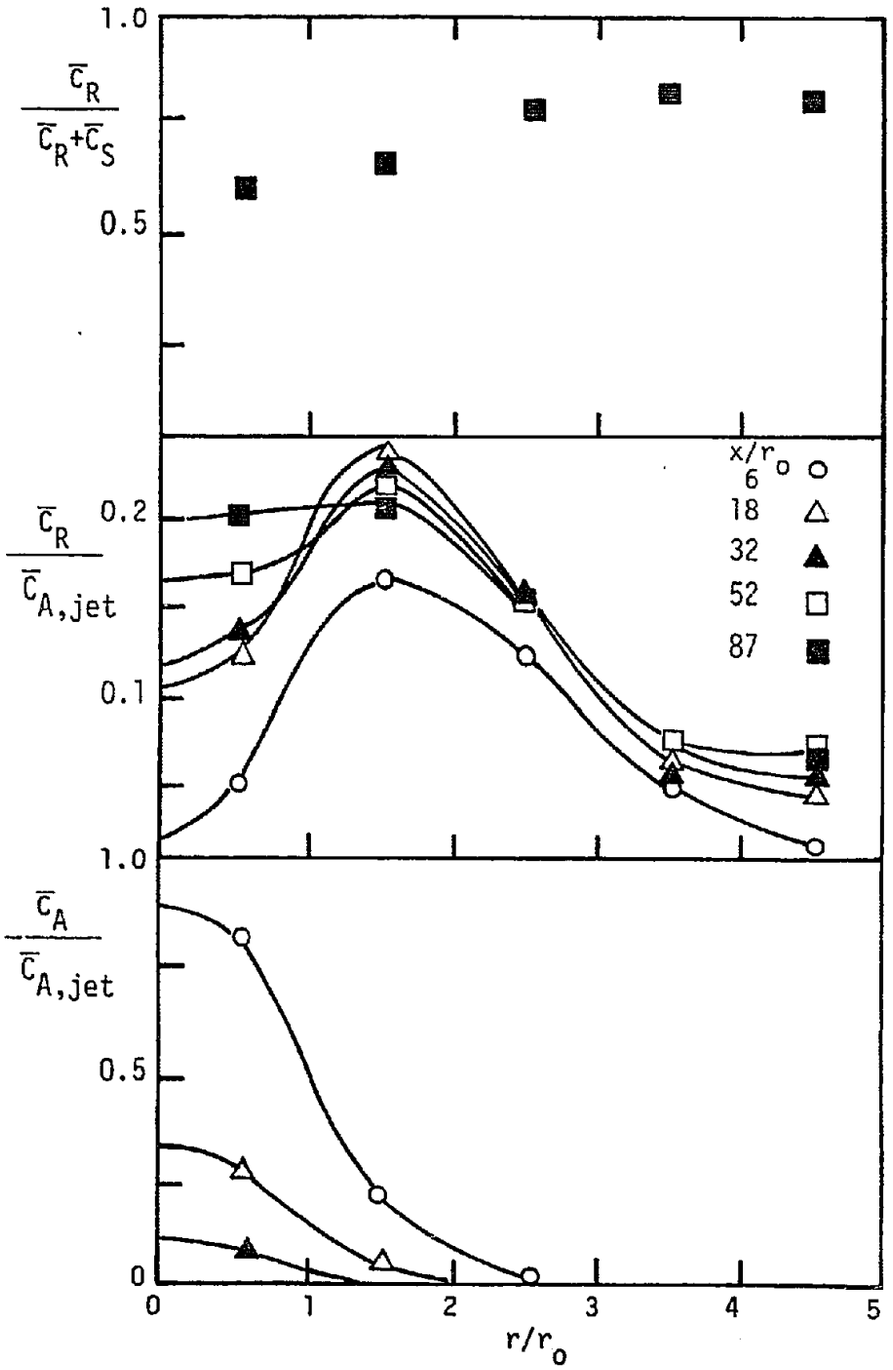

Fig. 31. Reactant A concentration, product-R concentration, and selectivity to product-R for the reaction A + B→R; A + R→S. (r_o = 1.0 cm; $\bar{u}_{jet}$ = 10 cm/s; K_{01} = 10 cc/gmole/s; K_{02} = 1.0 cc/gmole/s).

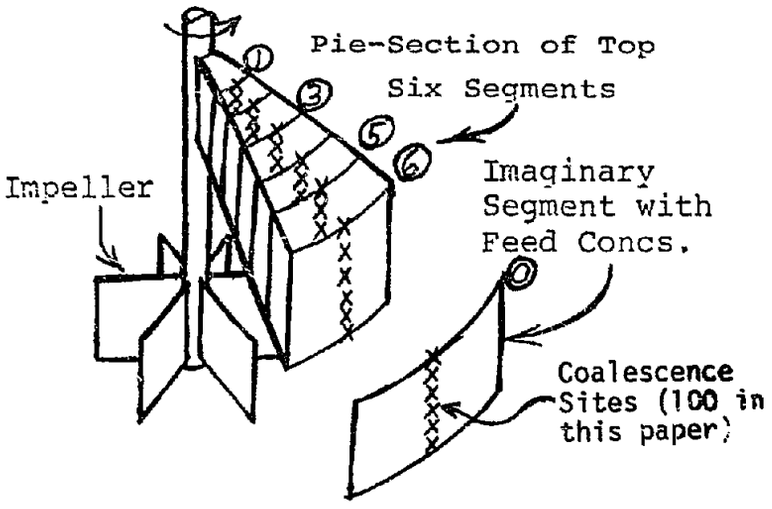

* Fig. 32. Diagram of tank reactor segment with C-D site locations.

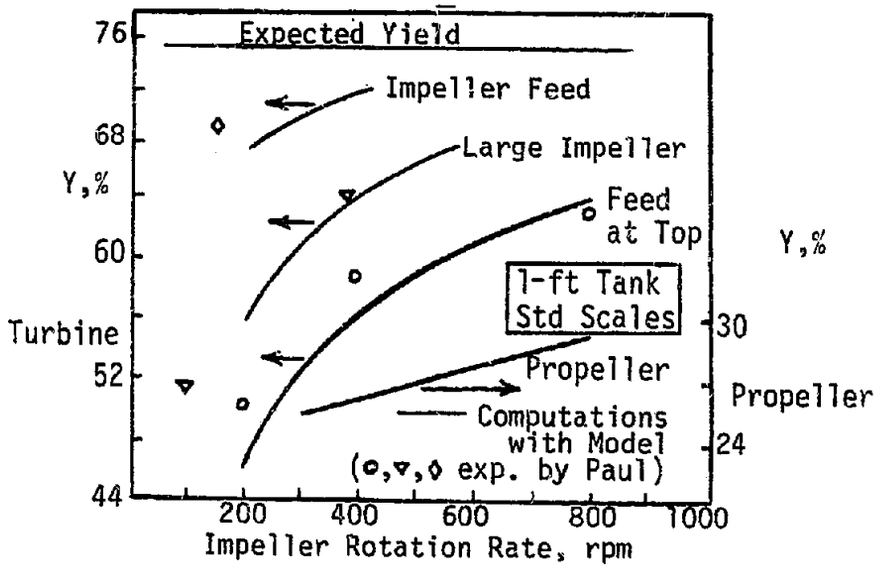

* Fig. 33. Comparison of experiment and model results for a semibatch reactor (1.0 ft diameter).

reaction occur at the same time, but this kind of evidence indicates good behavior.

*Reprinted with permission from CHEMICAL ENGINEERING SCIENCE, 32, 1349(1977).

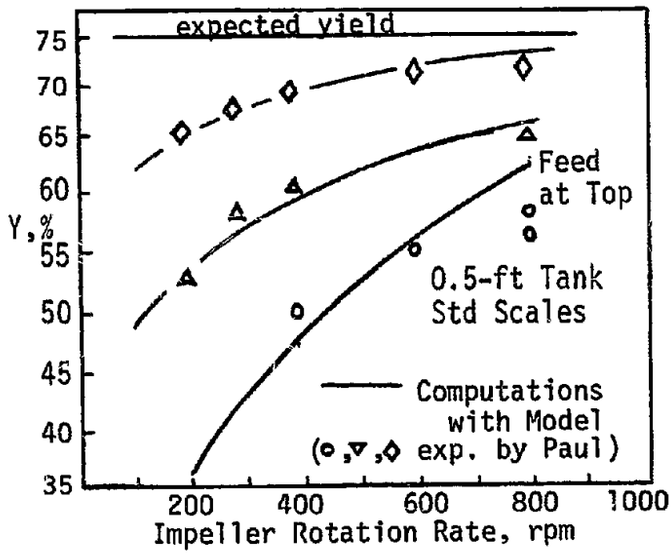

Fig. 34. Comparison of experimental and model results for a semibatch reactor (0.5 ft. diameter).

REFERENCES

1. Vassilatos, G., and Toor, H. L., *AIChE J.* 11, 10 (1965).

2. McKelvey, K. N., Yieh, H. N., Zahanycz, S., and Brodkey, R. S., *AIChE J*, 21, 1165 (1975).

3. Patterson, G. K., *Fluid Mecahnics of Mixing*, Proc. of ASME Meeting, Fluids Eng. Div., Atlanta, June 1973.

4. Corrsin, S., *AIChE J.*, 10, 870 (1964).

5. Patterson, G. K., Lee, W. C., and Calvin, S. J., Symposium on Turbulent Shear Flows, Penn. State Univ., April 1977.

6. Jones, W. P., and Launder, B. E., *Int. of Heat Mass Transfer*, 16, 119 (1973).

7. Spalding, D. B., Chemical Engineering Science, 26, 95 (1971).

8. Durao, D. and Whitelaw, J. H., *J. Fluids Engineering*, Trans. ASME, 1973.

9. Canon, R. M., Smith, A. W., Wall, K. W., and Patterson, G. K., Chemical Engineering Science, 32, 1349 (1977).

10. Patterson, G. K., 70th Annual AIChE Meeting, New York, Nov. 1977.

11. Paul, E. L., and Traybal, R. E., *AIChE J.*, 17, 718 (1971).

12. Pratt, D. T., *Prog. Energy Comb. Sci.*, 1, 73, (1976).

13. Patterson, G. K., *Application of Turbulence Theory to Mixing Operations*, ed. R. S. Brodkey, Acad. Press, New York, 1975.

14. Patterson, G. K., 4th Intern. Symposium on Chemical Reaction Engineering, Heidelberg, 1976.

15. Truong, K. T., and Methot, J. C., Can. J. Chem. Eng., 54, 572, (1976).

16. Nabholz, F., Ott, R. J., and Rys, P., 2nd European Conference on Mixing, Cambridge, England, April, 1977.

17. David, R., and Villermaux, J., Chem. Engineering Science, 30, 1309 (1975).

18. Patterson, G. K., 71st Annual AIChE Meeting, Miami Beach, November, 1978.

Comments and Replies on

"Modeling Chemical Reactions in a Mixing Environment - Basic Considerations"

by G. K. Patterson

R. Edelman: What you have said is that at this plane, the chemical reactions depend on laminar diffusion of the chemical components.

G. Patterson: No. I'm not necessarily down to that point. This is just a cut through the thing at some particular time; that time may be when the fluid regions have been stretched to the point that they are very small. All I'm saying is that at any particular time, if you take a picture, it may look something like this. Nothing is being said about what the scale is, yet. If they are very small, the diffusion between the two components and the equalization of concentrations will be very rapid. If they are very large, with the same diffusivity, the equalization of concentration will be slower.

M. Zlotnick: Are the velocity and temperature in the two components of importance?

G. Patterson: We're not talking about temperature effects in the beginning. We're assuming that we have got an isothermal system; a fairly idealized situation, because that's what we are going to draw some of our conclusions from.

T. Blake: Could you say a little bit about the geometry of the straight tube jet itself?

G. Patterson: The tube was filled with little, very long tubes, and since there were so many of them, the velocity profile in the tubes, themselves, really wasn't important for the overall problem. Once you get several diameters downstream, there is not more effect from them anyway.

S. Goren: In the Toor reactor, were the reactants alternated between adjacent jets?

G. Patterson: Yes, reactants were alternated between adjacent jets. It wasn't a random pattern. Alternating reactants in the jets.

A. Varma: This is the laminar Schmidt number, not the turbulent Schmidt number, in the Corrsin equation?

G. Patterson: Yes, the laminar Schmidt number. The Schmidt number based on molecular diffusivity. In order to carry out the modeling we had to know something about the rate of turbulence energy dissipation and length scale and we use measured values for those, which Brodkey and his students obtained.

J. Bett: Gary, is it possible to relate - in the picture of mixing and diffusion you showed - the sequence of the pictures to the concentration gradient.

G. Patterson: The way that would have to be done is this: if consider the way Corrsin derived his equation for the rate of scalar segregation decay, he hypothesized a spectrum which was easy to handle for the scalar component. What that means, of course, is he's including all the possible scales of segregation that might occur. The smallest globs of fluid and the biggest. The length scale that turns out in his equation is a characteristic large scale that is in the spectrum that he hypothesized. As that characteristic large scale changes, then the rate of mixing changes because it is a function of that.

M. Zlotnick: What measurements did you actually make?

G. Patterson: We didn't make any. The measurements were made by a series of two or three students working for Herb Toor at Carnegie-Mellon University, and we simply used their measurements to test our model.

M. Zlotnick: What were their measurements?

G. Patterson: Their measurements were the temperature profile on the axis downstream to indicate the level of conversion of the acid-base reaction.

P. Ponzi: Why did you write your balance equations as a series of stirred-tanks instead of just a variation with a distance downstream?

G. Patterson: That was the simplest way for us to carry out the modeling we did.

R. Edelman: Is the temperature for these cases nearly constant?

G. Patterson: There were very small temperature changes. A degree or two. In order to get the level of conversion, they had to measure to precisions of 0.01 degree approximately, which is not bad, but that was simply a temperature effect of the reaction. In other words, there is some heat evolved because of the exothermic reaction, so you get some heating. The temperature increase was not enough, though, to affect the fluid

mechanics. It was just a tool for measuring the level of conversion in the chemical reaction.

R. Edelman: Is the reaction then assumed to be irreversible?

G. Patterson: Yeah, it's assumed to be essentially irreversible second order reaction.

R. Edelman: Second order in C_1 or first order in C_1 and C_2?

G. Patterson: First order in both.

J. Bett: What are the units of K_2?

G. Patterson: In this case, they were the metric units that the chemists use, so they would be liters per gram mole per second.

X. Reed: When you write a μ_T, is that the turbulent vs. the molecular?

G. Patterson: Yeah, Launder usually separates them and says, "this is the eddy viscosity and this is the molecular viscosity, so the sum of them is a total viscosity." In most cases, the eddy viscosity is so much bigger, the molecular viscosity doesn't show up.

A. Varma: I was just thinking about whay you said about the segregation production term. That doesn't require the differential equations for modeling?

G. Patterson: No. It may look like it involves a differential equation, all we're doing is calculating some gradients and then combining them together to get a source term.

R. Edelman: What is the composition of C_1?

G. Patterson: Just two streams of air in the no-reaction case. One stream has a very light loading of small particles like you'd use for laser-Doppler anemometry and the other stream has no particles, so concentration profiles are measured as a function of light scattering intensity.

K. Wray: And the jet contained particulates?

G. Patterson: The inside jet contained particulates.

S. Goren: What size were the particulates?

G. Patterson: They were the same particules we used for the laser-Doppler anemometry, so they were a little bit larger than a micron. They essentially followed the flow. We had to use a little higher loading than we used for for the laser-Doppler anemometry in order to get

scattering levels which gave us good enough precision to measure.

R. Edelman: How about the initial conditions in the modeling?

G. Patterson: For the initial conditions, we used a parabolic profile in the center jet and essentially a flat profile for the angular jet. That's now exactly the kind of a condition that you would expect, but for a fineness of grid we were using, we couldn't do very much better than that.

B. Gerhold: These data were for the formation of ammonium chloride particles in those two streams? You put HCl in one and ammonia in the other. You measure it by measuring the light scattering from the particles. Did I understand that correctly?

G. Patterson: That's right.

B. Gerhold: What do you do about particle size and agglomeration and knowing how much you really reacted when you made your measurements?

G. Patterson: We are afraid that there probably are some effects like agglomeration in there, but we haven't studied that particle properties that are produced at the various points well enough to really know how much agglomeration is occurring.

B. Gerhold: There has to be some.

G. Patterson: I agree. This is a somewhat crude experiment.

K. Wray: What is the rate constant? Did you say it is essentially instantaneous?

G. Patterson: It's essentially instantaneous.

K. Wray: That's the rate constant for....

G. Patterson: For gaseous HCl reacting with gaseous ammonia to make ammonium chloride particles.

K. Wray: So it includes the condensation-precipitation growth phenomenon in that region?

G. Patterson: Yes.

R. Edelman: Were the initial conditions the same as for the non-reacting case?

G. Patterson: Yes, essentially.

R. Edelman: How did the chemical reaction affect the mixing rate?

G. Patterson: Through the term which arises in the segregation balance equation. There is a term which arose because of chemical reaction, which has the concentration correlation terms in it.

R. Edelman: It would appear that the effective Schmidt number in your calculations is substantially different in each case.

G. Patterson: Why?

R. Edelman: Well, I see if I go back to the non-reacting case you're still in the potential core region. Under the reacting conditions, your measurements show you're still in the potential core region.

G. Patterson: That's right. You get a very high rate of mixing occurring here. Are you saying that the diffusion in the potential core is faster than it looks like it should occur?

R. Edelman: Compared to the non-reacting case, that's what your calculated result shows.

G. Patterson: If you look at the stretching elements of fluid, if we can have no reaction there, then the only thing that's occurring which will enhance the rate that mixing occurs is the stretching itself. As the stretching occurs, this thins out the mixing regions and allows the molecular diffusion to mix the material more rapidly. If chemical reaction occurs, it enhances that diffusion process as well as the stretching itself, because the reaction steepens the concentration gradients.

I. Osgerby: I don't see how that applies in this particular system.

G. Patterson: In the non-reacting case, there were low levels of mixing very close to the jet even near the centerline (potential core). The model predicts rates of reaction for those mixtures less than for a homogenous case at the concentrations involved.

S. Goren: C_1 bar is the concentration of...

G. Patterson: Of a reacting component. I believe in this case it was the ammonia.

S. Goren: Measured along the center line?

G. Patterson: No. These are profiles at various distances downstream.

K. Wray: Is the ammonia in the center? Is that the jet?

G. Patterson: Yes. Ammonia is the jet. We put the ammonia in the center because we didn't like to smell it, which is the way I remember that's how we did it.

I. Osgerby: Are you familiar with model developed by Rhodes and Harsha?

G. Patterson: I'm not familiar with model developed by Rhodes and Harsha. Have they used something like random coalescence and dispersion?

I. Osgerby: I think you would benefit greatly from looking at their work. Correct me if I'm wrong, Ray, but they were taking each eddy as a small stirred reactor, allowing it to (whatever that composition was) react for a finite time and then coalesce with other eddies, then proceed with a pretty good mixing model to account for the lifetime of these eddies.

R. Edelman: I think the objective is the same, but the formalism involved in coalescence-dispersion modeling is quite different.

G. Patterson: Pratt has done some of this - he doesn't use the term "sites", he calls them"turbules". They didn't use that terminology?

R. Edelman: No.

I. Osgerby: The reason I brought it up is that I think Rhodes and Harsha originated that line of thought.

R. Edelman: They were the first to do a formal analysis with a multi-component system.

G. Patterson: Where is their data?

R. Edelman: It's been published.

G. Patterson: I'll get it from you. The first coalescence modeling that I know of was work by Evangelista.

P. Ponzi: Actually, it goes back further than that, right to...

G. Patterson: Yes, that's true.

R. Edelman: I think the point there is what one does for chemistry. For example, looking at things like NO_x, where the kinetics are extremely sensitive and multi-step kinetics are important. The Rhodes and Harsha work was the first time that any attempt was made to take into account the effects of fluctuating chemistry with a multi-step chemical reaction mechanism.

P. Ponzi: What was the flow situation like this?

R. Edelman: It was coaxial flow and they compared their predictions with the data of Kent and Bilger and got very good agreement.

G. Patterson: As far back as 1972 we were simulating polymerization using coalescence-dispersion. We were also simulating other kinds of complex chemical reactions. I think one of the problems in a lot of the cross communication between fields is we use different termninology. If, for instance, Harsha doesn't say coalescence-dispersion, many of us don't know what he is doing.

R. Edelman: No, it's not coalescence-dispersion, as a matter of fact.

G. Patterson: OK. So this is a somewhat different technology.

R. Edelman: It's different formalism.

G. Patterson: I'm glad you brought that up. I'll get the information on his work.

I. Osgerby: I'm having trouble with the coalescence-dispersion model equation. Is there a unit problem there?

G. Patterson: Not really, because "I" isn't coalescences per unit time. "I" is the number of coalescences that occur during the time "τ" per unit number of coalescences sites that are in the element itself. What we do in a computation is determine the maximum distance for a coalescence and we let it have a random distribution up to that maximum. That's simply one of the rules that we use in setting the formalism of the method and then we see how it works.

R. Edelman: What does MC mean?

G. Patterson: Monte Carlo. I don't call it that anymore. I call it random coalescence dispersion now. I don't like the term Monte Carlo.

S. Goren: In the HCl experiment, what do you actually measure?

G. Patterson: We actually measured the product. We had to back calculate the conversion of the reaction at various points.

MODELING OF CHEMICAL REACTIONS IN TURBULENT FLOW - A REVIEW

Ashok K. Varma
Aeronautical Research Associates of Princeton, Inc.

INTRODUCTION

Turbulent flows involving chemical reactions occur in many situations including industrial and home furnaces, chemical process plants, various propulsive devices such as jet engines, rocket motors and ram jets, chemical and gas dynamic lasers, exhaust plumes and wakes of high speed vehicles. In effect, almost every practical flow system involving chemical reactions also involves turbulent flowfields. The interaction between the chemistry and the turbulence is of significant importance in many of these systems. Turbulence affects flame speeds, combustion efficiency, ignition and extinction behavior, flammability limits, combustion stability and pollutant formation, etc. On the other hand, the chemical processes affect the turbulence as well, through energy release and density variations. Models for these interactions have to be developed in order to carry out predictive calculations of turbulent reacting flows. Many current calculation procedures completely ignore the coupling between turbulence and chemistry and are inadequate in this regard.

The main reason this problem has been ignored in the past is due to its complexity. The need for understanding the coupling between turbulence and the chemical processes has been appreciated and acknowledged by the early combustion researchers. However, until very recently the analytical and computational capabilities as well as the diagnostic tools to adequately characterize turbulence in reacting flows were not available. Considerable advances have been made in recent years in these areas and it now appears feasible to develop a rational model for turbulent reacting flows using a higher-order closure modeling approach.

This review will attempt to demonstrate the importance of the turbulence-chemistry interactions by examining a number of basic reacting flows and then attempt to outline the diverse approaches being used by different groups and the progress-to-date.

BASIC CONSIDERATIONS

Why Modeling is Required

This is a reasonable question in light of the fact that the governing conservation equations of fluid mechanics are well known and are generally accepted as being correct. Why not simply solve them numerically? There are two main considerations. Firstly, current computers are not yet large enough or fast enough to do an adequate job of solving the Navier-Stokes equations (even for the simpler nonreacting flow problems). Such capability is expected to be available in about a decade from now. Till such time, intelligent modeling is required to retain the important features of the flow and simplify the problem to the point that it can be solved on

currently available computers. Secondly, and more importantly, modeling is necessary because in many situations one is not interested in all the information contained in the equations. For example, in many engineering applications of turbulent flows one is only interested in the knowledge of the mean variables. It is probably not cost-effective to solve the instanteous equations and then extract the information on the means. Instead, one can derive the equations for the mean variables of interest and just solve these equations after appropriate modeling. In many cases, this process also leads to increased understanding of the physics of the problem.

Closure Problem of Turbulence

The conservation equations for the mean variables can be easily derived from the instantaneous hydrodynamic equations by expanding the instantaneous variable into a mean and fluctuating part. The mean equations involve correlations of the fluctuations. Simplified forms of the mean momentum and mean species mass fraction conservation equations are shown below:

Mean momentum equation

$$\bar{\rho}\bar{u}\bar{u}_x + (\bar{\rho}\bar{v} + \overline{\rho' v'})\bar{u}_y = -(\bar{\rho}\,\overline{u'v'})_y - (\overline{\rho' u' v'})_y - \bar{p}_x + \frac{1}{Re}(\bar{\mu}\bar{u}_y)_y + \ldots\ldots \quad (1)$$

Mean species conservation equation

$$\bar{\rho}\bar{u}\bar{\alpha}_x + (\bar{\rho}\bar{v} + \overline{\rho' v'})\bar{\alpha}_y = -(\bar{\rho}\,\overline{v'\alpha'})_y - (\overline{\rho' v' \alpha'})_y + \dot{\bar{w}} + \frac{1}{ReSc}(\bar{\rho}\bar{D}\bar{\alpha}_y)_y + \ldots\ldots \quad (2)$$

The equations contain second-order correlations like $\overline{'v'}$, $\overline{u'v'}$, $\overline{v'\alpha'}$ and third-order correlations like $\overline{\rho' u' v'}$, $\overline{\rho' v' \alpha'}$ etc. The mean chemical source term $\bar{\dot{w}}_\alpha$ contains many second- and third-order correlations. All these terms must be modeled to close the system of equations before they can be solved. Modeling at this stage is called first-order closure or eddy diffusivity modeling, and involves modeling all the higher-order correlations in terms of the mean quantities. Commonly used models are of the type,

$$\overline{u'v'} = C_{uu}\Lambda^2 \left(\frac{\partial \bar{u}}{\partial y}\right)^2$$
$$\overline{v'\alpha'} = C_{uT}\Lambda^2 \frac{\partial \bar{u}}{\partial y}\frac{\partial \bar{\alpha}}{\partial y} \quad (3)$$

C_{uu}, C_{uT} are model constants and Λ is the turbulence macroscale.

First-order closure modeling considers the turbulence correlations to be locally related to the mean flow variables. The modeling can usually be improved by considering the dynamics of the turbulence. Transport equations can be derived for the various second-order correlations. The typical form of two such equations is shown below. These equations contain third- and higher-order correlations and these now have to be modeled to obtain a closed set of equations. This is the closure problem of turbulence, that is, one cannot obtain a closed set of equations by going to higher orders of

Reynolds stress $\overline{u'v'}$ equation

$$\bar{\rho}\bar{u}\,\overline{(u'v')}_x + \bar{\rho}\,\bar{v}\,\overline{(u'v')}_y = -\overline{(v'v')\rho}\,\bar{u}_y - 2\bar{\mu}\,\frac{\overline{u'v'}}{\lambda^2} \qquad (4)$$

$$+ \ldots\ldots$$

Species correlation equation

$$\bar{\rho}\,\bar{u}\,\overline{(\alpha'\beta')}_x + \bar{\rho}\,\bar{v}\overline{(\alpha'\beta')}_y = -\bar{\rho}\,\bar{\alpha}_y\overline{(v'\beta')} - \bar{\rho}\,\bar{\beta}_y\overline{(v'\alpha')}$$

$$- \overline{\rho'v'\beta'}\,\bar{\alpha}_y - \overline{\rho'v'\alpha'}\,\bar{\beta}_y$$

$$+ \overline{\alpha'\dot{w}'_\beta} + \overline{\beta'\dot{w}'_\alpha} \qquad (5)$$

$$-2\bar{D}\,\frac{\overline{\alpha'\beta'}}{\lambda^2} + \frac{1}{ReSc} \qquad \text{molecular diffusion terms}$$

$$+ \ldots\ldots$$

correlations. Modeling has to be used to obtain closure. Aeronautical Research Associates of Princeton, Inc. (A.R.A.P.) has been one of the groups active in developing the full Reynolds stress closure or second-order closure approach to turbulence modeling and important successes have been achieved in analysis of nonreacting flows (Donaldson, 1971, Lewellen, 1977). The same procedures are now being extended to reacting flows, and will be discussed in this paper.

Another approach to turbulent flowfield modeling is intermediate between first-order closure and second-order closure. This is the two-equation turbulence model developed originally by the group at Imperial College in England (Launder and Spalding, 1972). Instead of solving all the transport equations for the various turbulence correlations, this procedure solves only one equation for the turbulence kinetic energy $k = \overline{u'u'} + \overline{v'v'} + \overline{w'w'}$ and one equation for the turbulence dissipation rate ε,

to obtain a measure of the turbulence scale lenghts. It is proposed that the turbulence can be adequately characterized by these two quantities. The procedure is obviously simpler than full second-order closure and has been quite successful in a number of applications. However, it does require additional modeling and these modeling assumptions break down for some flow problems - for example, swirling flows. In these flows, the breakup of the turbulent kinetic energy into the individual normal stress components is different than it is for nonrotating flows and the basic two-equation $k\varepsilon$ model requires additional empirical modeling. A three equation $k\varepsilon g$ model has been proposed (Spalding, 1971a) for problems involving scalar transport, for example, thermal transport, species mixing and reacting flows. An additional equation for $g = \overline{\phi'\phi'}^{1/2}$ (ϕ, scalar variable of interest) is solved in this formulation to characterize all the scalar second-order correlations.

The use of the two- or three-equation turbulence models is a significant improvement over first-order closure or eddy diffusivity modeling, and is being increasingly used. Complete second-order closure procedures are expected to be more generally applicable to a wider class of problems but do require the solution of a larger number of equations. Two- and three-equation turbulence models have been used for simple reacting flow problems but the proper treatment of turbulence-chemistry coupling may require the use of complete second-order closure models.

MODELING OF TURBULENT REACTING FLOWS

Turbulence-Chemistry Interactions

Consider a very simple chemically reacting system. Two reactant species α and β undergo a one step irreversible reaction to form a product γ.

$$\alpha + \beta \rightarrow \gamma$$

Using the Law of Mass Action,

$$\frac{d\gamma}{dt} = k\,\alpha\,\beta$$

$$\frac{d\bar{\gamma}}{dt} = \overline{k\,\alpha\,\beta}$$

$$= \bar{k}\,\bar{\alpha}\,\bar{\beta}\left(1 + \frac{\overline{\alpha'\beta'}}{\bar{\alpha}\,\bar{\beta}} + \frac{\overline{k'\beta'}}{\bar{k}\,\bar{\beta}} + \frac{\overline{k'\alpha'}}{\bar{k}\,\bar{\alpha}} + \frac{\overline{k'\alpha'\beta}}{\bar{k}\,\bar{\alpha}\,\bar{\beta}}\right) \qquad (6)$$

The second- and third-order correlations in the above expression represent some of the turbulence-chemistry interaction effects. There is additional coupling of turbulence and chemistry in the term k. The turbulence-chemistry interaction effects are neglected in many current models of turbulent reacting flows. The chemical source term is evaluated by ignoring the fluctuations of species and temperature and,

$$\frac{d\bar{\gamma}}{dt} = k(\bar{T})\ \bar{\alpha}\ \bar{\beta} \qquad (7)$$

We term this as the "laminar chemistry" or fully mixed chemistry approach. Note that $\bar{k} \neq k(\bar{T})$.

A number of idealized combustion systems have been studied to evaluate the importance of the turbulence-chemistry interaction effects. These studies have been reported by Fishburne and Varma (1977), and a few typical results are discussed here. Consider a reacting two-dimensional shear layer without heat release. Streams of reactant species α and β mix and react downstream of a splitter plate. Figure 1 shows the variation of the mixedness correlation $\alpha'\beta'/\alpha\ \beta$ along the centerline of the flow. For no reaction, the correlation approaches an asymptotic value of -0.2. The correlation will always be negative for a diffusive mixing/reacting system. The value of -0.2 is in agreement with the experiments of Konrad (1976) at CalTech. As the reaction rate is increased, the value of the mixedness correlation approaches -1. Thus, the neglect of this term in the chemical source expression (Eq. 6 note that for isothermal systems, the k' terms are zero) can lead to very significant errors. Figure 2 shows the calculated mean product concentration $\bar{\gamma}$ along the centerline of the shear layer with and without the inclusion of the mixedness correlation term. For slow reactions, considerable molecular diffusion occurs and the predictions for $\bar{\gamma}$ are not too different. However, as the reaction rate increases, the predicted product formation with "turbulent chemistry" will be significantly slower than that calculated with the neglect of the turbulence-chemistry interactions.

Figure 3 shows corresponding results for a reacting two-dimensional shear layer with heat release. The predictions for the temperature are substantially higher when the species and temperature fluctuations are neglected. Thus, the inclusion of the turbulence-chemistry interactions is quite important in the modeling of turbulent reacting flows, and procedures have to be developed to properly incorporate these effects due to species and temperature fluctuations in calculation procedures for turbulent reacting systems.

Turbulent Flowfield Models - These have already been briefly discussed in the section on the closure problem of turbulence. The three main classes of models are:

- Eddy diffusivity or first-order closure
- Two equation $k\varepsilon$ and the three equation $k\varepsilon g$
- Reynolds stress closure

Models for Turbulence/Chemistry Interactions - The various modeling approaches can be divided into two main classifications: 1) models within the Eulerian framework and 2) those in the Lagrangian framework. The Eulerian framework models are:

- No interaction - Laminar or Fully-Mixed Chemistry
- Eddy Break-up Models

- One-dimensional pdf's
- Multi-dimensional pdf's
- Solution of pdf equations
- Stirred reactor approaches
- Superequilibrium and Quasiequilibrium approximations

The Lagrangian framework models are:

These will not be discussed in any detail here. The Coalescence/Dispersion approach has been mainly developed by Pratt (1978) and Patterson (1977, 1978) and is reviewed in the presentation of Patterson in this workshop. The ESCIMO model is being developed by Spalding (1978), and in some features it is similar to the coalescence/dispersion approach. The acronym ESCIMO stands for Engulfment, stretching, Coherence, Interdiffusion and Moving Observer. The approach is to construct a population of eddies and follow them in a Lagrangian sense from birth (formation) to death (decay, breakup or coalescence). The eddies are pictured as one-dimensional sandwiches of the reactants that are formed at the edges of the mixing layer. These structures are convected downstream and undergo stretching and scale reduction due to the turbulent shear. Molecular mixing and complex multi-step chemistry are considered to occur within the individual sandwiches. The approach is promising and intuitively attractive, but probably much more difficult than claimed. The main difficulty is in determining the correct sources and sinks for the sandwich elements at various points in the flow and determining the species present in individual sandwiches in a multispecies, multistep reaction system. Further progress in the development of this model should be carefully monitored.

The remainder of this presentation will review the models that use the Eulerian approach.

The no interaction or laminar chemistry model is self explanatory. The turbulence/chemistry interactions are neglected and the mean chemical source term is evaluated by using the mean values of the species and temperatures.

$$\overline{\dot{w}} = k(\overline{T})\ \overline{\alpha}\ \overline{\beta}$$

This formulation is used in many current calculation procedures for turbulent reacting flows and is not correct. It is used because no simple, generally valid approach for considering these interactions has been established. A number of alternative approaches have been proposed and are now being tested.

Eddy Break-up (EBU) Models

The model was proposed by Spalding (1971). It applies to fast chemical reactions where the reaction rate is controlled by turbulent mixing. Then the rate of chemical reaction is determined by the rate of breakup of large turbulent eddies into smaller eddies all the way down to the molecular scales and the turbulence dissipation rate provides a measure of this rate. The chemical source term is written as

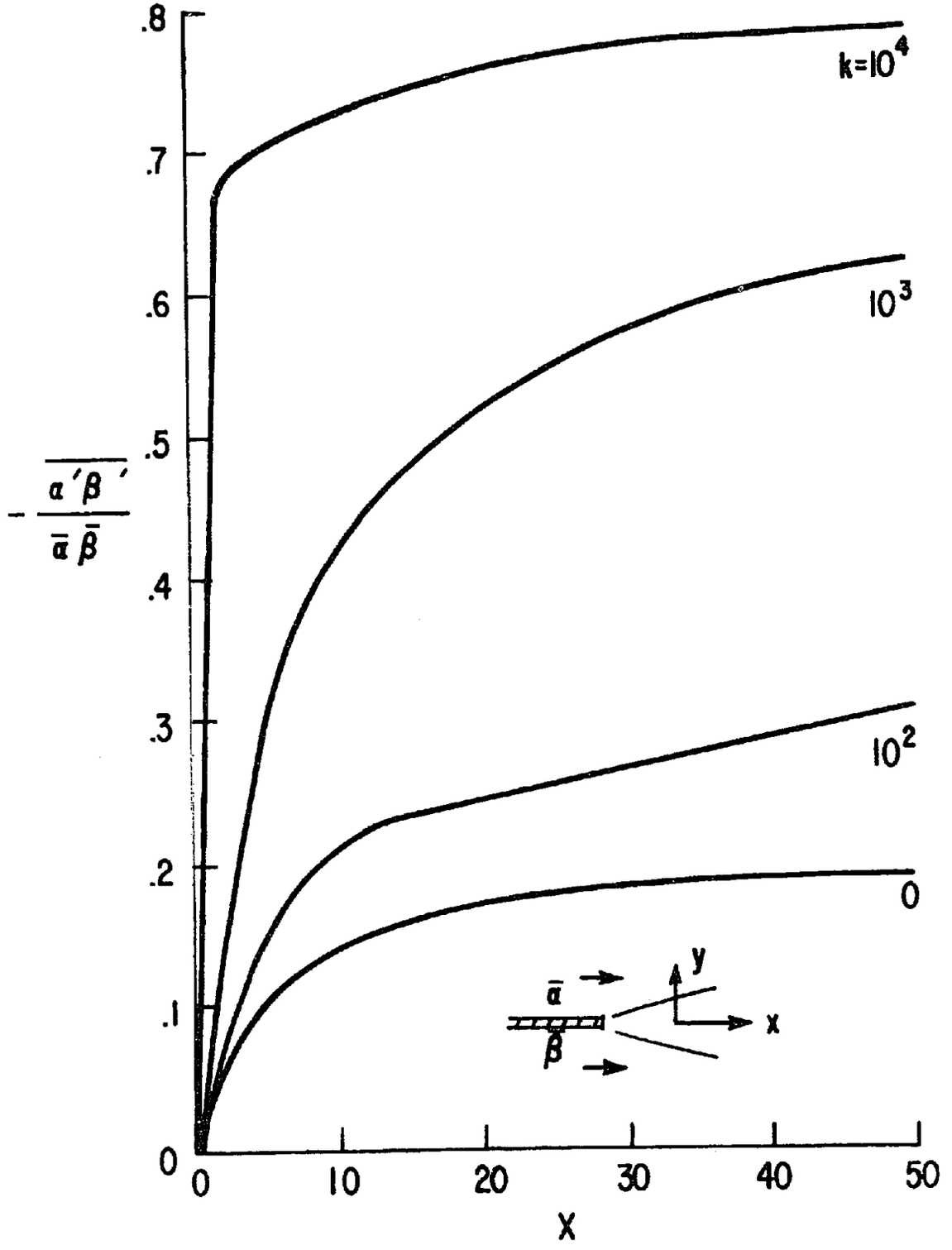

Fig. 1. Effect of reaction rate on mixedness correlation in reacting shear layer with no heat release.

° Coalescence/Dispersion Models

° ESCIMO Approach

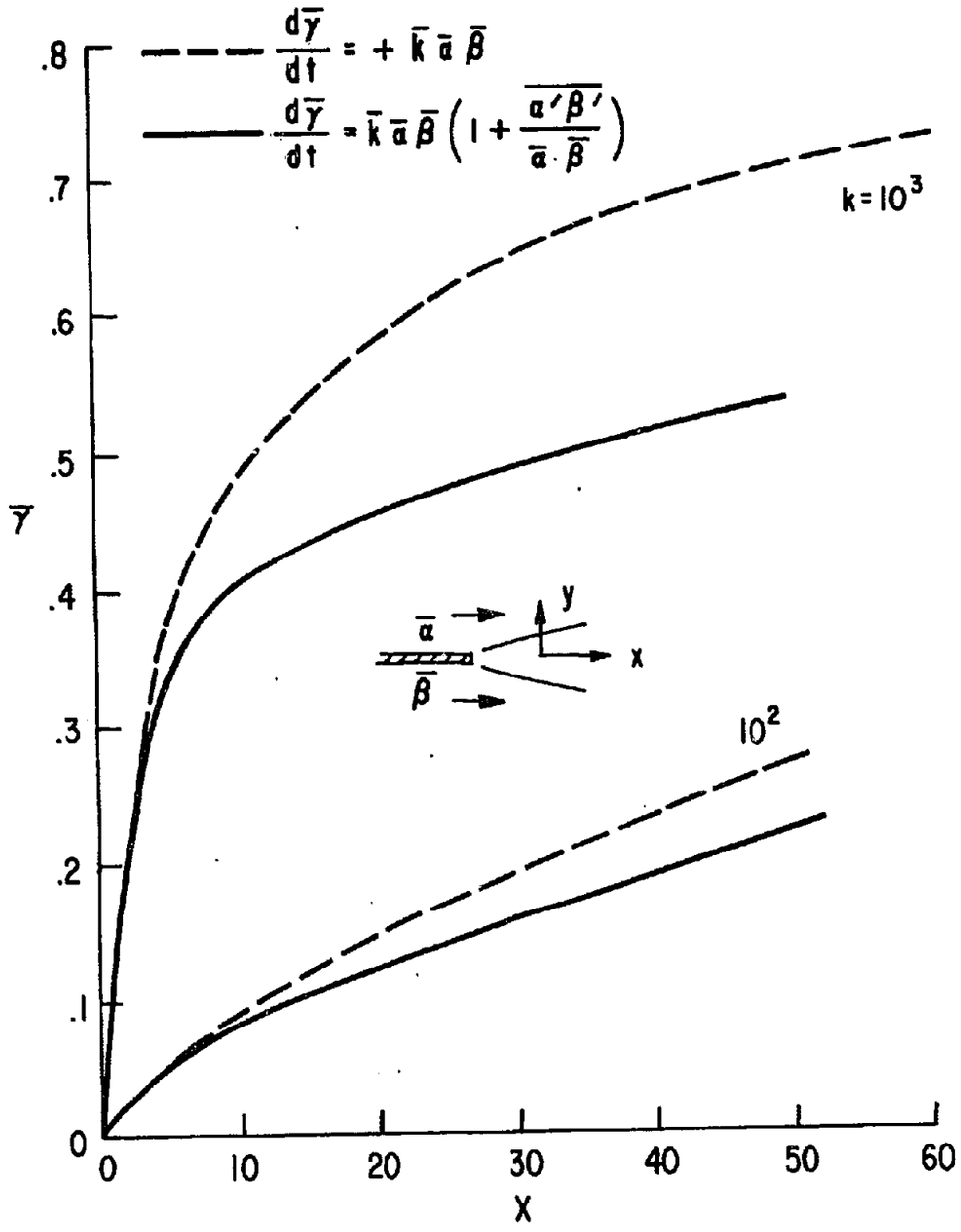

Fig. 2. Effect of mixedness correlation on product formation in reacting shear layer with no heat release.

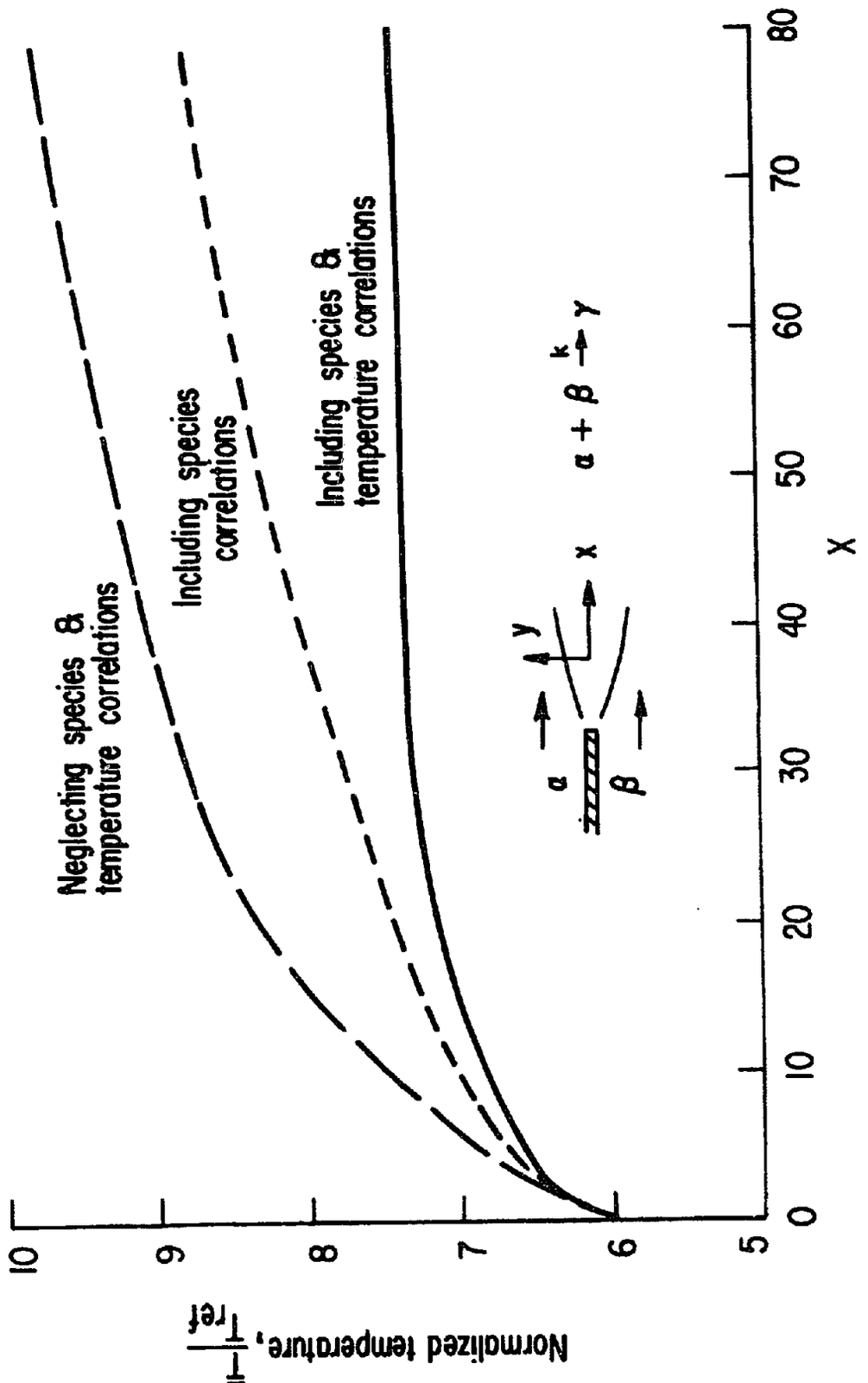

Fig. 3. Axial development of maximum flame temperature in reacting shear layer with heat release.

$$\bar{\dot{w}} = C_{EBU} \sqrt{\overline{c'c'}}\, \frac{\bar{\rho}\varepsilon}{k}$$

C_{EBU} is an empirical constant. ε is the turbulent dissipation rate and k is the turbulent kinetic energy. A major shortcoming of the model is the lack of any chemical kinetic influences. Attempts to modify the model for moderately fast reactions have not been very successful. El Khalil *et al.* (1975) have shown good agreement with data by using this model for calculations of jet diffusion flames in two-dimensional furnaces. The model is used in a modified form in that the eddy breakup rate is compared to the reaction rate obtained from a chemical kinetic expression using mean quantities and the smaller of the two rates is used at all points. This corresponds to model 3 in a few representative figures shown below. Models 1 and 2 are simpler non-kinetic models (see Figures 4 and 5).

A number of other empirical modifications of this type have been used by other investigators. Magnussen and Hjertager (1977) have carried out calculations for city gas diffusion flames and premixed flames by using the following modified EBU models. For diffusion flames, the smaller of the following two chemical production rates is used

$$\bar{\dot{w}}_f = A\, c_f \frac{\varepsilon}{k} \qquad\qquad \dot{w}_f = A\, \frac{\bar{c}_o}{r}\, \frac{\varepsilon}{k}$$

A is an empirical constant. c_f and c_o are the mean fuel and oxidizer concentrations. r is the stiochiometric ratio.

For premixed flames,

$$w_f = A\, \frac{\bar{c}_p}{1 + r}\, \frac{\varepsilon}{k}$$

$\bar{c}_p$ is the mean product concentration. This formulation is simpler than the original EBU proposal as it depends only on the mean quantities and the species correlation is not required. The figures below indicate that with proper choice of the empirical parameters in the combustion model and the turbulence dynamics model, reasonable agreement with measurements can be achieved for combustion systems involving fast chemical reactions. However, we lack a comprehensive, generally valid model for turbulence/chemistry interactions (see Figures 6, 7, and 8).

One-Dimensional PDF Models

With the use of a number of simplifying assumptions, it is possible to relate all the scalar variables in the flow to one scalar variable. Thus, if the chemistry can be reduced to a one-step reaction, the Schvab-Zeldovich coupling functions can be used to express all scalars in terms of reaction progress variable ξ. There are several other scalar variables that are conserved during chemical reactions and these can be used to formulate other scalar functions that characterize the behavior of all other scalars. The joint pdf of all the scalar variables is simply related to the one-dimensional pdf of this characteristic scalar ξ.

(From El Khalil *et al.* (1975))

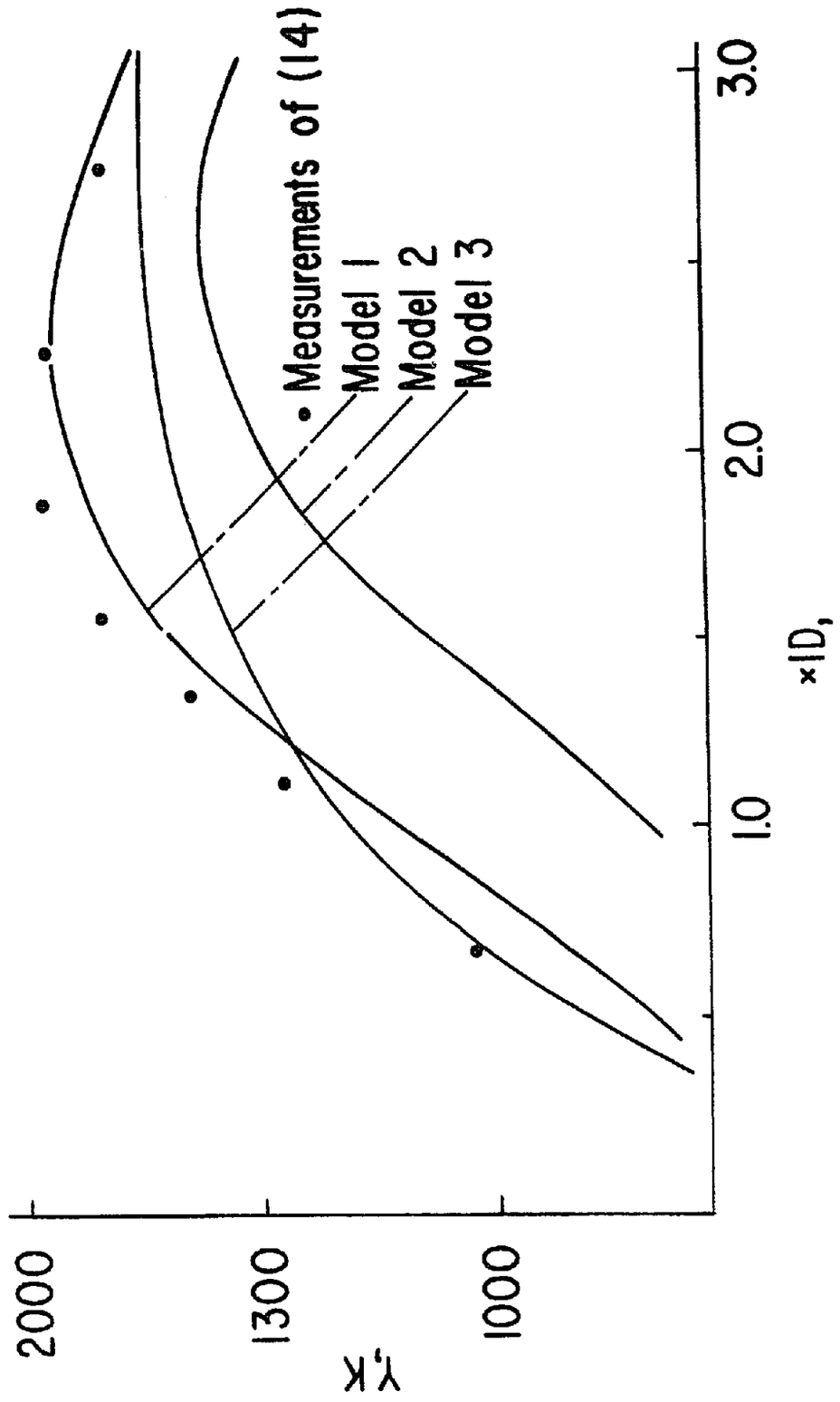

Fig. 4. Centerline distribution of mean temperature: comparison with results of [14].

(From El Khalil *et al.* (1975))

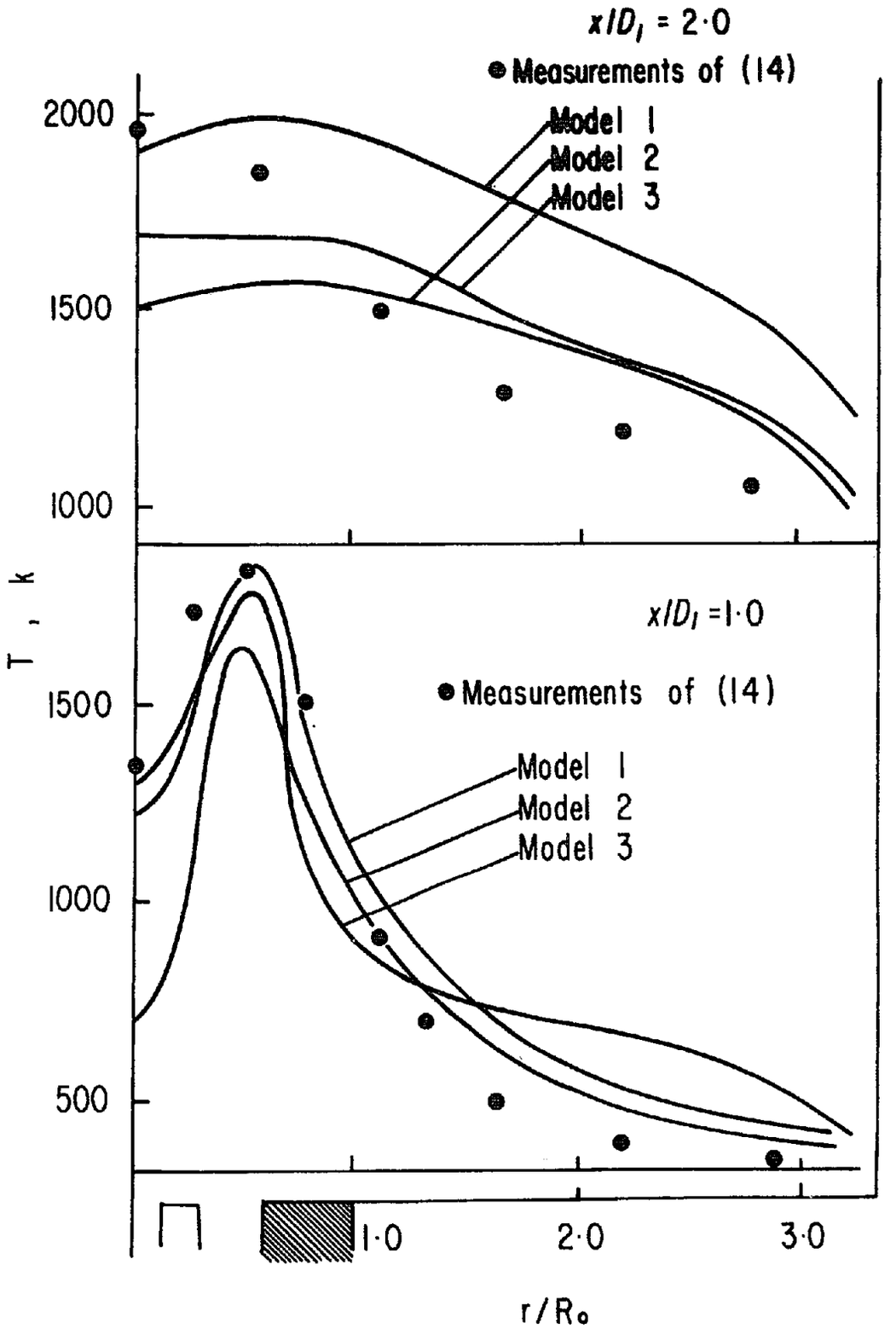

Fig. 5. Radial profiles of mean temperature: comparison with results of [14].

(From Magnussen and Hjertager (1977))

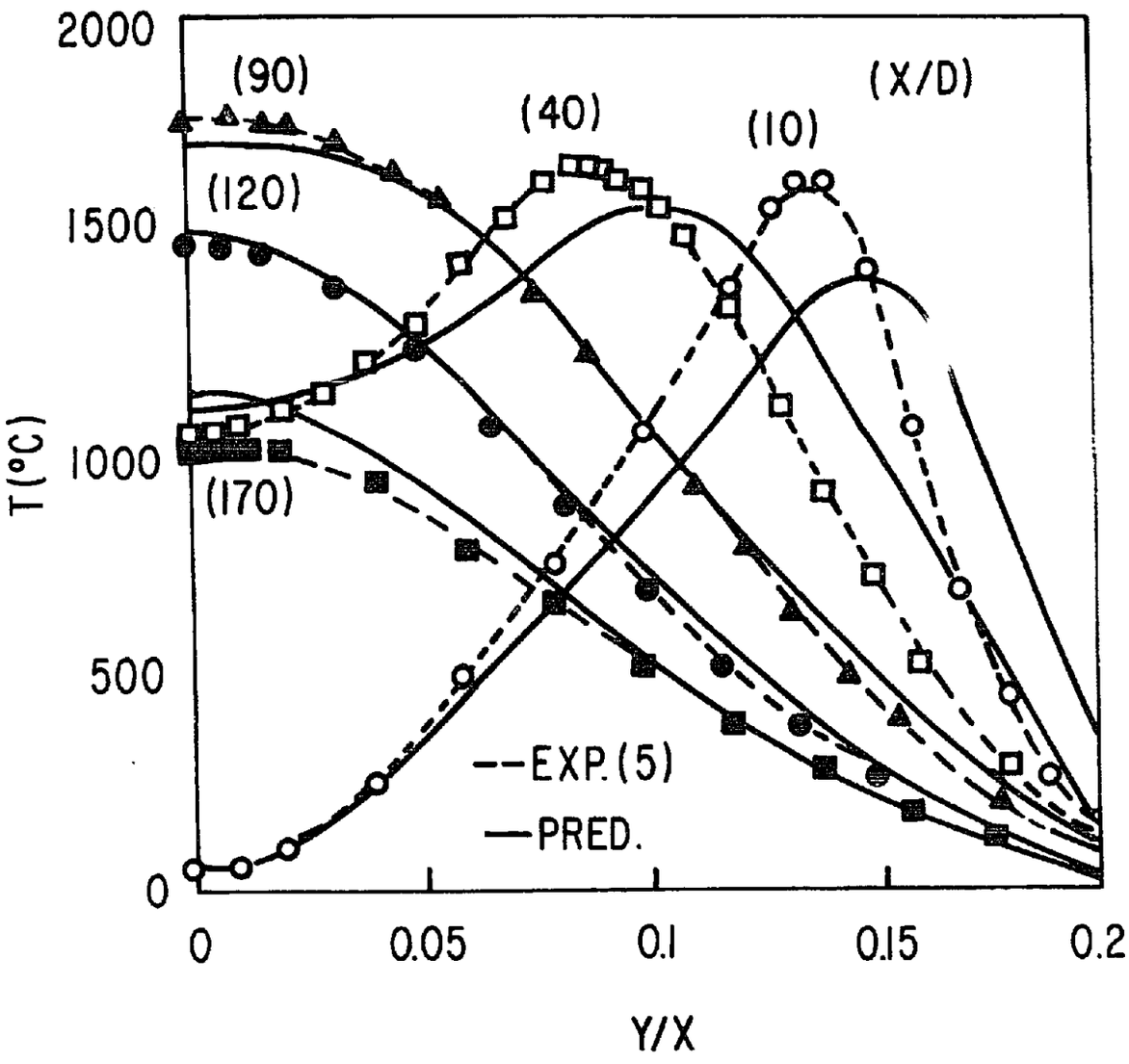

Fig. 6. Experimental and predicted local mean temperatures of a city gas diffusion flame (Re 24000).

(From Magnussen and Hjertager (1977))

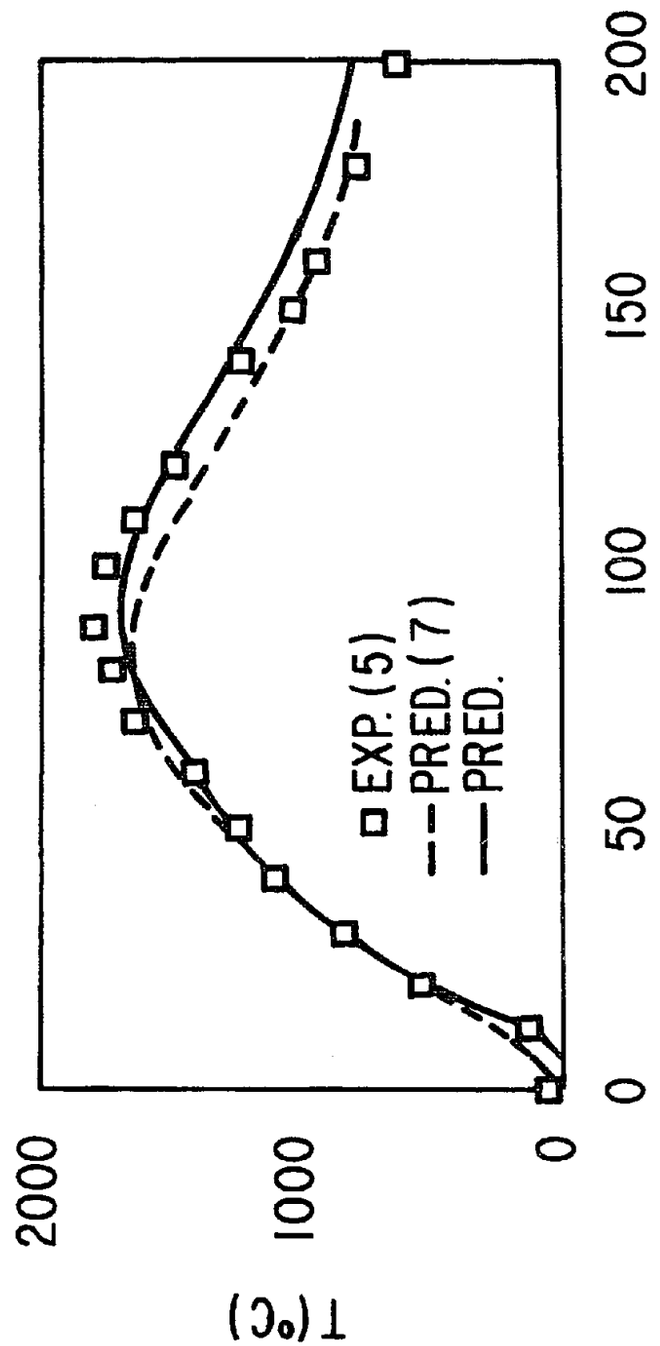

Fig. 7. Experimental mean temperature on the axis of the city gas diffusion flame (Re 24000) compared with predictions by Lockwood and Naguib and predictions according to present model.

(From Magnussen and Hjertager (1977))

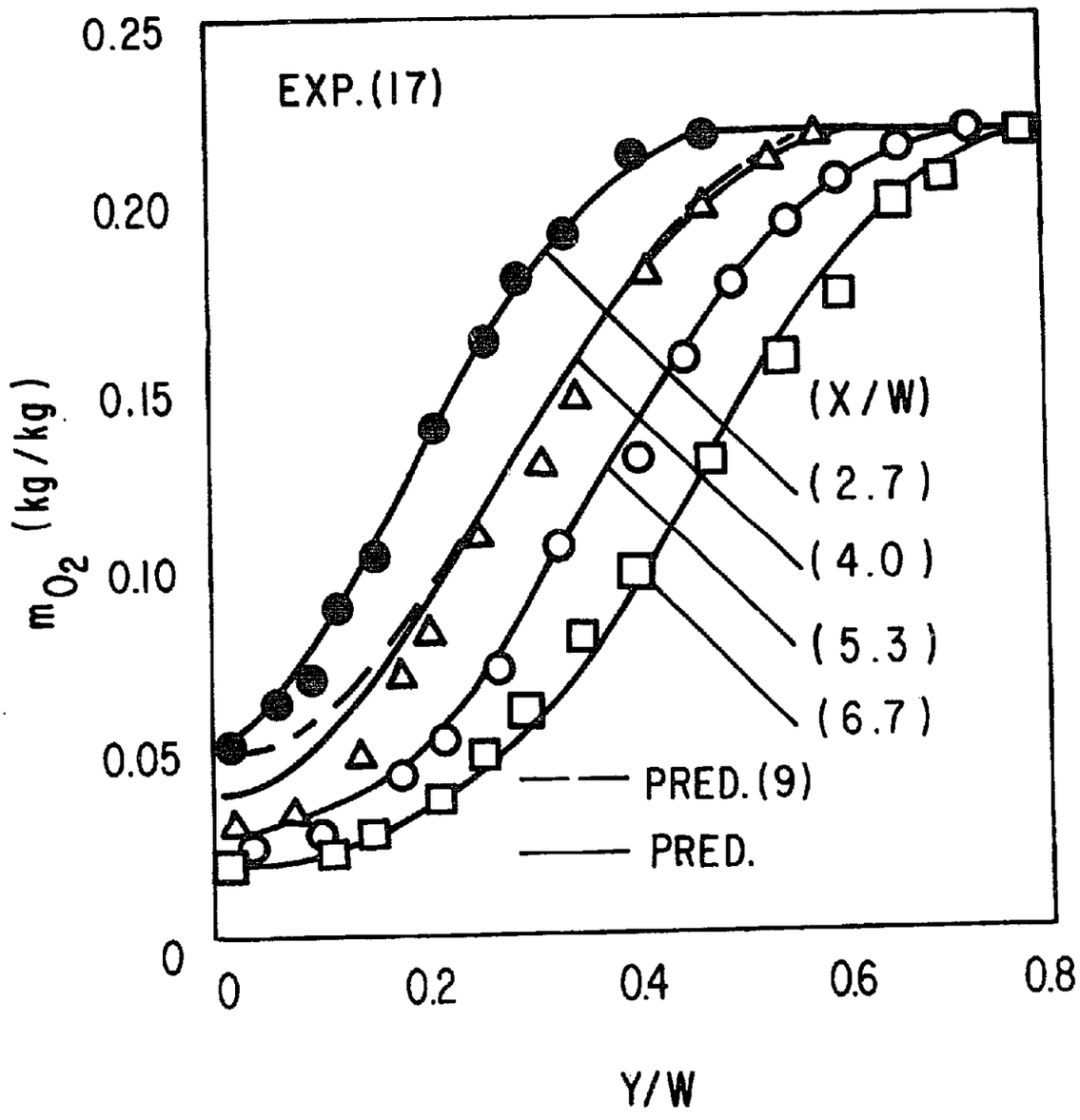

Fig. 8. Experimental and predicted local time mean values of oxygen concentration for the premixed 31 m/s flame.

Typically, ξ is defined to range between 0 and 1. Many different assumptions for the pdf of ξ have been used in the literature. Hawthorne (1949) proposed a Gaussian pdf and recently Becker (1974) has also used a Gaussian pdf. The regions outside 0 and 1 are physically implausible. As the sketch below shows, for small fluctuations, the portion of the pdf outside the 0 - 1 limits may not be too important, but for large fluctuations, there may be significant errors. Richardson (1953) used a Beta function pdf that correctly ranges between the 0 to 1 limits. However, measurements indicate that real pdf's are not this simple and have a lot more structure. Lockwood and Naguib (1975) have used a clipped Gaussian function, restricted to the region 0 to 1, with the unwanted tails of the distribution outside this region being lumped into delta functions at 0 and 1. The pdf is

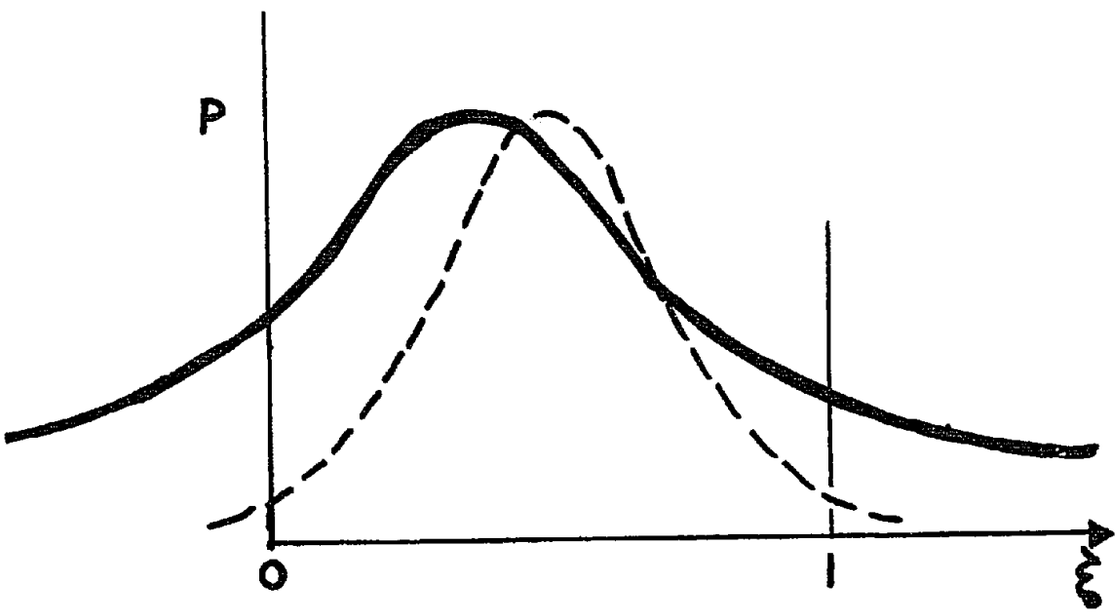

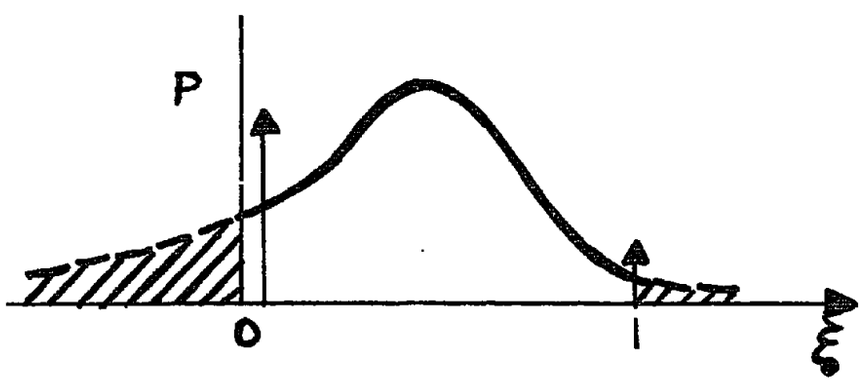

constructed using the calculated values for $\bar{\xi}$ and $\overline{\xi'^2}$ from the corresponding transport equations. The model leads to good results for axisymmetric turbulent jet diffusion flames as is illustrated by a few representative figures shown below (see Figures 9 and 10).

(From Lockwood and Naguib (1975))

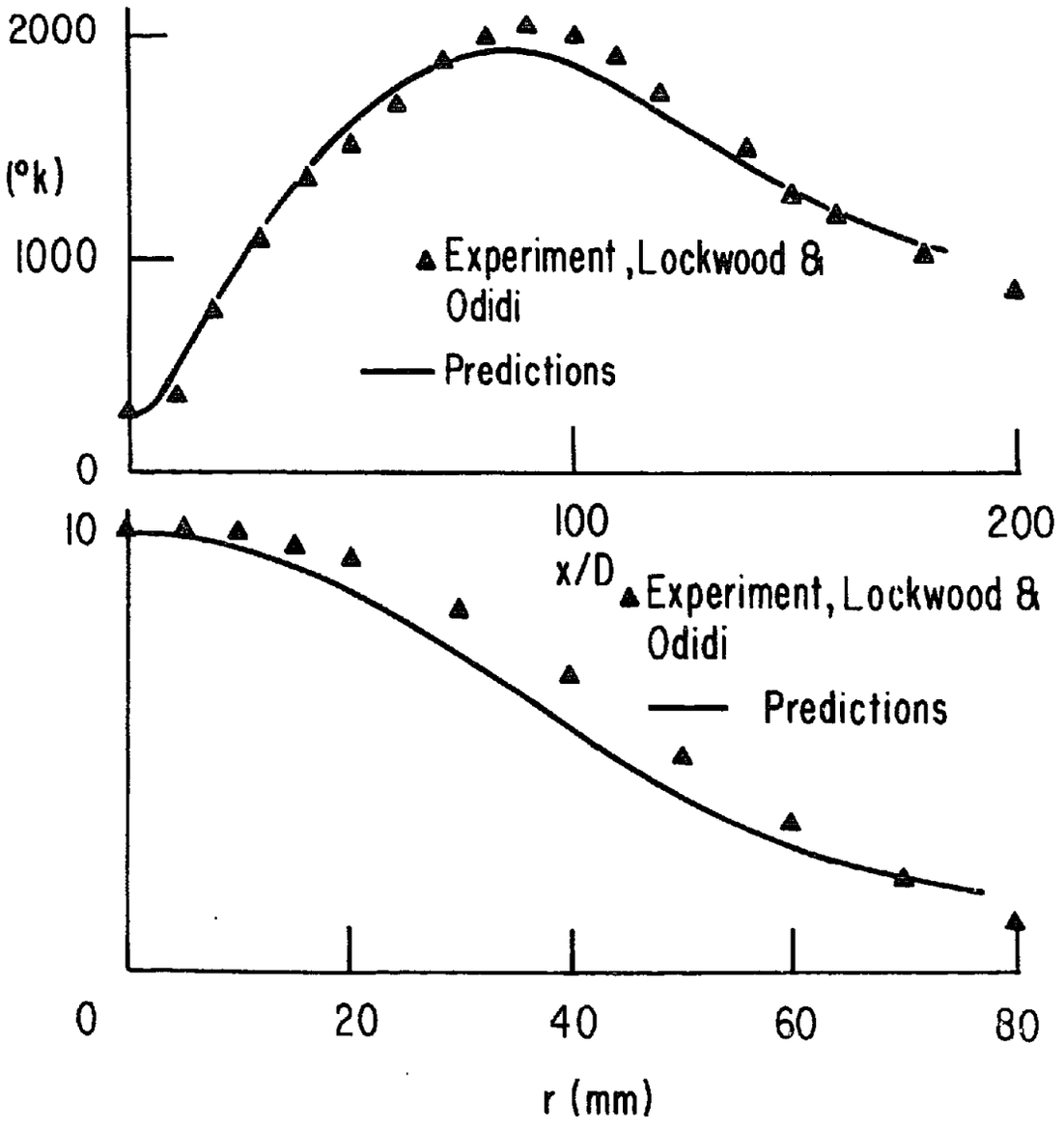

Fig. 9. Free jet diffusion flame: axial distribution and radial profile of temperature for town-gas fuel, Re = 2.4×10^4.

(From Lockwood and Naguib (1975))

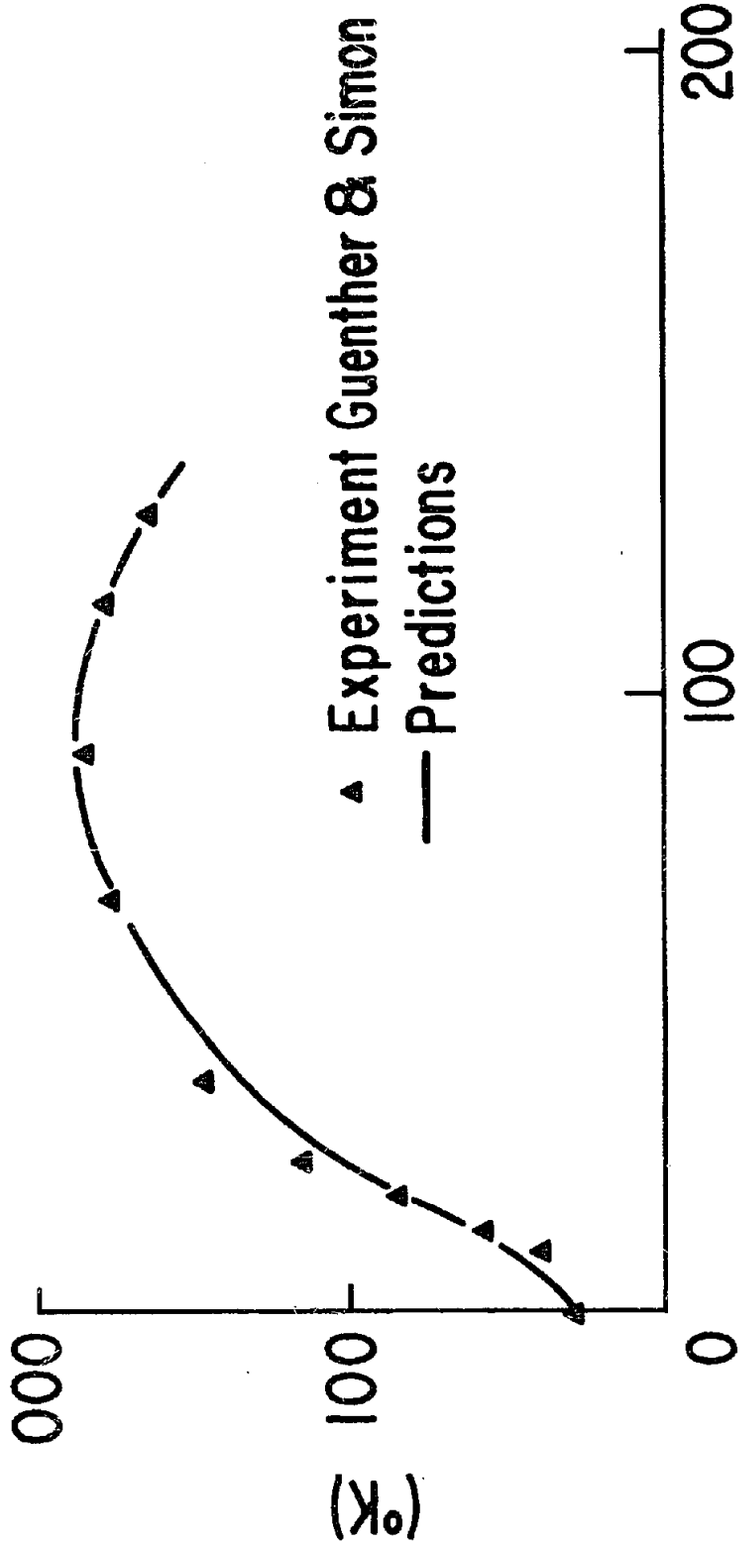

Fig. 10. Free jet diffusion flame: axial distribution of temperature for town-gas fuel, Re = 43,000.

Hutchinson *et al.* (1977) have used the same pdf model for predicting NO formation in furnaces. A one-step gas phase reaction is used for the main energy release processes along with the one-dimensional pdf model. Subsequently, NO formation is calculated using the Zeldovich mechanism. The predictions for the temperature profile are quite reasonable. The paper is of interest for it shows the effect of carrying out the calculations with and without the inclusion of transport equations for $\rho'u'$ and $\rho'v'$. The results are shown below. These equations are normally not solved in a two- or three-equation turbulence modeling approach. A complete second-order closure approach of the kind being developed at A.R.A.P. does include the transport equations for the various density correlations. The significant effects on the results demonstrated by the calculations of Hutchinson indicates the inadequacies of simpler approaches and a great deal of work remains to be done to increase our understanding of the dynamics of turbulent reacting flows, before realistic simplifications can be made (see Figure 11).

The previous pdf model with the clipped Gaussian does not appear to lend the proper emphasis on the intermittency features of the flow. The strengths of the delta functions at $\xi = 0$ and 1 are simply whatever is left over. Bray and Moss (1974) have developed an alternate, and perhaps better, pdf model. The model consists of two delta functions and an assumed function over the range $\xi = 0$ and 1. η is the

$$P(\xi) = \alpha\,\delta(\xi) + \beta\,\delta(\xi - 1) + \left\{\eta(\xi) - \eta(\xi - 1)\right\}\gamma\, f(\xi)$$

Heavyside function and $f(\xi)$ is a known assumed function. The strengths of the two delta functions α and β and the weighting factor γ is calculated from known values of ξ and ξ'^2.

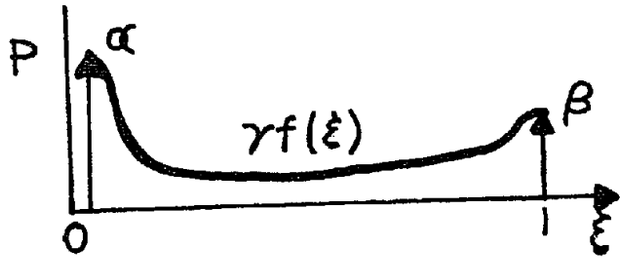

The model was originally developed for problems of one-step reactions, but has since been extended to problems involving sequential chemistry with the construction of two-dimensional pdf's. The procedure has been used by Borghi *et al.* (1977) for a problem of hydrocarbon combustion followed by oxidation of CO, and by Bray and Moss (1977) to study NO formation. With two sequential reactions, the proposed pdf is shown below.

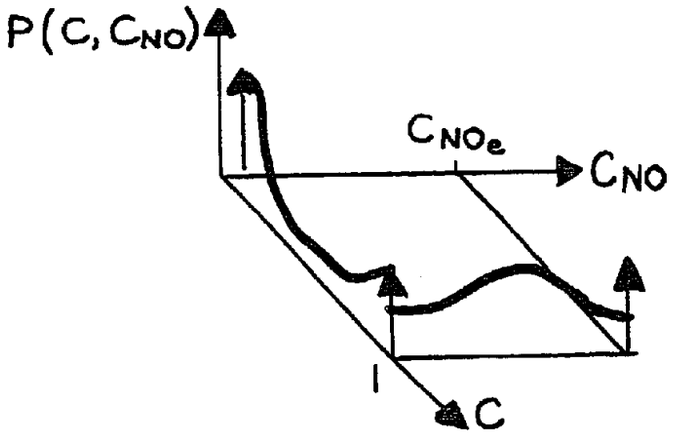

The model has not yet been verified by comparison with data.

Multi-Dimensional PDF Models

A more general approach to the modeling of turbulent reacting flows requires the development of multi-dimensional pdf's, so as to avoid assumptions regarding relationships between the individual scalars. The only model proposed in this category is the A.R.A.P. "typical eddy" model (Donaldson, 1975, Donaldson and Varma, 1976). The concept of the "typical eddy" model is to assume the shape of the pdf and to then calculate the shape parameters by ensuring that the first- and second-order moments of the model pdf are in agreement with the moments obtained from the transport equations. The use of a complete second-order closure approach provides information on a large number of means and second-order correlations that are used to construct a joint pdf of the scalars. The "typical eddy" model currently being developed consists of a number of delta functions of variable strengths and positions in the scalar phase space. It has been demonstrated (Varma *et al.* 1978a) that,

- A physically realistic pdf composed of delta functions can always be constructed at all points in the statistically valid moment space.
- The model provides adequate accuracy in the calculation of higher-order moments for closure of the transport equations.

The delta function "typical eddy" model has been extensively tested for a two species variable density mixing flow. Starting from basic statistical theorems such as the Cauchy-Schwarz inequality, we have derived statistical constraints on the means and second-order correlations that will be calculated from transport equations. The constraints are useful in a number of ways. They enable us to check the sensitivity of the results to the pdf models. Another important use is in the question of the realizability of a second-order closure procedure. A large number of modeled

(From Hutchinson *et al.* (1977))

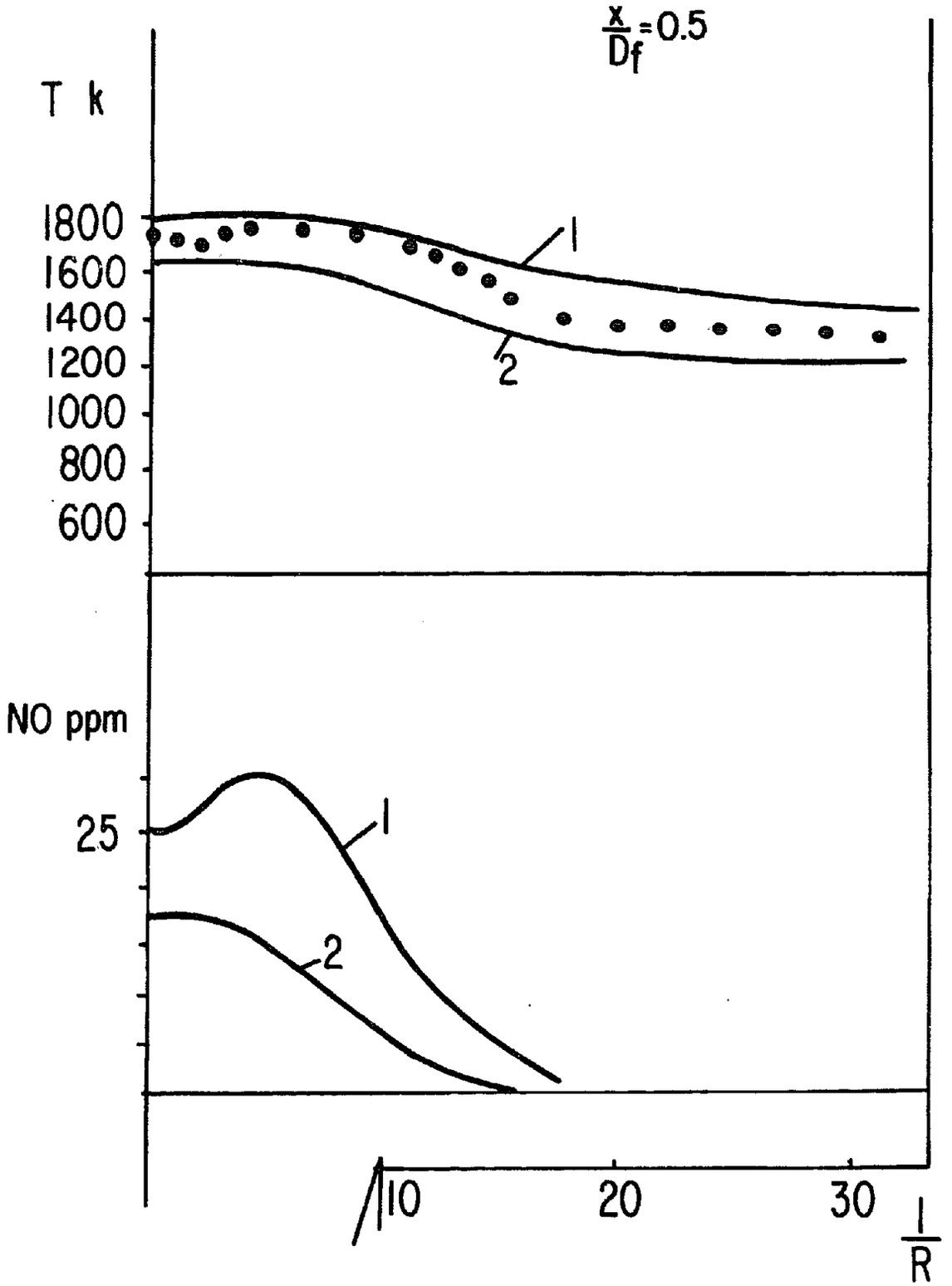

Fig. 11. Temperature and NO profiles at $x/D_f = 0.5$ for S = 0.5: 1. Calculations including conservation equations for $\overline{\rho' u'}$ and $\overline{\rho' v'}$. 2. Calculations excluding conservation equations for $\overline{\rho' u'}$ and $\overline{\rho' v'}$.

partial differential equations are solved in this procedure and it is necessary to ensure that the calculated values of the correlations are statistically correct, that is, they must lie inside the derived bounds. If there is a violation of the statistics, there must be an error in the modeling. The derived constraints are tabulated in Figure 12.

$$0 \le \bar{\alpha} \le 1$$

$$\bar{\alpha}^2 \le \overline{\alpha^2} < \bar{\alpha}$$

$$\frac{\overline{\alpha^2}^2}{\bar{\alpha}} \le \overline{\alpha^3} \le \overline{\alpha^2} - \frac{(\bar{\alpha} - \overline{\alpha^2})^2}{1-\bar{\alpha}}$$

$$\bar{\alpha}^3 \le \overline{\alpha^3} \le \bar{\alpha}$$

$$\frac{\overline{\alpha^2}}{\bar{\alpha} - \Delta\,\overline{\alpha^2}} \le \overline{\rho_* \alpha} \le \frac{1}{1-\Delta} \frac{\bar{\alpha}(1-\bar{\alpha}) - \Delta(\bar{\alpha} - \overline{\alpha^2})}{(1-\bar{\alpha}) - \Delta(\bar{\alpha} - \overline{\alpha^2})}$$

Fig. 12. Statistical Constraints on Correlations

The constraints on $\overline{\alpha^3}$ shown in the box on the left are for specified values of α and $\overline{\alpha^2}$; the box on the right shows the constraints on $\overline{\alpha^3}$ if only $\bar{\alpha}$ is specified. These bounds are compared in Figure 13. The significant narrowing of the bounds on $\overline{\alpha^3}$ when α and $\overline{\alpha^2}$ are specified is very promising as far as pdf modeling is concerned. $\overline{\alpha^3}$ can only have a very limited range of values, and results from all statistically valid pdf models will lie within these bounds.

The delta function pdf is simply a model for the actual continuous pdf. It is proposed that by suitable placement of delta functions of different strengths, one can obtain a reasonable estimate of the higher-order moments needed for closure of the equations. The delta function models for two and

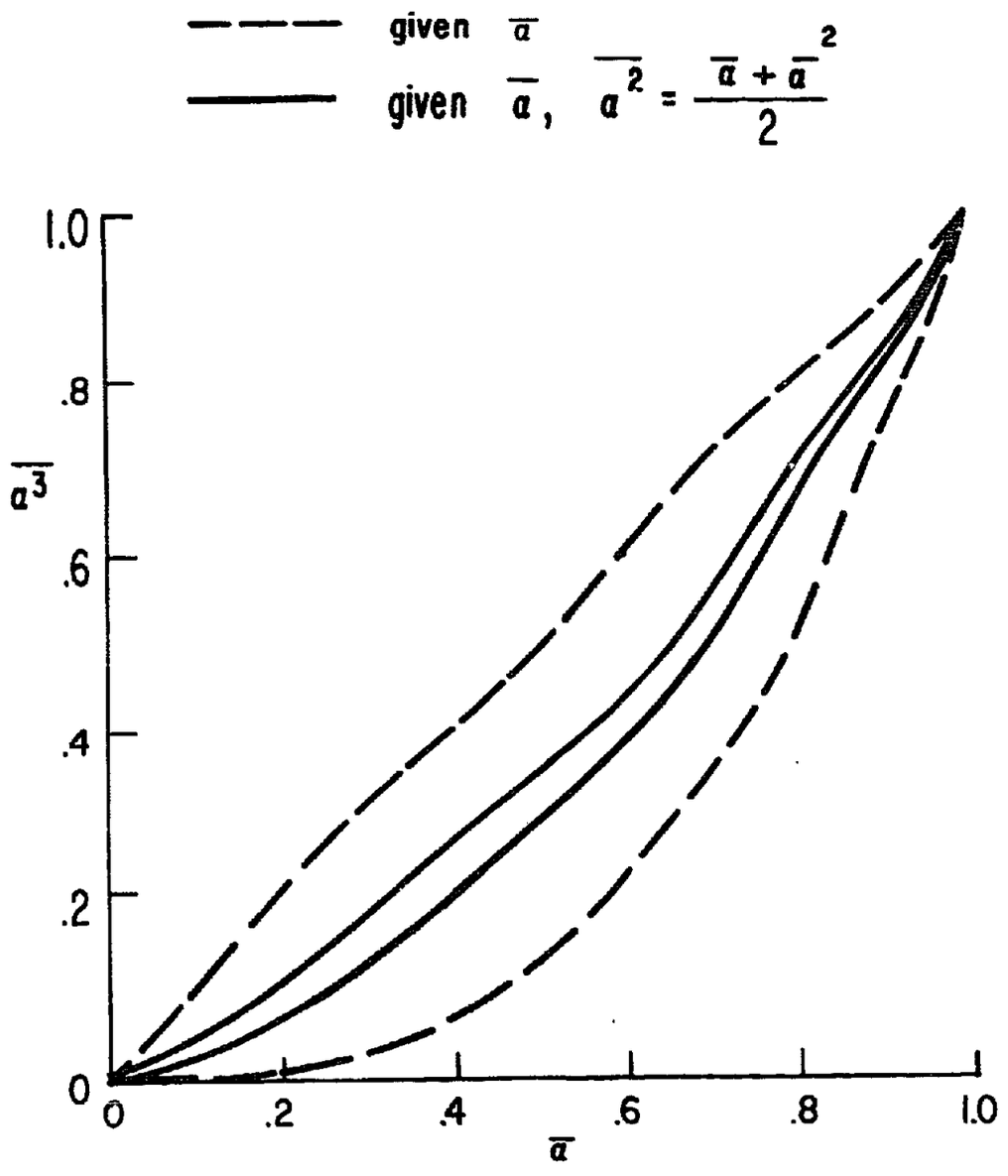

Fig. 13. Comparison of the statistical bounds on $\overline{\alpha^3}$ for specified lower-order moments.

three species are shown in Figure 14. The available first- and second-order moments that will be used to construct the model are also listed. The box diagrams should be interpreted as follows to relate them to the more usual probability diagrams. The joint pdf $P(\alpha, \beta)$ for two species consists of 4 delta functions of strengths ε_1, ε_2, ε_3, and ε_4 located at α, β positions of (1,0), (0,1), (α_3, β_3) and (k, 1-k). Similar considerations hold for the 3 species model that consists of 7 delta functions. Further details of the model construction can be seen in Varma *et al.* (1978a).

The delta function "typical eddy" model has been directly compared to pdf measurements in a variable density shear layer flow (Konrad, 1976). The

Two Species Model

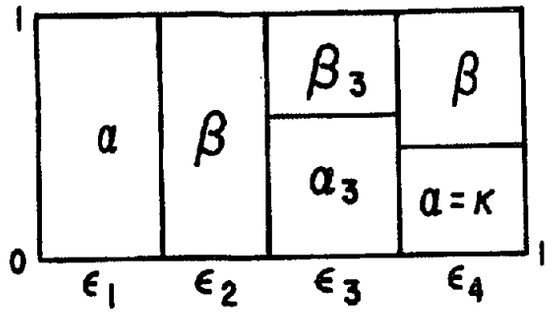

$1,\ \bar{\alpha},\ \overline{\alpha'\alpha'},\ \overline{\alpha'\rho'},\ \overline{\rho'\rho'}$

Three Species Model

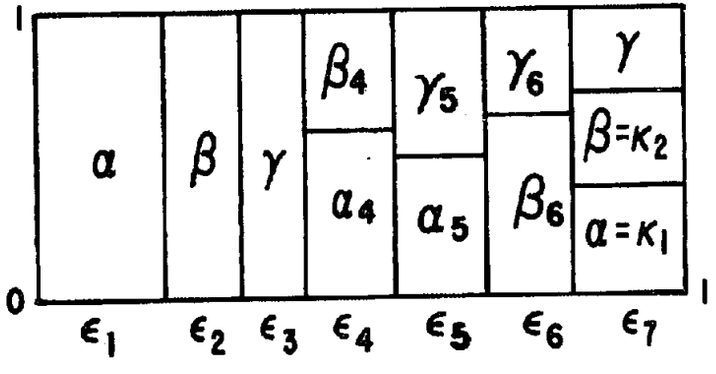

$1,\ \bar{\alpha},\ \bar{\beta},\ \overline{\alpha'\alpha'},\ \overline{\alpha'\beta'},\ \overline{\beta'\beta'},\ \overline{\alpha'\rho'},\ \overline{\beta'\rho'},\ \overline{\rho'\rho'}$

Fig. 14. Delta Function Typical Eddy Models

results are shown in Figure 15. The pdf measurements at various positions across a He-N_2 shear layer with a velocity ratio of 0.38 and a density ratio of 7 are used to determine the values of four lower-order moments -- α, $\overline{\alpha^2}$, $\overline{\alpha\rho}$, and $\overline{\rho^2}$ -- that are needed to construct the two-species "typical eddy" model. The measured pdf is also used to calculate the experimental value for a third-order correlation $\overline{\alpha\beta^2}$. The same third-order moment is also calculated from the model and the results compared to the measurements. A simpler version of the "typical eddy" model that neglects the density fluctuations is also constructed and the results for $\overline{\alpha\beta^2}$ calculated. The dotted lines show the upper and lower bounds on the third moment when only two lower-order moments are used for the model construction. In this case $\overline{\alpha\beta^2}$ model has a large range of possible values and some pdf models within the statistical range can lead to significant errors compared to the experiments. However, when 4 lower order moments are specified, the model values of $\overline{\alpha\beta^2}$ are very tightly constrained as shown by the solid lines. In fact, now any statistically valid model is able to calculate $\overline{\alpha\beta^2}$ (and other third-order moments) to better than 10% accuracy. This is significantly better accuracy than the expected error-bounds on experimental measurements of third-order moments. Therefore, any statistically valid pdf model that matches the values for the lower-order moments will provide adequate accuracy for closure of the transport equations.

A qualitative comparison of the delta function "typical eddy" pdf and the measured pdf is shown in Figure 16. The experimental pdf (thin lines) is reproduced from the report by Konrad (1976). The delta function representation (thick lines) of the pdf seems to be capable of capturing the important features of the experimental pdf structure.

A delta function pdf model for reacting flows is being developed along the same lines as the model for mixing flows of variable density described above.

It must be pointed out that the concept of the "typical eddy" model is not restricted to delta functions. The same ideas can be used to construct pdf models composed of delta functions and a clipped Gaussian. Such a model for two species flow is shown in Figure 17. Using the 5 available second-order moments in a complete second-order closure analysis, we can determine the strengths of the delta functions and the 3 parameters for the Gaussian curve. However, the delta function pdf model is simpler to construct and as it appears to provide adequate accuracy for closure, we recommend its usage.

Solution of PDF Equations

In this approach one avoids some of the assumptions in the pdf modeling approach by deriving a transport equation for the pdf, which governs the development of the pdf from some initial structure. The transport equation has to be closed by suitable modeling of terms involving interactions between the pdf and other flow variables and this is the main difficulty that a number of investigators are trying to solve. We cannot go into any details of this approach here and the reader is guided to the following references as a good starting point. Dopazo and O'Brien (1974), Pope (1976), and Bonniot and Borghi (1977).

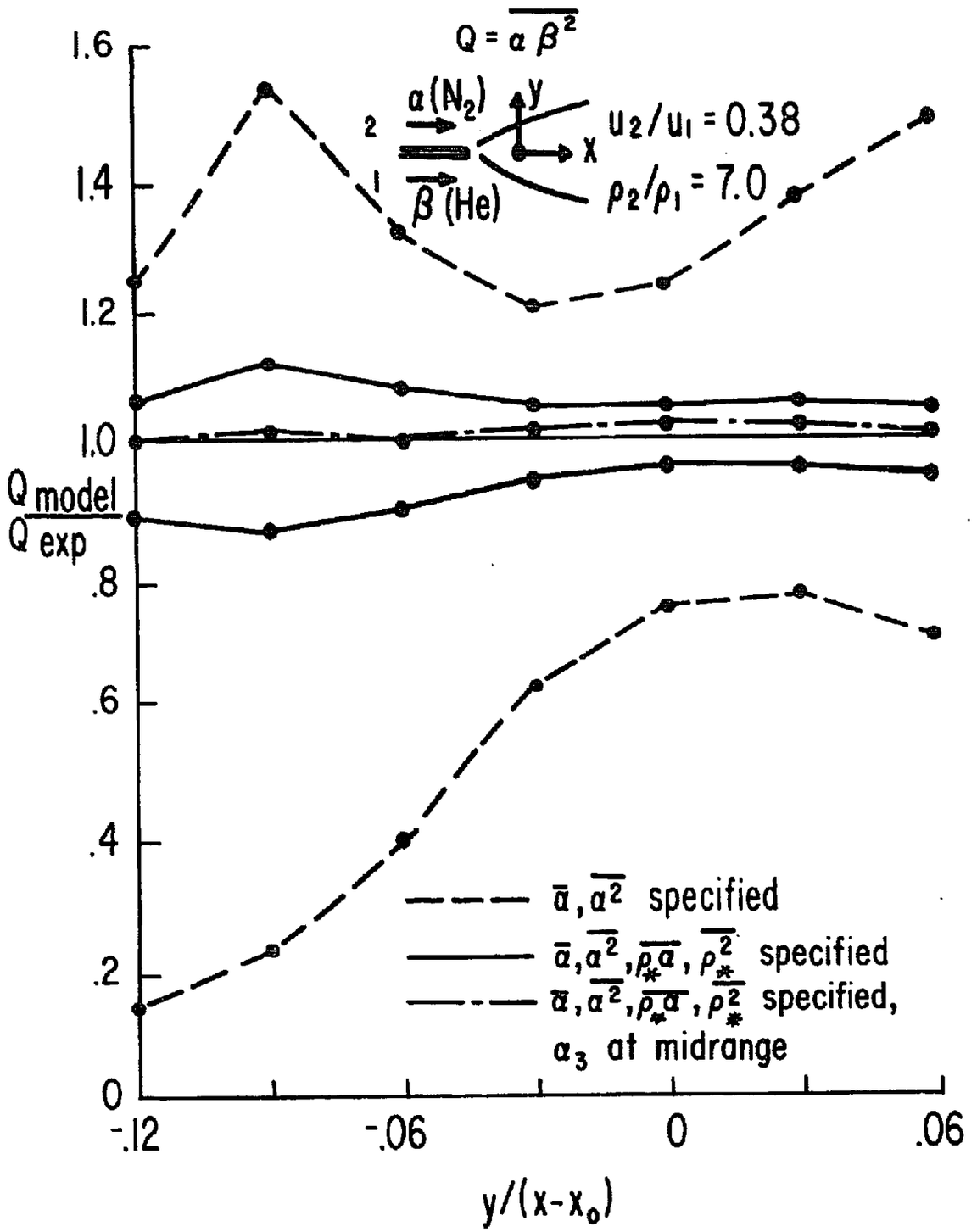

Fig. 15. Comparison of model predictions and experiments for the third moment $\overline{\alpha\beta^2}$. He-N_2 shear layer.

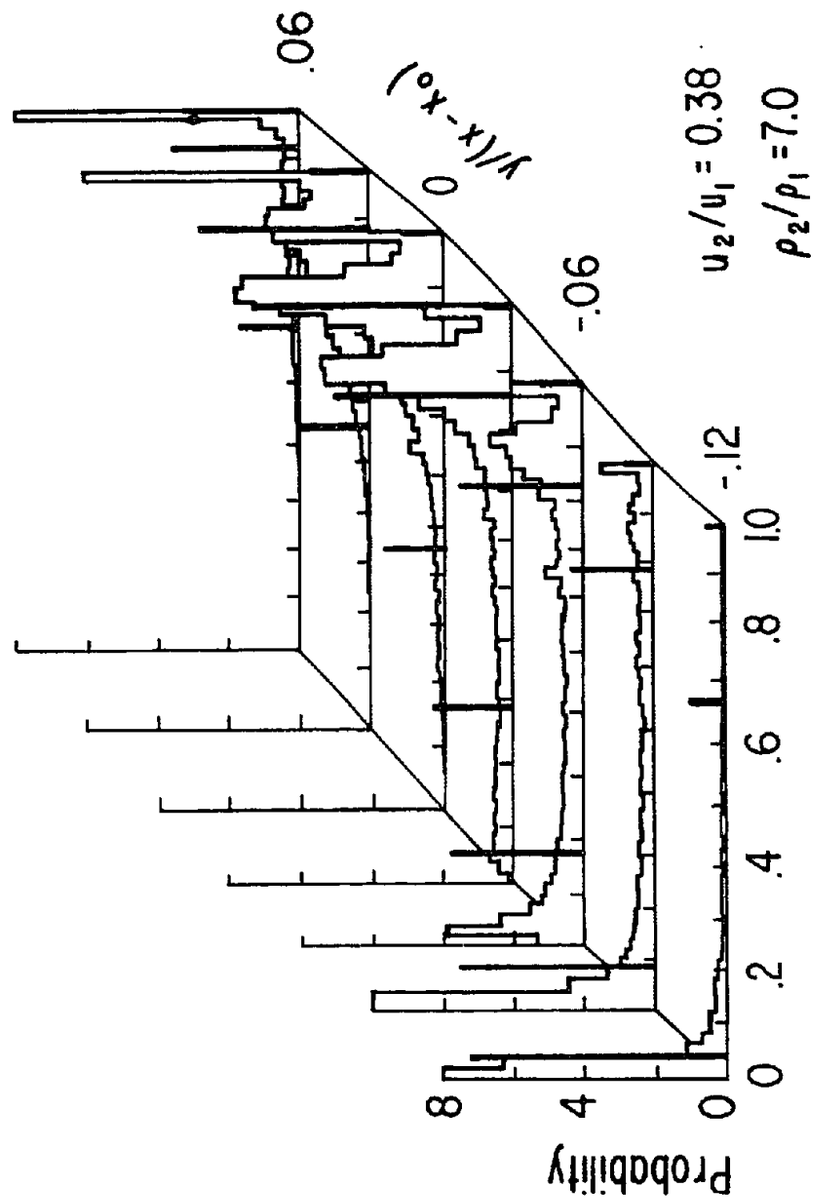

Fig. 16. Comparison of delta function pdf with measured pdf. Minimum entropy of mixing model. He-N_2 shear layer.

Two Species Flow

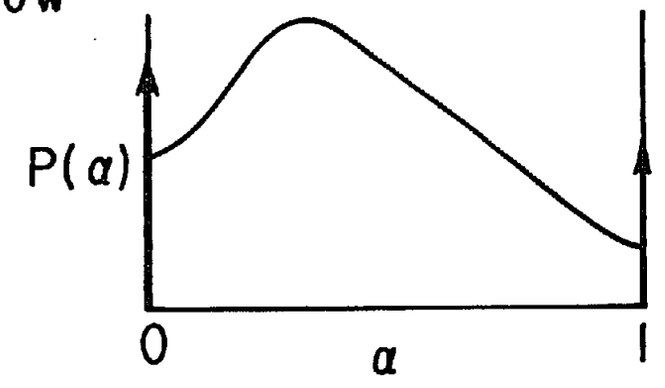

$$P(\alpha) = W_1 \delta(\alpha) + W_2 \delta(\alpha - 1) + N_{exp} - \frac{(\alpha - \alpha_0)^2}{\sigma^2}$$

model parameters	5	W_1	W_2	N	α_0	σ
available moments	5	1	$\overline{\alpha}$	$\overline{\alpha^2}$	$\overline{\rho\alpha}$	$\overline{\rho^2}$

Fig. 17. Typical Eddy Model with Delta Function and Clipped Gaussian.

Stirred Reactor Approaches

These approaches actually combine Eulerian and Langrangian features. Rhodes *et al.* (1974) have studied a diffusion flame problem. The turbulent flowfield is first solved for using a parabolic computer program and a one-equation turbulence model. An empirical relationship between species composition fluctuations and velocity fluctuations is then assumed and all the fluid in the mixing layer is divided into "classes," each representing an elemental composition. A stirred reactor analysis with complex chemistry is carried out for each class. A simple triangular shape pdf model is assumed for the species. Swithenbank *et al.* (1978) carry out an elliptic finite difference prediction of the three-dimensional flow pattern in a gas turbine combustor and combine it with a network of interconnected plug flow reactors and stirred reactors to handle the multi-step chemical kinetics. The crucial assumption is in the breakup of the flow field into the network of reactors. For further details, the reader is referred to the quoted references.

Superequilibrium and Quasiequilibrium Approximations

Finally, I would like to discuss some approximate procedures for estimating the magnitude of various second-order correlations of interest in determining turbulence-chemistry interaction effects. The approximations reduce the number of partial differential equations that need to be solved and are suitable for use with other simpler computer programs for calculations of turbulent reacting flows. The first of these procedures is the superequilibrium approximation.

In this procedure the convection and diffusion terms in the transport equation for the correlation are neglected and the equation reduces to a balance of the production and dissipation terms. Typically, for many turbulent flows, these are the larger terms in the equation. The use of this procedure for a set of transport equations leads to a linear coupled set of algebraic equations relating the various correlations and these can be solved (Donaldson, 1973) to obtain algebraic expressions relating various turbulence quantities. Higher-order correlations are neglected in this approach.

Calculations have been carried out (Varma *et al.*, 1978b) for a turbulent hydrogen-air jet diffusion flame using the superequilibrium approach. A procedure has been developed to handle multi-step chemistry within the framework of a three species turbulent reacting flow program. The results of the calculations have been compared to the experimental measurements of Kent and Bilger (1972) and are shown in Figures 18 and 19. Figure 10 shows the results for the mean species H_2, O_2, and H_2O with the use of both the "laminar chemistry" (neglecting turbulence-chemistry interactions) and the "turbulent chemistry" approach. There is much better agreement with the experimental data with the inclusion of the scalar species and temperature fluctuations in the reaction source terms. With the use of the "laminar chemistry" approximation, the flame thickness (region of overlap of the reactants H_2 and O_2) is quite small and is the thickness determined by the chemical kinetic rates. The turbulence-chemistry interaction effects have to be included to predict the thick turbulent flame region. The results demonstrate how important features of turbulent reacting flows will not be

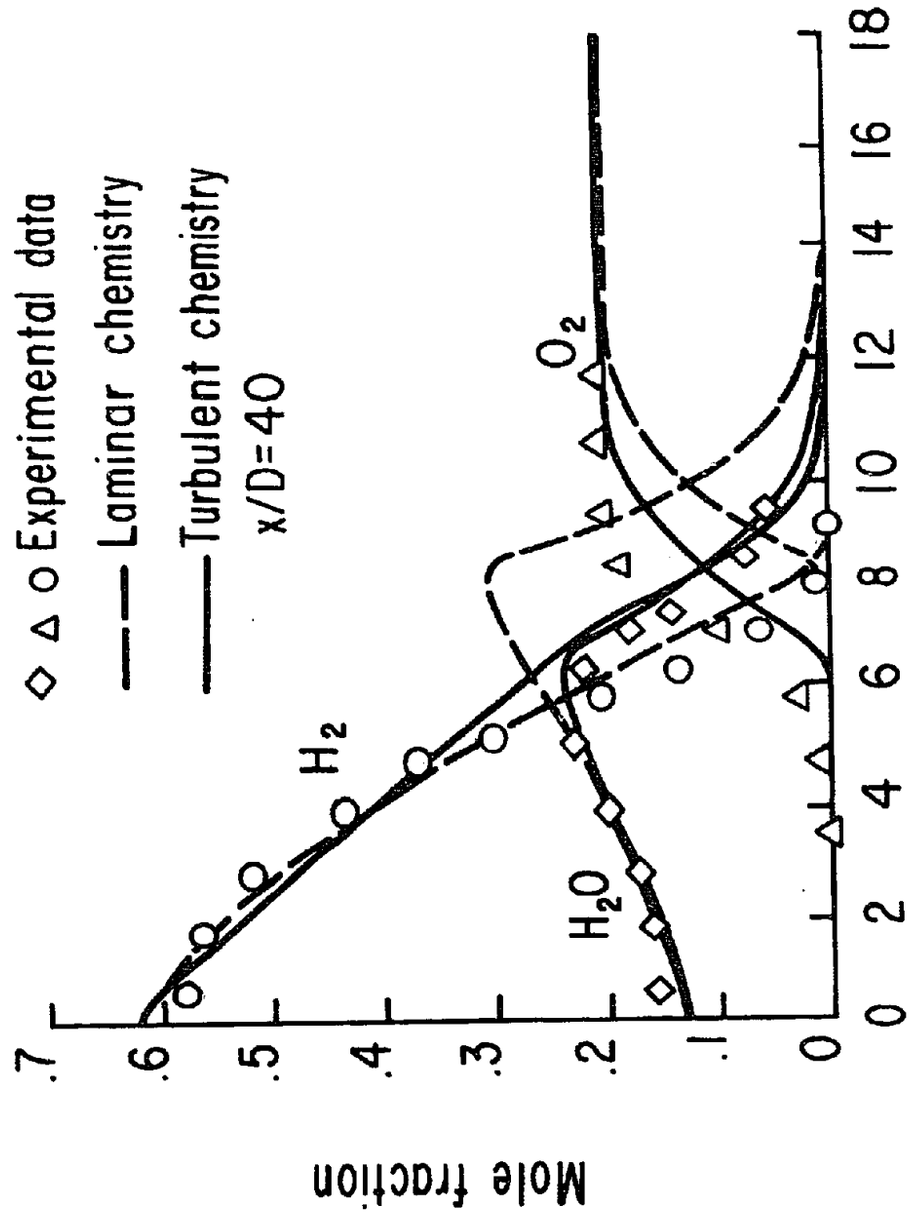

Fig. 18. Mean species radial profile in hydrogen-air diffusion flame. Secondary model. Superequilibrium procedure.

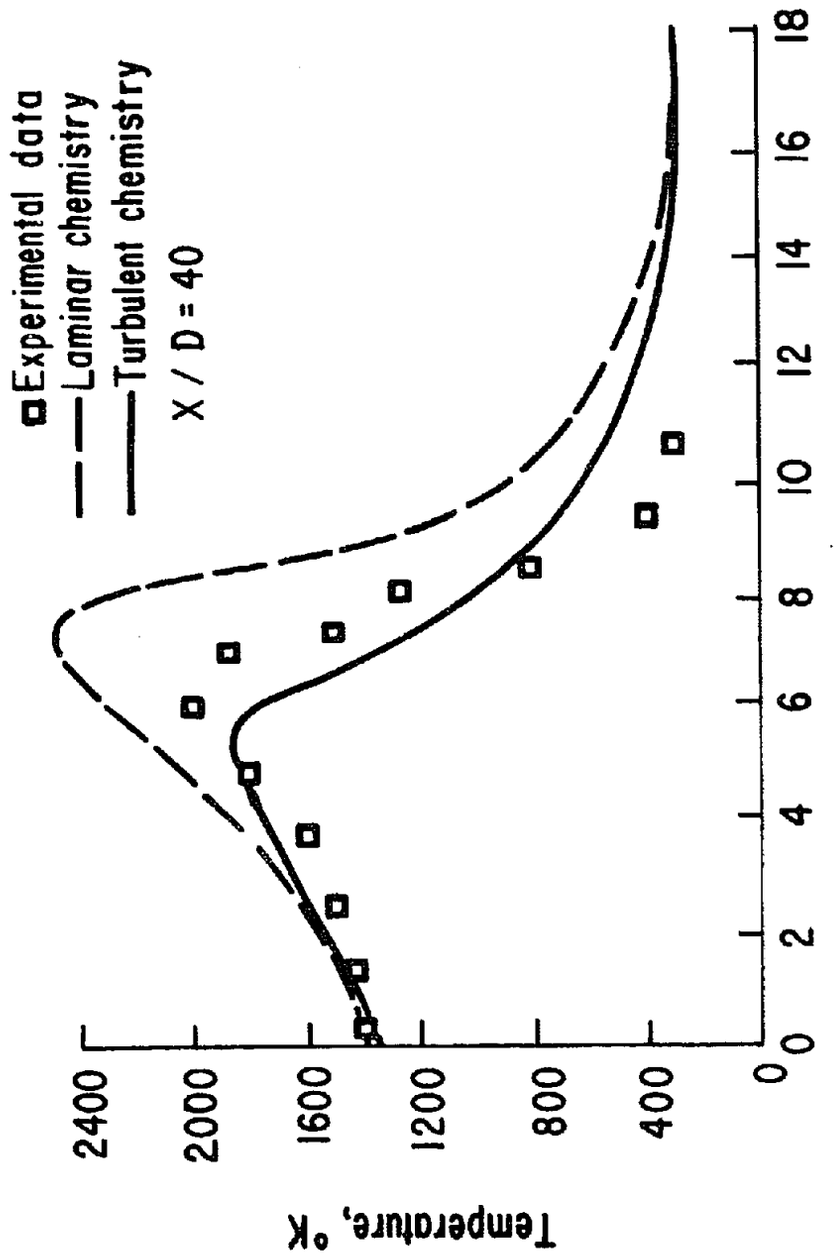

Fig. 19. Mean temperature radial profile in hydrogen-air diffusion flame. Secondary model. Superequilibrium procedure.

correctly predicted if turbulence-chemistry interactions are neglected. The results for the temperature profile shown in Figure 11 also indicate better results with the turbulent chemistry approach. These calculations will soon be repeated with the pdf model and complete second-order closure instead of the superequilibrium procedure.

A quasiequilibrium procedure has also been formulated but has not yet been tested. This will be a step better than the superequilibrium approach. It is proposed to solve a few typical transport equations for the second-order correlations, for example, $\overline{v'\alpha'}$, $\overline{h'\alpha'}$, $\overline{\alpha'\beta'}$, and then to compare the values obtained from the transport equation to the superequilibrium values and determine appropriate correction factors for various groups of correlations.

$$R_v = \frac{\overline{v'\alpha'} \text{ equation}}{\overline{v'\alpha'} \text{ superequilibrium}} \qquad R_h = \frac{\overline{h'\alpha'} \text{ equation}}{\overline{h'\alpha'} \text{ superequilibrium}}$$

The other correlations will then be obtained by calculating the superequilibrium value and applying the correction factor for that particular group, before using the correlation in the chemical source terms or in closure of the mean equations.

A complete multiequation second-order closure computer program of the kind being developed at A.R.A.P. can be used to construct and test simpler approximations of the above types, which can then be used in other simpler codes which are faster and oriented towards engineering design calculations.

CONCLUSIONS

Significant progress has been made in the last few years in the understanding and modeling of turbulent reacting flows. A number of different approaches are currently being pursued by many investigators. The central problem for reacting flows is the modeling of the joint scalar probability density function and the various modeling efforts in combination with detailed experimental measurements should lead to rapid development of computational procedures for calculations of these flows.

REFERENCES

1. Becker, H. A. *Effects of Concentration Fluctuations in Turbulent Flames*. Queen's University, Kingston, Ontario, Chem. Eng. Dept., April, 1974.

2. Bonniot, C. and Borghi, R. *On the Joint Probability Density Function of Reactive Species in Turbulent Combustion*. Presented at the Sixth International Colloquium on Gasdynamics of Explosions and Reactive Systems, Stockholm, Sweden, August, 22-26, 1977.

3. Borghi, *et al. Theoretical Prediction of a High Velocity, Premixed, Turbulent Flame*. Presented at the "Levich Birthday Conference," International Conference on Physiochemical Hydrodynamics, Oxford, England, July 11-13, 1977.

4. Bray, K. N. C. and Moss, J. B. *A Unified Statistical Model of the Turbulent Premixed Flame*. University of Southampton Report AASU No. 335. Accepted for publication in Acta Astronautica.

5. Bray, K. N. C. and Moss, J. B. *A Closure Model for the Turbulent Premixed Flame with Sequential Chemistry*. Combustion and Flame, 30, (1977) 125-131.

6. Donaldson, C. duP. *Atmospheric Turbulence and the Dispersal of Atmospheric Pollutants*. AMS Workshop on Micrometeorology (D. A. Haugen, ed.), Science Press, Boston, pp. 313-390 (1973).

7. Donaldson, C. duP. *On the Modeling of the Scalar Correlations Necessary to Construct a Second-Order Closure Description of Turbulent Reacting Flows*. Turbulent Mixing in Nonreactive and Reactive Flows (S. N. B. Murthy, ed.), Plenum Press, New York, pp. 131-162 (1975).

8. Donaldson, C. duP. and Varma, A. K. *Remarks on the Construction of a Second-Order Closure Description of Turbulent Reacting Flows*. Combustion Science and Technology, 13, pp. 55-78 (1976).

9. Dopazo, C. and O'Brien, E. E. *An Approach to the Autoignition of a Turbulent Mixture*. Acta Astronautica, 1, pp. 1239-1266 (1974).

10. Fishburne, E. S. and Varma, A. K. *Investigations of Chemical Reactions in a Turbulent Media*. Presented at the Sixth International Colloquim on Gasdynamics of Explosions and Reactive Systems, Stockholm, Sweden, August, 22-26, 1977. Accepted for publication in Acta Astronautica.

11. Hawthorne, W. R., Weddell, D. S., and Hottel, H. C. *Mixing and Combustion in Turbulent Gas Jets*. Third Symposium on Combustion and Flame and Explosion Phenomena, Williams and Wilkins Co., Baltimore, p. 255, 1949.

12. Hutchinson, P., Khalil, E. E., and Whitelaw, J. H. *Measurement and Calculation of Furnace-Flow Properties.* Turbulent Combustion (L. A. Kennedy, ed.), Vol. 58, American Institute of Aeronautics and Astronautics, pp. 211-228 (1978).

13. Kent, J. H. and Bilger, R. W. *Turbulent Diffusion Flames.* Charles Kolling Research Laboratory, University of Sydney, TN-F-37, 1972.

14. Khalil, E. E., Spalding, D. B., and Whitelaw, J. H. *The Calculation of Local Flow Properteis in Two-Dimensional Furnaces.* Int. J. Heat Mass Transfer, Vol. 18, pp. 775-591 (1975).

15. Konrad, J. H. *An Experimental Investigation of Mixing in Two-Dimensional Turbulent Shear Flows with Applications to Diffusion-Limited Chemical Reactions.* Project SQUID Technical Report CIT-8-PU, (1976).

16. Launder, B. E. and Spalding, D. B. *Mathematical Models of Turbulence.* Academic Press, London and New York (1972).

17. Lewellen, W. S. *Use of Invariant Modeling.* Handbook of Turbulence, Vol. 1, (W. Frost and T. Moulden, eds.) Plenum Publishing Corp., pp. 237-280 (1977).

18. Lockwood, F. C. and Naguib, A. S. *The Prediction of the Fluctuations in the Properties of Free, Round-Jet, Turbulent, Diffusion Flames.* Combustion and Flame, 24, pp. 109-124 (1975).

19. Magnussen, B. F. and Hjertager, B. H. *On Mathematical Modeling of Turbulent Combustion with Special Emphasis on Soot Formation and Combustion.* Sixteenth Symposium (International) on Combustion, The Combustion Institute, Pittsburgh, PA, pp. 719-729 (1977).

20. Patterson, G. K. *Modeling Complex Chemical Reactions in Flows with Turbulent, Diffusive Mixing.* Presented at the 70th Annual Meeting of the American Institute of Chemical Engineers, New York, November, 1977.

21. Patterson, G. K. *Methods for Computing Yield for Turbulently Mixed Complex Reactions.* Presented at the 71st Annual Meeting of the American Institute of Chemical Engineers, Miami, FL, November, 1978.

22. Pope, S. B. *The Probability Approach to the Modelling of Turbulent Reacting Flows.* Combustion and Flame, 27, pp. 299-312 (1976).

23. Pratt, D. T. *Coalescence/Dispersion Modeling of High-Intensity Combustion.* Presented at the 71st Annual Meeting of the American Institute of Chemical Engineers, Miami, FL, November, 1978.

24. Rhodes, R. P., Harsha, P. T., and Peters, C. E. *Turbulent Kinetic Energy Analyses of Hydrogen-Air Diffusion Flames.* Acta Astronautica, Vol. 1, pp. 443-470 (1974).

25. Richardson, J. M., Howard Jr., H. C., and Smith Jr., R. W. *The Relation Between Sampling-Tube Measurements and Concentration Fluctuations in a Turbulent Gas Jet.* Fourth Symposium (International) on Combustion, Williams and Wilkins, p. 814 (1953).

26. Spalding, D. B. *Concentration Fluctuations in a Round Turbulent Free Jet.* J. Chem. Eng. Sci. 26, 95 (1971a).

27. Spalding, D. B. *Mixing and Chemical Reaction in Steady Confined Turbulent Flames.* Thirteenth Symposium (International) on Combustion, The Combustion Institute, Pittsburgh, PA, pp. 649-657 (1971b).

28. Spalding, D. B. *A General Theory of Turbulent Combustion.* J. Energy, January-February, pp. 16-23 (1978).

29. Swithenbank, *et al.* *Three-Dimensional 2-Phase Mathematical Modelling of Gas Turbine Combustors.* Presented at Project SQUID Workshop on Gas Turbine Combustor Design Problems, Purdue University, West Lafayette, IN, May 31-June 1, 1978.

30. Varma, *et al.* *Modeling of Scalar Probability Density Functions in Turbulent Flows.* Project SQUID Technical Report ARAP-1-PU, Purdue University, West Lafayette, IN, 1978a.

31. Varma, *et al.* *Aspects of Turbulent Combustion.* Progress in Astronautics and Aeronautics, Volume 58 - Turbulent Combustion, (L. A. Kennedy, ed.), American Institute of Aeronautics and Astronautics, New York, NY, pp. 117-140 (1978b).

Comments and Replies on

MODELING OF CHEMICAL REACTIONS IN TURBULENT FLOW - A REVIEW

by Ashok K. Varma

R. Edelman: Do you have any experimental comparisons?

A. Varma: Yes, we have carried out comparisons with the Kent-Bilger data on hydrogen-air turbulent diffusion flames using a model in which third-order scalar correlations are neglected. (Figures 10 and 11 of the text). Some characteristic features of turbulent flames such as a thick reaction zone can only be predicted by including these interactions.

R. Edelman: In general, the interaction needs to be taken into account. However, I think it is worth pointing out that in many cases of practical interest ignoring the interaction terms has a very small effect on such things as overall heat release, which is a very important parameter in combustion problems. When it comes to things that are dependent on trace quantities such as NO_x emissions, soot formation, etc., then the story would be different. This has to be kept in perspective relative to the problems we wish to address, so that a practical approach can be selected.

A. Varma: I assume the calculations used an ad hoc model such as eddy breakup to reduce the reaction rate in the cases you mentioned.

R. Edelman: No. I was talking about the use of laminar kinetics along with a model for the turbulent transport.

A. Varma: Yes, I have seen some of these results. However, I have a great deal of difficulty understanding why this happens, for the interaction terms should clearly be included in turbulent reacting flows. The main energy release reactions are usually fast and there the interaction effects should be large. One should not be anywhere slose to the right result with laminar chemistry. I presume that other empiricisms and uncertainties in the total model mask the effects of the error in neglecting turbulence-chemistry interactions.

G. Patterson: How many model constants are required in the second-order closure approach?

A. Varma: That is a good question and I will try to explain the modeling approach used. The chemistry modeling, that is, the pdf model does not require any additional

empirical constants. All the constants were required for the modeling of the dynamics of the turbulence and are the same as for non-reacting flows. In non-reacting flows, all the transport equations have terms representing dissipation, diffusion and pressure correlations. For low speed flows, the program has five model constants, and a model turbulent macroscale, that have all been fixed by comparison with basic data on flat plate boundary layers, shear layers, jets and wake flows. Compressible flows will require the modeling of a few additional pressure correlations, but the model constants for these have not yet been evaluated. The approach is to hold these constants invariant after they have been fixed by comparison with basic test flows and then use them for predictive calculations of more complex flows. This has already been done with significant success for many non-reacting flow problems and further applications are now being investigated.

P. Ponzi: Can the pdf approach handle reactions of fractional order? The minute you take a "mean" of something to the half times something to some other odd power, you are sort of stuck, aren't you?

A. Varma: Actually, this is a major advantage of the pdf approach. There is no need to expand the reaction rate term and cut it off at a certain point. If the joint pdf of all the independent scalars is known, one can calculate a pdf for the instantaneous reaction rate term (it is simply another scalar) and then compute the mean reaction rate, etc.

AUTOTHERMAL REFORMING AND ROCKET INJECTOR MIXING TECHNOLOGY

John Houseman
Jet Propulsion Laboratory

The basic steps for producing hydrogen from hydrocarbons by the autothermal reforming process are discussed in this paper. The potential use of rocket injector mixing technology to overcome some of the problems in the entry section of the reactor are presented.

The first slide shows the different topics that will be discussed, starting with the equilibrium yields and the various steps in the autothermal process. The JPL approach and the JPL experimental results in autothermal processing will then be presented.

The mixing and pre-reactions problems will then be discussed, followed by the rocket injector mixing characteristics. Some comments on modeling for mixing of reactive components will conclude this presentation.

- EQUILIBRIUM YIELDS
- NECESSARY STEPS IN AUTOTHERMAL PROCESS
- JPL APPROACH
- EXPERIMANTAL RESULTS
- MIXING AND PRE-REACTION PROBLEMS
- MIXING FOR ROCKET COMBUSTORS
- MODELING FOR MIXING OF REACTIVE COMPOUNDS

Fig. 1. Outline of Presentation

Figure 2 shows the chemistry of hydrogen generation.

There are two basic reactions for the generation of hydrogen from hydrocarbons. The first one is steam reforming, where steam and the vaporized hydrocarbon react to form a mixture of primarily hydrogen and carbon monoxide. This reaction is exothermic and heat must be supplied to the reactor. The

carbon monoxide is converted into hydrogen by further reaction with steam in a separate shift convertor.

$$HC + AIR + STEAM \xrightarrow{CAT.} SYNGAS + N_2$$

PARTIAL OXIDATION

$$(1)\ -CH_2- + 1/2\ O_2 \longrightarrow CO + H_2$$

STEAM REFORMING

$$(2)\ -CH_2- + H_2O \longrightarrow CO + 2H_2$$

OBJECTIVE: OBTAIN AS MUCH STEAM REFORMING AS POSSIBLE FOR MAXIMUM HYDROGEN YIELD ($\equiv$MAX. $CO + H_2$)

APPROACH: FIND OPTIMUM OPERATING CONDITIONS USING EQUILIBRIUM THEORY AND TRY TO APPROACH THIS CONDITION WITHOUT FORMING CARBON AND WITHOUT SULFUR POISONING OF CATALYST

Fig. 2. Hydrogen from No. 2 Fuel Oil

The second method is partial oxidation where the vaporized hydrocarbons react with oxygen or air to produce again a mixture of primarily hydrogen and carbon monoxide. This reaction is exothermic and no heat supply is required. Steam reforming is the more efficient process, but is limited in the type of fuels it can handle.. The heaviest fuel that can be processed is a light naptha.

Autothermal reforming uses a mixture of steam and air to react with vaporized hydrocarbons. This process can handle heavier hydrocarbons like No. 2 Fuel Oil. Most of the hydrogen is produced by partial oxidation (of the order of 80%), while the rest of the hydrogen is produced by steam reforming. The overall reaction is exothermic. To make the process as efficient as possible, the aim is to make as much hydrogen as possible by the steam reforming reaction. The formation of carbon or soot is normally the limitation to this aim.

To understand these limitations, it is essential to first examine the chemical equilibrium limits to soot-free operation.

Figure 3 shows the product composition as a function of the air/fuel mass ratio (no steam added). As the air/fuel ratio is reduced from the stoichiometric value (close to 15), hydrogen and carbon monoxides start to form. At an air/fuel ratio of 5.5 methane starts to form, soon followed by carbon formation at 5.1.

Air/fuel mass ratios above 5.1 thus represent the carbon-free operating regime. The addition of steam moves this ratio to lower values.

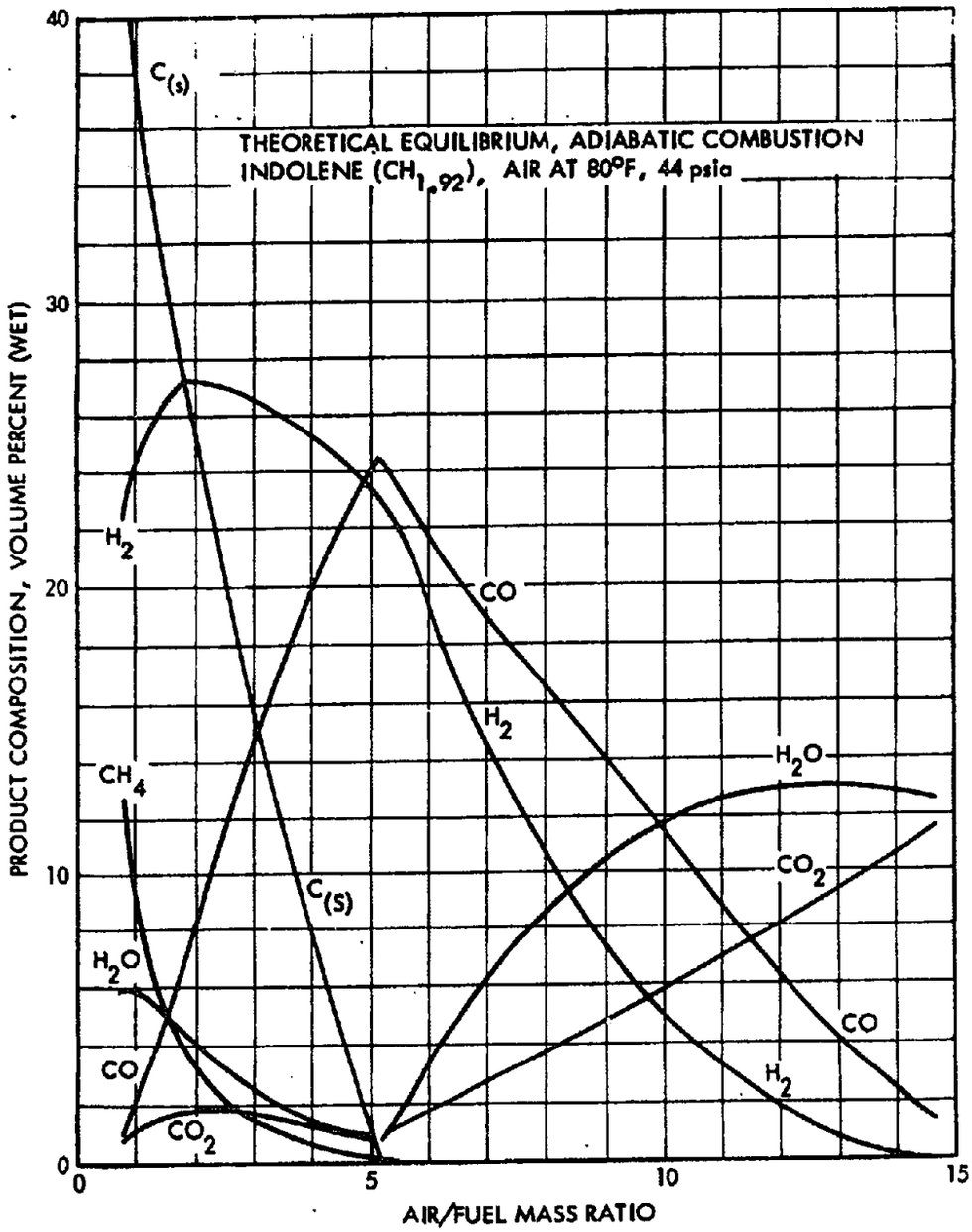

Fig. 3. Product Composition as a Function of the Air/Fuel Mass Ratio (no steam added).

Figure 4 shows the yield of hydrogen (after 100% shift conversion) as equivalent hydrogen or $(H_2 + CO)/C$ or EH, this time as the molar air/carbon ratio, where the air/carbon soot point for zero steam is at 2.3.

For zero steam addition (S/C = 0) the maximum EH is 1.9 (no steam reforming), both for 600°F and 1000°F preheat. By adding steam at a S/C = 3, the EH increases to 2.1 for 600°F preheat and to 2.25 for 1000°F preheat. These increases take place by additional steam reforming action. Note

however, that these maxima shift to the left, that is towards the theoretical soot point in terms of air/C ratio.

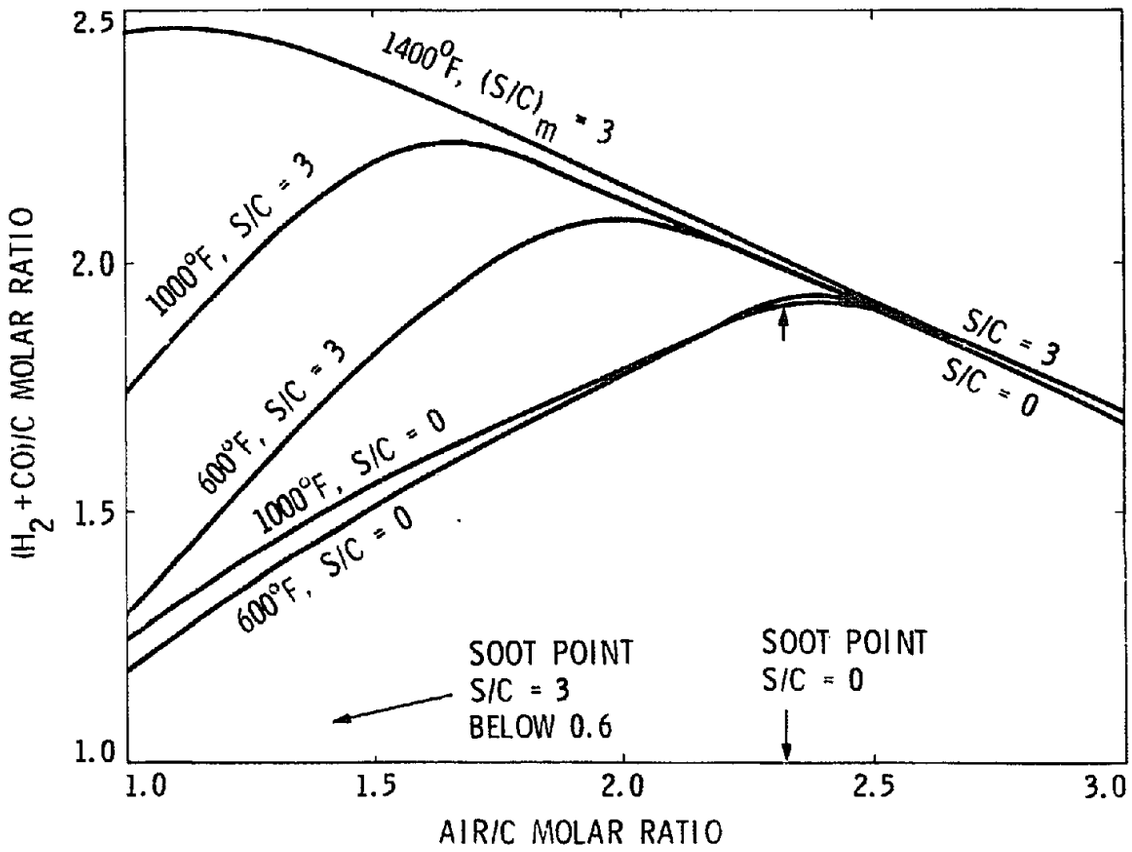

Fig. 4. Equilibrium Prediction for $CH_{1.92}$ 1 atm

It turns out that in practice soot formation occurs much sooner than predicted by equilibrium theory, that is at a higher air/C ratio than the equilibrium value.

Figure 5 shows the various steps of the autothermal process and the potential problem areas that must be avoided.

The reactants must be brought to the vaporization temperature, vaporized, further preheated and then mixed thoroughly prior to entering the catalytic reactor. Within the reactor, the catalyst bed will further preheat the reactant mixture to say 1800°F, after which the main reaction takes place. A secondary slower reaction of converting residual methane takes place further down in the bed.

Figure 6 shows these same steps in a block diagram that represents the JPL autothermal reactor system.

STEPS	POTENTIAL PROBLEMS
• PREHEAT REACTANTS	• HC CRACKING ABOVE $1100^{0}F$ • FOULING OF H.E. BY HC.
• VAPORIZE HC	• INCOMPLETE VAPORIZATION LEADS TO CARBON FORMATION • SLOW DROPLET VAPORIZATION.
• MIX REACTANTS	• INCOMPLETE MIXING MAY RESULT IN A LOCAL STEAM/C AND AIR/C RATIOS THAT ARE NOT IN CARBON FREE REGION. • MIXING OF GASES IS A SLOW PROBESS. • HIGH MIXING TIME MAY LEAD TO PREMATURE REACTIONS THAT PRODUCE CARBON.
• HEAT MIXTURE TO REACTION TEMPERATURE ($1400^{0}F$ $1800^{0}F$)	• PREMATURE REACTION IN ABSENCE OF CATALYST WILL PRODUCE CARBON. • RELEASE OF SULFUR AS H_2S WILL POISON CATALYST BELOW $1800^{0}F$
• MAIN REACTION ZONE ($1800^{0}F$ $2100^{0}F$)	• POOR CATALYST PERFORMANCE MAY RESULT IN HIGH RESIDUAL METHANE CONCNETRATION.
• SECONDARY REACTION ZONE	• HEAT LOSSES DECREASE REACTION TEMPERATURE. • HIGH EXIT METHANE REPRESENTS HYDROGEN LOSS.

Fig. 5. Steps in Autothermal Reforming

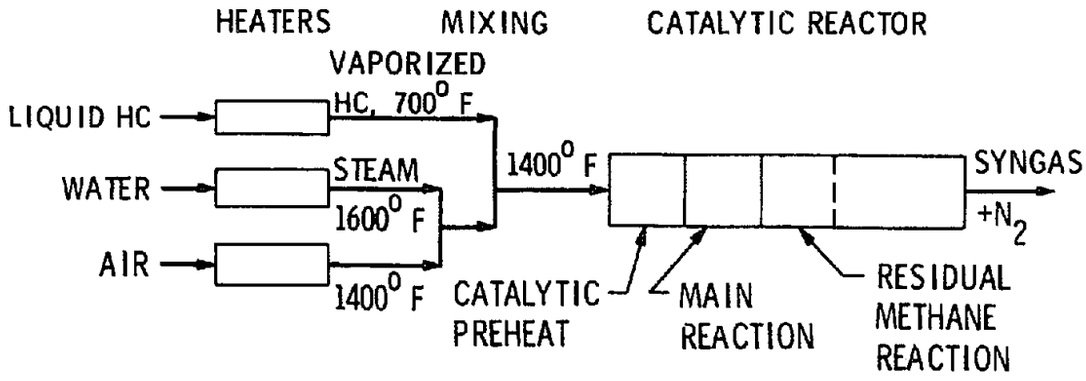

- VAPORIZE HC SEPARATELY, KEEP TEMPERATURE LOW
- PUT HIGH PREHEAT INTO STEAM AND AIR
- PREVENT REACTION AHEAD OF CATALYST BED
- USE LOW ACTIVITY CATALYST TO BRING REACTANTS FROM 1400°F TO 1800°F.
  MECHANISM: RADIATION, CONDUCTION AND SOME EXOTHERMAL REACTION
- USE MEDIUM ACTIVITY CARBON-TOLERANT CATALYST FOR MAIN REACTION
- USE HIGHLY ACTIVE CATALYST FOR STEAM REFORMING OF RESIDUAL METHANE

Fig. 6. JPL Approach to Autothermal Reforming

Figure 7 shows the experimental results that were obtained with this reactor, relative to the equilibrium predictions.

The lower square represents the EH values. The reactor used was not long enough to further steam reform the methane product from the hydrocarbon. This is indicated by the dotted line in the reactor section of Fig. 6. By making the reactor longer the one to two percent of methane in the product gas can be converted into hydrogen as the equilibrium yield of methane is close to zero under the conditions used. The symbol TH is used to show the total hydrogen that can be generated as one mole of methane will result in 4 moles of hydrogen (after total shift conversion):

$$TH = (H_2 + CO + 4CH_4)/C$$

Values for EH and TH of 1.75 and 2.1 were obtained respectively. The value for TH is very close to the equilibrium values, indicating a good material balance in the experiments.

These results at an air/C ratio of 1.9 represent the lowest air/C ratio that could be used without producing soot.

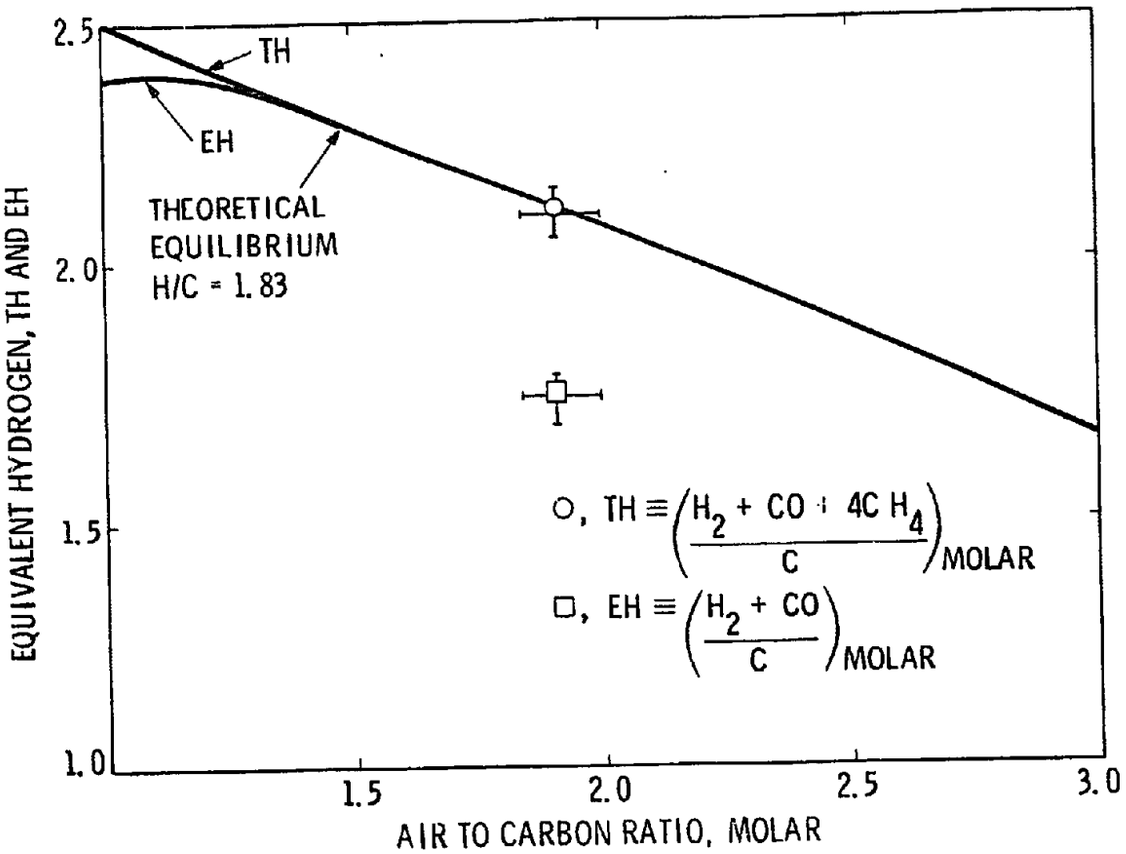

Fig. 7. Theoretical vs Experimental Results at T_p 1400°F and $(S/C)_m$ 3.0

The equilibrium line shows that a decrease in air/C should lead to higher EH and TH values. Equilibrium residual methane does not occur until air/C = 1.4, as shown by the differences between EH and TH.

To be able to operate at lower air/C ratios will require a more effective catalyst and/or higher preheat (see Fig. 4 predictions).

The amount of preheat is limited by hydrocarbon cracking reactions that take place at 1100°F and beyond. Such cracking reactions can result in soot formation that will deactivate the catalyst.

Hydrocarbon cracking at a given temperature can be minimized by fast efficient mixing of the reactants and a fast heating rate (minimum residence time) from 1100°F to the reaction temperature of 1800°F. As the presence of the catalyst has a soot suppressing action, it would be preferred if the heating from 1100°F to 1800°F could be done in such a manner. We will refer to such a method as "catalytic preheat".

We will now examine the effect of two different reactant mixers on the pre- and post-reactor gas composition.

Figure 8 shows an autothermal reactor with an inlet system (Mixer A) in which the vaporized fuel is first mixed with steam, and the resulting steam/fuel mixture is then mixed with hot air. The total mixture then passes through a mixing section that incorporates a 12 inch section of steel balls and a 4 inch section of swirler tubes ahead of the catalyst bed. The residence time of the reactants from first mixing to reactor inlet was 8 milliseconds.

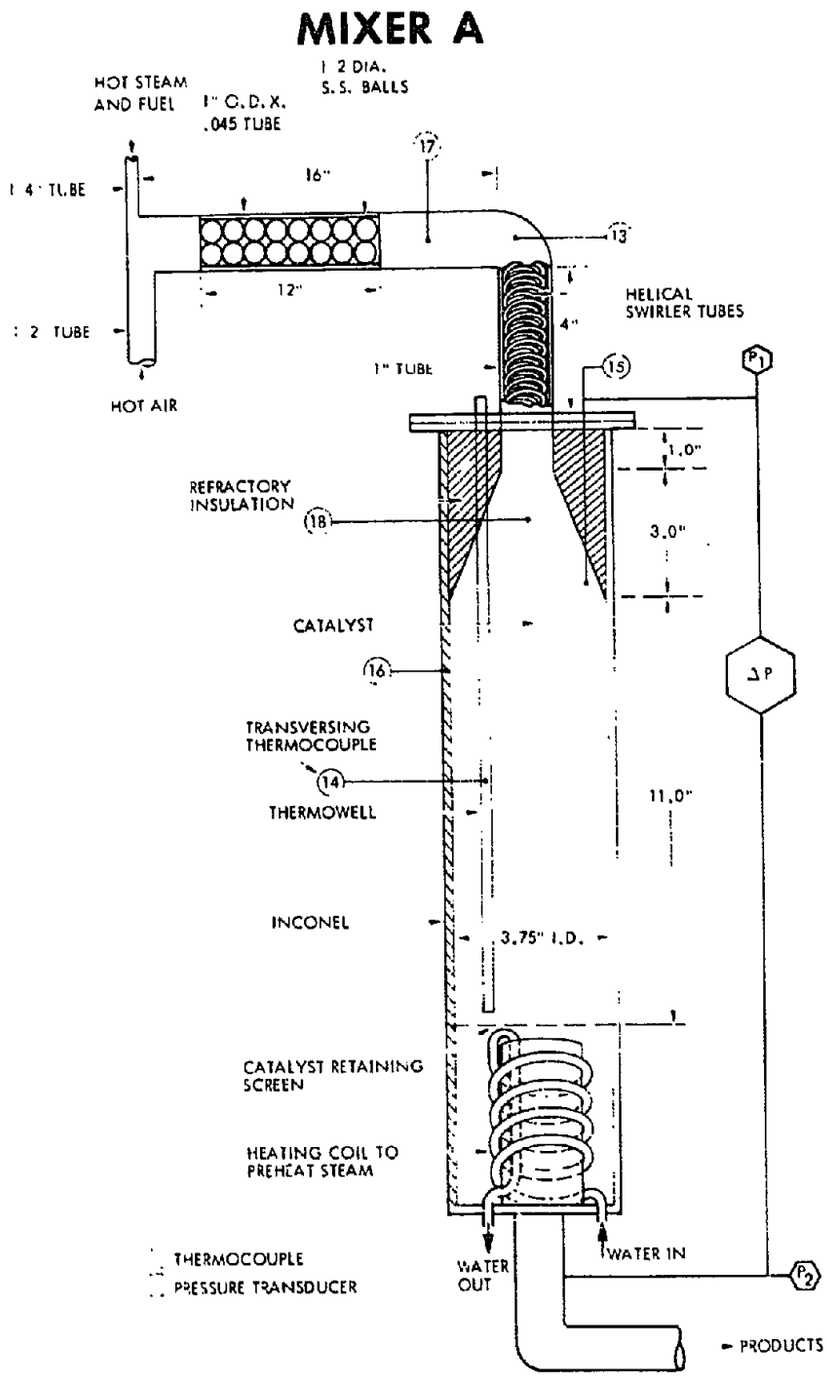

Fig. 8. Autothermal Reactor

Figure 9 shows the Mixer B configuration where the vaporized fuel is introduced later into a steam/air mixture. The residence time from initial fuel mixing till reactor inlet is now only 3 milliseconds. Figure 10 shows the temperature profiles for Mixers A and B. The higher temperatures for Mixer A are partly due to heat release as a result of cracking and premature reactions.

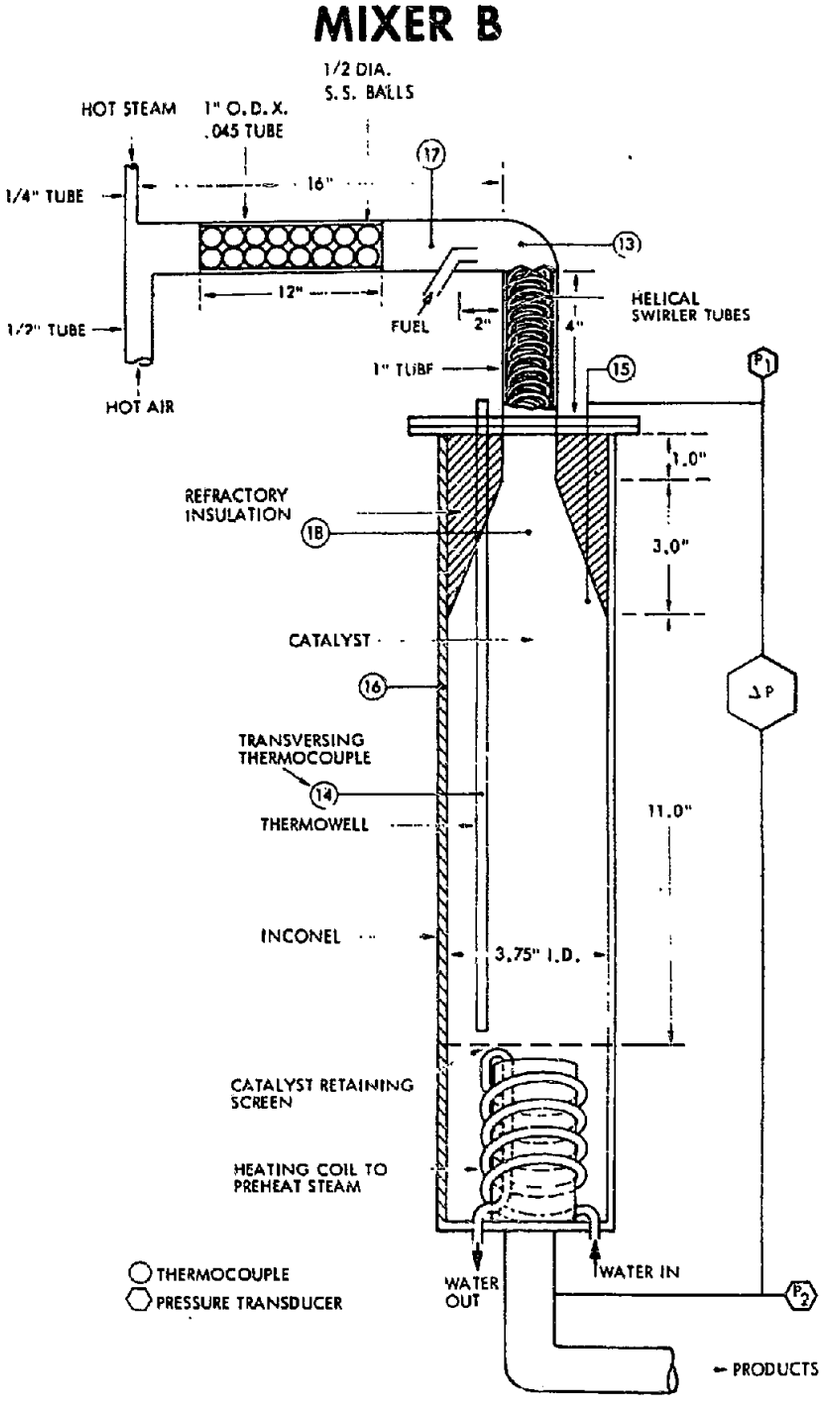

Fig. 9. Mixer B Configuration

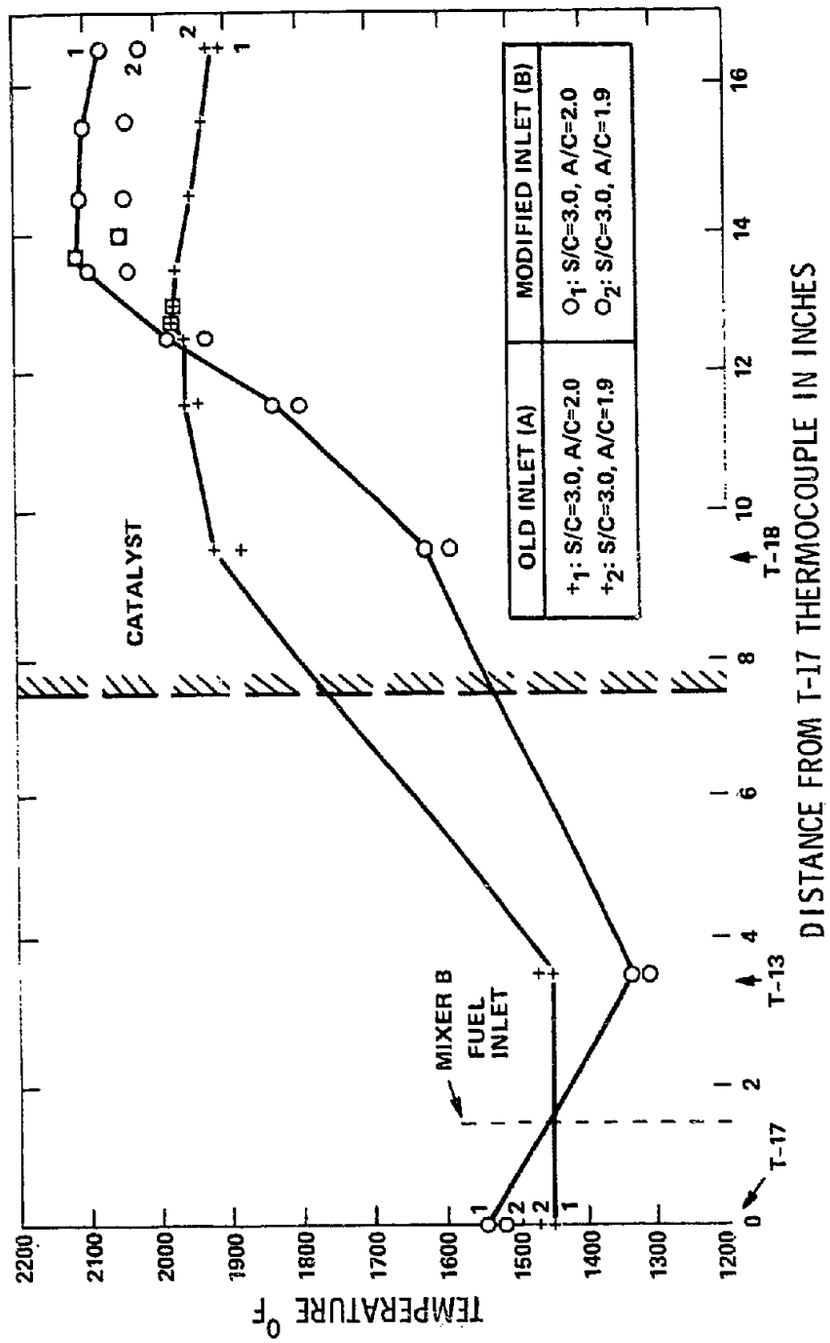

Fig. 10. Temperature Profiles for Mixers A and B

The Mixer B reactants enter the catalyst bed at a lower temperature (very little pre-reaction) and further preheat now takes place within the catalyst bed as "catalytic preheat". The final reaction temperature for the Mixer B configuration was actually higher than for Mixer A.

Figure 11 shows an analysis of the reactant gas at the catalyst bed inlet and at the reactor exit.

It is apparent that Mixer A produces considerably more cracking than Mixer B as evidenced by the high concentration of light hydrocarbons. It is even more interesting to note that an equivalent difference in C1, C2 and C3 concentrations exists in the reactor exit gas.

Apparently, Mixer A has a small enough mixing residence time to reduce the pre-reactions to a very low level, while the mixing process is good enough to produce a homogeneous reactant mixture at the inlet to the catalyst bed.

As the production of unsaturated light hydrocarbons is normally a precursor to soot formation, the prevention of such reactions is highly desirable. A fast and efficient mixer is thus needed.

The problem of fast, efficient mixing has been dealt with at length in liquid rocket injectors. The very short residence times in rocket

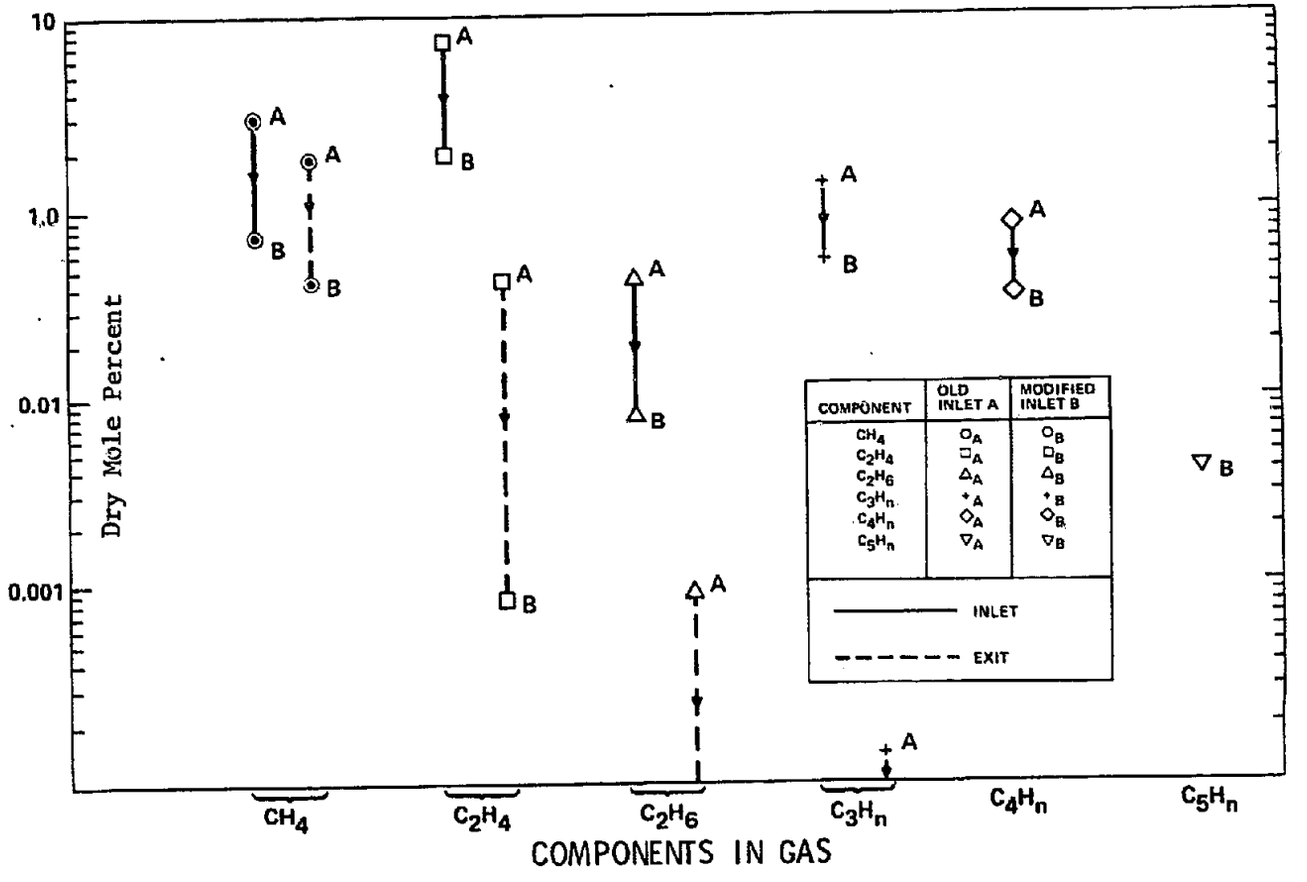

Fig. 11. Hydrocarbon Gas Compositions for Mixers A and B

combustion chambers result in very little stream tube or lateral mixing. It then becomes essential to ensure complete primary mixing, as a non-homogeneous mixture greatly reduces performance. Impinging jet mixing provides such mixing.

Figure 12 shows the basic geometry of impinging jet mixing for liquids. Upon contact of the jets, a liquid sheet is formed that gets thinner as it travels away from the impact point. As the sheet reaches a minimum thickness, it breaks up into small droplets of mixed liquids. Thus well mixed droplets of liquids are produced in a few jet diameters.

Figure 13 shows some typical configurations. Figure 14 shows some typical characteristics of impinging jets. The important one for our application is that the mixing time is proportional to the ratio of the jet diameter to the jet velocity which is usually of the order of milliseconds in rocket engines. Figure 15 lists various other configurations that have been used in rocket engines, including gas/liquid injectors.

There is a considerable body of design data on liquid jets, some examples of which are shown in Figure 16. It has also been shown that gaseous jet mixing is very similar to liquid jet mixing. A NASA design handbook on gas injectors is available.

In the JPL experiments described earlier all the reactants were first converted to gases before mixing. Gaseous jet mixing can be used here. In industrial practice it is common to atomize fuels into droplets and to inject sprays of such fuel droplets into a hot gas to achieve vaporization of the fuel and subsequent mixing of the reactants. The gas/liquid rocket injectors referenced in Figure 15 could be used for such a case to achieve rapid vaporization and efficient mixing.

It must be mentioned at this point that in rocket injectors it has been found that it is difficult to scale up jet mixers and maintain good mixing characteristics. Instead, the practice has been to use many small injector elements in parallel. It appears that the same practice could be used to advantage in autothermal reactor inlet systems.

Rigorous theoretical modeling of the flowfield of impinging jets has been very difficult as turbulence and mixing are not well understood, even at the academic level. Any modeling of inlet systems will have to take into account the velocity profiles and the turbulence levels, which are both hardware dependent, as well as the basic chemical reaction rates. Any modeling results therefore will need extensive experimental verification. These factors are summarized in Figure 17.

In conclusion, it may be said that rocket injector technology should be able to help solve some problems in rapid, complete mixing of the reactants in the inlet systems of autothermal reforming. It may be noted that rocket injector technology is already being used successfully in coal gasification for rapid heating and gasification of cold coal particle sprays with hot gaseous reactants.

IMPROVED MIXING AND ATOMIZATION BY UTILIZATION OF IMPINGING JETS

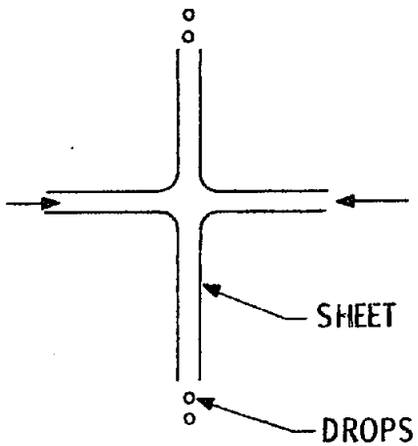

- EQUAL MOMENTUM
- PLANAR SHEET
- SHEET BECOMES THINNER WITH INCREASING RADIUS AND BREAKS UP INTO DROPLETS

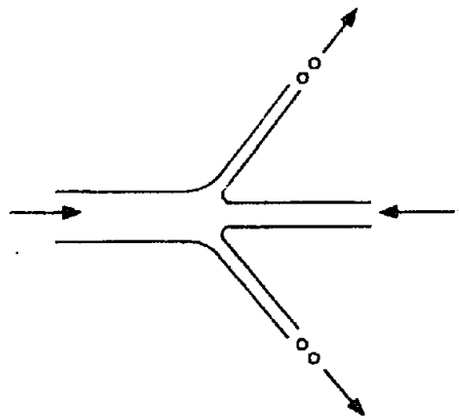

- UNEQUAL MOMENTUM
- CONICAL SHEET

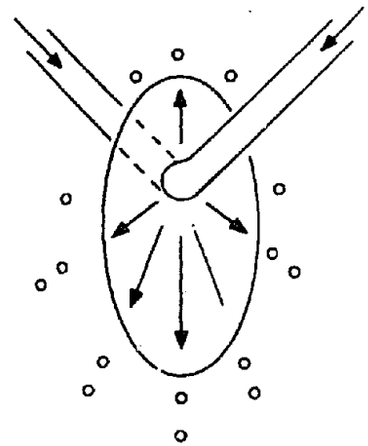

- EQUAL MOMENTUM
- ANGLE LESS THAN 180^0
- SHEET MAINLY DOWNSTREAM OF IMPINGEMENT POINT

Fig. 12.

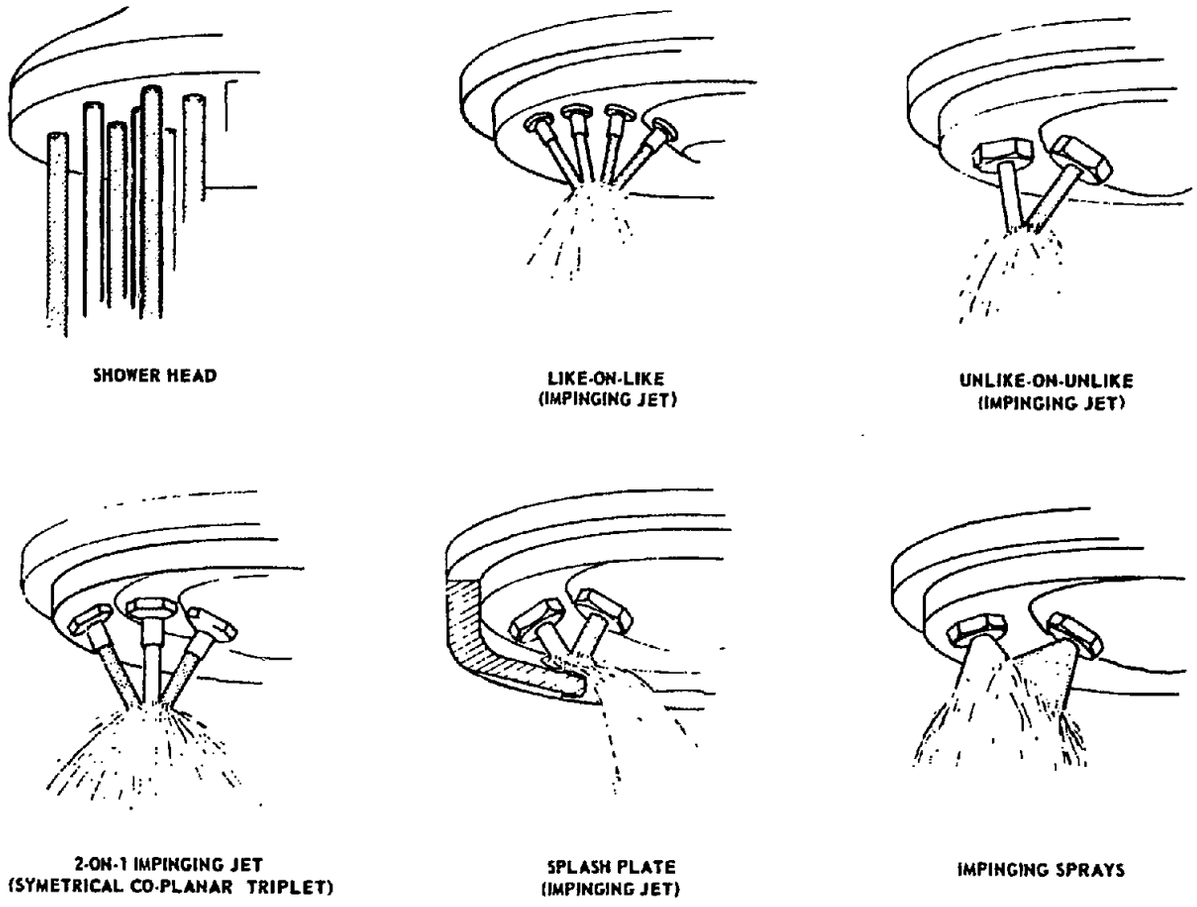

Fig. 13. Typical Configurations for Rocket Motor Injectors

DROPLET SIZE

$$D = 1.73 \frac{D_j^{0.15}}{V_j^{0.5}} \left(\frac{\sigma}{\rho}\right)^{0.25}$$

TANASAWA, SASAKI & NAGAI

σ = SURFACE TENSION

OPTIMUM MIXING

- 60^0 ANGLE
- $\frac{\rho_1 V_1^2 D_1}{\rho_2 V_2^2 D_2} = 1$ (RUPE CRITERIA)
- MIXING TIME $\equiv D_j/V_j \equiv$ MILLISECONDS

Fig. 14. Characteristics of Impinging Jets

- IMPINGING SHEETS
  - TRW: ANNULAR SHEET + RADIAL JETS FROM WITHIN
- VORTEX INJECTOR
  - REACTION MOTORS: RADIALLY OUTWARD JETS IMPINGE ON SWIRLING SHEET INSIDE A CUP
- GAS/LIQUID INJECTORS
  - BELL: COAXIAL: GAS IN CENTER, LIQUID IN ANNULUS, ATOMIZATION BY SHEAR, $V_g / V_\ell \geq 15$
- POROUS PLUG INJECTORS
- PLATELET INJECTORS (MICRO-ORIFICE)
  - AERO JET & VACCO: PHOTO-ETCHED FLOW CHANNELS TO MAKE IMPINGING JETS

Fig. 15. Other Configurations

- LIQUID JETS
  - CHARACTERIZED AT JPL IN 50'S:
    - J. H. Rupe, JPL REPORT NO. 20-209, 1956
    - R. W. Riebling, J. SPACECRAFT & ROCKETS, VOL. 4 NO. 6, 1967
- GASEOUS JETS
  - ROCKETDYNE SHOWED APPLICABILITY OF LIQUID JET CORRELATIONS TO GASEOUS JETS
  - NASA LEWIS CR-121234 (1973), CONTRACT TO AEROJET, LEWIS CONTACT: Dick Priem "HANDBOOK FOR GAS INJECTORS"
- MODEL OF INJECTION, ATOMIZATION, VAPORIZATION AND COMBUSTION IN ROCKET COMBUSTION CHAMBERS JPL CONTACT: Ray Kushida

Fig. 16. Available Information on Injectors

- ROCKET INJECTOR TECHNOLOGY CAN HELP SOLVE CRITICAL PROBLEMS IN RAPID, COMPLETE MIXING OF REACTANTS FOR AVTOTHERMAL REFORMING
- ROCKET INJECTOR TECHNOLOGY IS ALREADY BEING USED IN COAL GASIFICATION:
  - ROCKWELL: $(CH) + H_2 \xrightarrow{0.5\ \text{sec.}} CH_4$
    AMBIENT T 2200^0 F 1800^0 F
    COAL
  - BELL + TRW: $(CH) + AIR \xrightarrow{0\text{-}045\ \text{sec.}} CO + H_2 + (N_2)$
    AMBIENT T 600^0 F 2400^0 F
    COAL

Fig. 17. Conclusions

DEVELOPMENT OF SCALING METHODS FOR A CRUDE OIL CRACKING REACTOR USING SHORT DURATION TEST TECHNIQUES

J. D. Kearns, D. Milks and G. R. Kamm, Union Carbide Corporation

Presented by Gerard R. Kamm

*Reprinted from "Thermal Hydrocarbon Chemistry," ADVANCES IN CHEMISTRY SERIES No. 183, Copyright 1979 by the American Chemical Society. Reprinted by permission of the Copyright Owner.

ABSTRACT

Union Carbide's co-development with Kureha and Chiyoda has resulted in an Advanced Cracking Reactor (ACR) technology primarily for ethylene production. In the ACR process, a selected crude oil or distillate is injected into high temperature combustion gases. The vaporized feedstock and combustion gases flow through a venturi-reactor chamber where adiabatic cracking occurs. The products are rapidly quenched and then processed further. The unique reactor conditions produce high value chemicals directly from the world's limited oil resources. The reactor technology has been extensively investigated through a series of research and development programs. Of particular interest are the fluid dynamic, vaporization, and gas yield interactions leading to scale-up techniques and their associated experimental programs. Geometric, kinematic, and dynamic process similarity concepts have been investigated to scale-up typical ACR pilot data to a commercial reactor basis. Testing of these concepts has been accomplished using short duration testing during which steady state fluid dynamics and chemical performance are reached in a matter of seconds. The testing programs have included cold gas flow wind tunnel experiments where the injected liquid particle sizes and liquid trajectory have been measured. Full scale reactor tests at the commercial process temperatures and mass rates were also conducted. The tests verified the commercial ACR scale criteria and gas yield cracking patterns.

INTRODUCTION

The Process

Union Carbide Corporation, Kureha Chemical Industry Company, Ltd. and Chiyoda Chemical Engineering and Construction Company, Ltd., entered into a co-developmental program in 1973 to commercialize a new ethelyne technology based on flame cracking of crude oil and crude oil fractions. This unique Advanced Cracking Reactor (ACR) technology results in producing 60-70 percent of high value chemical products, including over 30 percent ethylene from selected crude oils or a wide range of distillate feedstocks[1]. This process offers a step change in the yields of non-fuel products from the world's valuable and limited resources of crude oil.

In this process, (see Fig. 1), crude oil or distillate is injected into somewhat less than two times its weight in high temperature gases (~2000°C) which are generated by pure oxygen combustion with an excess of fuel. The vaporized feedstock and combustion gases ("steam") are accelerated through a venturi nozzle reaction chamber where an adiabatic cracking reaction occurs at pressures significantly higher than those commonly used. The reaction products are rapidly quenched at about 20 msec residence time by a unique heat recovery system[2]. After gas-liquid phase separation and fractionation, the product gas is compressed and processed in a specially developed acid gas absorption system for the removal of H_2S and CO_2. The sweet gas is processed through somewhat conventional separation devices for the recovery of ethylene, propylene, acetylene and other cracking byproducts. The extreme flexibility with regard to feedstocks and product yields combined with the intrinsically high chemical yields results in a decided economic advantage over conventionally produced ethylene. In addition, this process offers chemical companies greater independence on their raw material supply from oil companies with whom they must compete in petrochemical markets.

The Development Effort

The ACR technology has been extensively investigated during the last four years through a series of research and development programs. Six major test facilities have been operated at Carbide's Technical Center in South Charleston, W. VA, and Kureha's facilities in Nishiki, Japan. These tests led to an extended pilot plant run demonstrating all of the key elements of the process including acid gas removal.

In addition, geometric, kinematic, and dynamic process similarity concepts have been investigated to scale-up typical ACR pilot data to a commercial reactor basis. Selected fundamental experiments were performed in which the scale-up criteria was refined. These tests included heat transfer studies as well as wind tunnel studies and other fluid dynamic tests which employed three dimensional imagery (holography), laser shadow photography, spark shadow photography, ultra high speed motion pictures, as well as conventional photography. Several of these tests and techniques employed the facilities of aerospace contractors. The data obtained from this work was used to mathematically correlate and estimate the position, size, slip velocity, and vaporization time of the injected oil droplets as a function of the characteristics of the injector, reactor geometry and operation conditions.

This technology led to testing of a full scale 100 million pound per year ethylene reactor. The full scale tests have verified scale criteria and gas yield cracking patterns. In order to further minimize the technical risk and complete the development effort, Union Carbide is constructing a $15 MM ACR prototype unit at Seadrift, Texas, primarily to prove long-term equipment operability. This demonstration unit will be completed in 1979 and can lead to the construction of a world-scale ethylene unit by the mid-1980's.

SCALING

Similarity in Scale-Up

Scale-up implies a change from a small configuration to a larger one. To successfully perform the scale-up of a chemical process, one must first establish the categories for which similarity must be ensured. The difficulty that arises is that techniques based on the governing differential equations or dimensional analysis provide only a means for identifying pertinent dimensionless groups. Their absolute relationships in complex processes must be developed from small-scale experiments which usually cannot provide complete similarity. Ideal similarity is often unattainable because it requires the ratio of corresponding measurements in both the small and large scale process to be identical. It then becomes economical to isolate and experiment only those conditions critical to the scale-up of the process. Given the known desirable performance of the small reactor system, variables important in scale-up may be studied in terms of the following similarity categories from Johnstone and Thring[3]; geometric, mechanical (static, kinematic, dynamic), thermal and chemical.

Critical Scale-Up Conditions

In an effort to maintain equivalent chemical performance or product yields in the ACR, we are in effect attempting to develop chemically similar reactor systems. Due to the two-phase flow in the reaction section of the ACR process, it is important to note that there are two principal chemical reaction subdivisions. The first is controlled by mass-action (homogeneous), while the second depends upon the surface or interface between the phases (heterogeneous).

By 1975, pilot-plant development studies of the ACR process had proceeded to the stage where the associated potential scale effects were being investigated. Computer simulation of the ACR reaction system revealed that (1) the initial vapor phase cracking reactions were extremely fast in comparison with the vaporization of sprayed feedstock particles, and (2) vaporization was essentially complete by the end of the reactor throat. This meant that, although the scaling situation would be complicated by having a so-called "mixed regime", that difficulty pertained mainly to the reactor throat section and was not a problem in the diffuser section of the reactor venturi.

The rate of chemical pyrolysis in the ACR, to a large extent, depends upon the temperature profile while the rate of bulk flow depends upon the flow pattern. Hence, ACR chemical similarity requires both thermal and kinemetic similarity. Damköhler[3] proposed a set of dimensionless similarity groups which apply to continuous reacting systems. Assuming that the ratio of heat liberated to heat transported will be similar because thermal similarity is maintained, most of the Damköhler numbers have little bearing on the ACR process. This is due to the essentially adiabatic ACR cracking process for which molecular diffusion can be neglected compared to bulk flow.

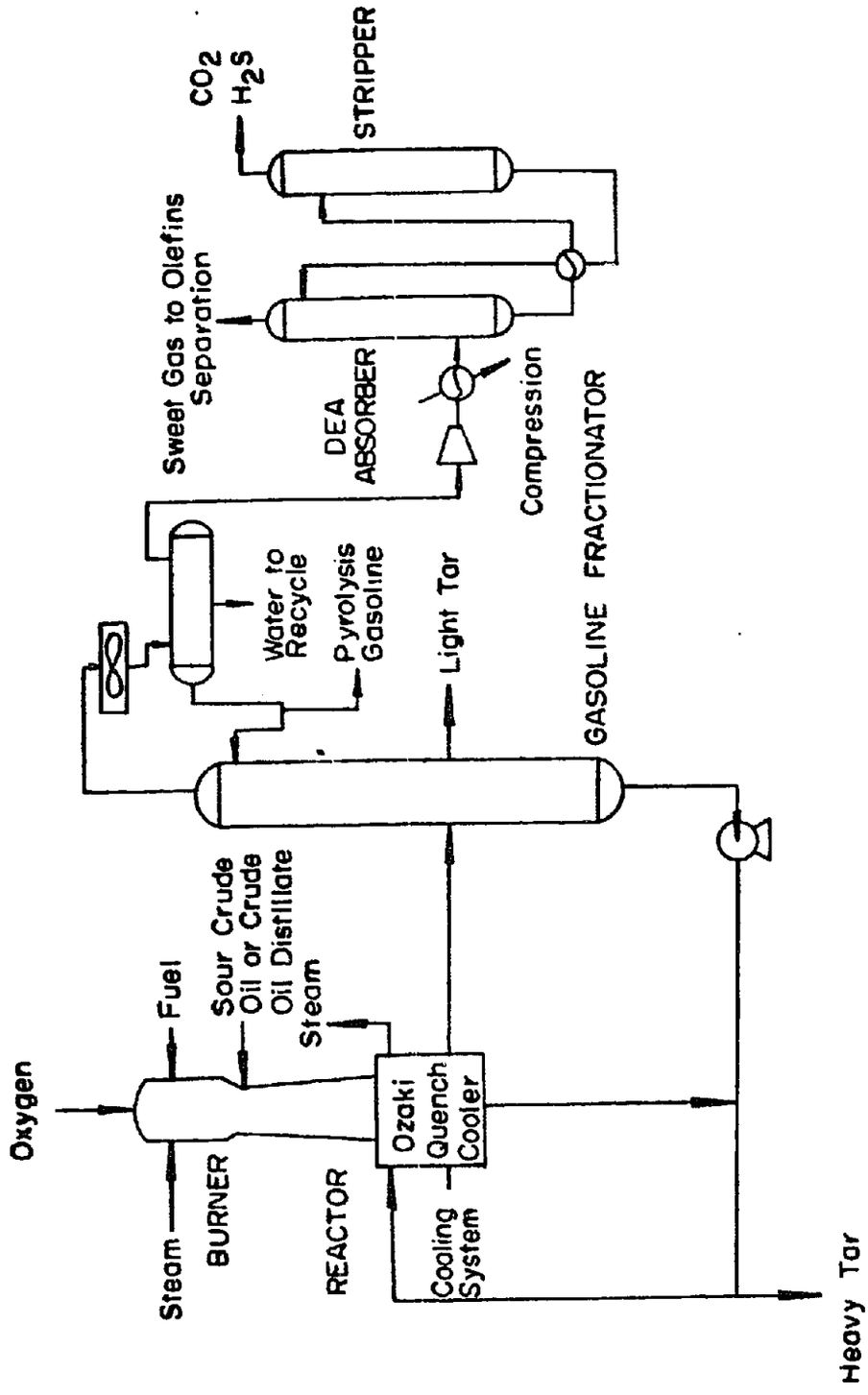

Fig. 1. Schematic diagram of ACR Process.

The Reynolds number should be kept constant during scale-up, but the ACR flow is well into the turbulent range so that viscous forces are relatively unimportant.

Chemical similarity in the diffuser section of the ACR can thus be defined in terms of the remaining (first) Damköhler number.

$$D_{a_I}{}^{*} = \frac{\text{Rate of Chemical Formation}}{\text{Rate of Bulk Flow}} = \frac{P}{T} = \frac{P}{F(1+S/F)} = \frac{Y}{1 + S/F} \qquad (1)$$

where P = production rate, lb/hr
T = reactor throughput, lb/hr
F = feed (cracking stock) rate, lb/hr
S = heat carrier (cracking medium) rate, lb/hr
Y = yield, lb product/lb feed

The similarity criteria which applies to this section, controlled by mass-action, ultimately requires equal residence time (or space velocity) when scaled.

Since particle vaporization is the controlling factor in the reactor throat, the reaction rate depends upon the fluid dynamics. Chemical similarity in this region is, therefore, subject mainly to a dynamic regime rather than a chemical one. Thus, dynamic similarity applies for the detailed scale-up of the reactor throat section.

Dynamic similarity requires that the ratio of corresponding forces is equal in geometrically similar systems. The principal force ratio operating in the ACR venturi throat section is the dynamic pressure ratio, $\bar{q}$,

$$\bar{q} = \frac{q_{liq}}{q_{gas}} = \frac{(\rho V^2)_{liq}}{(\rho V^2)_{gas}} \qquad (2)$$

When scaling the injection system, it is more effective to accommodate the desired higher oil flow rates by increasing nozzle capacity than by increasing the number of nozzles. However, to satisfy kinematic similarity, the relative position of particles or trajectory should correspond in geometrically similar ACR throat sections. It turns out that $\bar{q}$ is not particularly useful as a similarity criteria, but may be used to predict conditions required for kinematic similarity of the sprayed particles. For example, the radial

---

*The more familiar representation, $D_{a_I} = \frac{rL}{uC}$, indicates that chemical similitude depends upon reaction rate, r; reaction time, L/u; and initial concentration, C.

position of a particle is a function of $\bar{q}$, injector capacity, and downstream distance from injection. Thus, kinematic similarity of the particle trajectory, when constrained by the required change in injector capacity, can only be achieved by varying $\bar{q}$ during scale-up. In this instance, kinematic similarity becomes the desired objective.

Some of the heterogenous flow difficulties in the throat section can be avoided if the particle surface per unit volume is maintained constant. If the Sauter mean diameter of sprayed particles could be held constant during scale-up, the surface area per unit volume (or mass for constant density) of feed would be fixed. Because the ratio of heat carrier to feed will have to be fixed to obtain consistent yields (Eq. 1), the constant surface area per unit mass of heat carrier would imply that the oil droplet surface per unit volume would also be constant. This is analogous to the situation described by Walas[4] of equal activity (vaporization rate) in heterogenous catalysis when the specific surface per unit volume is constant; the scale equations then revert to a homogenous reaction form so that equality of residence time (or space velocity) again becomes the important similarity criteria.

Thermal similarity is achieved in the ACR by providing a temperature profile which can be held geometrically similar when scaled. The temperature profile drives the ACR chemical kinetics and is a combined result of the heat transfer due to cracking and the heat effects caused by the bulk fluid movement. Thus, true thermal similarity in the ACR can only be achieved in conjunction with chemical and kinematic similarity. Kinematic similarity in the ACR is made possible during scale-up by forcing geometrically similar velocity profiles. The ACR temperature, pressure and velocity profiles are governed by compressible gas dynamics, so that an additional key scale parameter is the Mach number.

The method for achieving kinematic similarity in the ACR, when scaling from a known pilot scale reactor to a commercial scale reactor, includes Mach number matching. The following equation from Shapiro[5] may be used in the Mach number scaling technique to obtain estimates of the diameters in each of the reactor sections.

$$\frac{W}{A} = \sqrt{\frac{k}{R}} \frac{P_o}{\sqrt{T_o}} \frac{M}{\left(1 + \frac{k-1}{2} M^2\right)^{\frac{k+1}{2(k-1)}}} \qquad (3)$$

where W = mass flow rate through a given cross-section
A = area of cross-section
k = specific heat ratio
R = specific gas constant = Ru/MW
Ru = universal gas constant
MW = molecular weight of the gas
P_o = stagnation pressure of the gas flow
T_o = stagnation temperature of the gas flow
M = Mach number at the given cross-section

Applying Eq. 3 with the assumption of Mach number matching between a desired commercial scale (subscript c) and a known pilot scale (subscript p) leads to

$$\frac{D_c}{D_p} = \sqrt{\left.\frac{W\sqrt{T_o}}{P_o\sqrt{MW}}\right|_c \Bigg/ \left.\frac{W\sqrt{T_o}}{P_o\sqrt{MW}}\right|_p} \qquad (4)$$

where D's are diameters and the effect of small changes in k have been neglected. Equation 4 may be used to determine the commercial diameters from the known pilot data and desired commercial flow conditions. Equation 3 may also be used directly to estimate the required diameters, provided Mach number information is available.

In order to satisfy physical limitations, modifications to the diameters are made depending upon the magnitude of the compressible flow effects in each of the reactor sections. Lengths are geometrically scaled in the reactor throat. However, the diffuser angle is forced below a maximum angle of 6° to avoid flow separation. Residence times are controlled by appropriate variation of the length of the reactor's cylindrical section.

Consistent performance of the ACR during scale-up depends upon thermal and kinematic similarity throughout, but with a dynamic influence on kinematic similarity in the throat and chemical similarity necessary in the diffuser. As a result of the above considerations, it was felt that the ACR process could be scaled in a geometrically similar reactor based on matching Mach numbers, S/F ratio, and residence time in the reaction section--provided two critical conditions could be met. When scaled, the sprayed particle size distributions would have to be approximately equal--(i.e., equality of Sauter mean diameter) while a kinematically similar oil particle trajectory would also be required.

EXPERIMENTAL

Droplet Size Experiments

The hydrocarbon feedstock is injected into the ACR's high temperature carrier gas from a circular array of nozzles. The atomized spray emitted from these injector nozzles is comprised of many droplets of varying size. Both small scale and commercial capacity spray nozzles were extensively studied during the ACR development.

The conditions necessary for equality of particle size distribution were determined under ambient conditions. The nozzles used in the investigation can be classified as swirl spray pressure nozzles. They accommodate a swirl insert which imparts a tangential velocity to the exiting fluid and from conventional swirl nozzles (see Putnam, et al.[6]) to require an experimental study of particle size distribution.

Particle size measurements were made using an ultraviolet laser shadow photographic technique. The particle sizing system displayed real-time droplet images onto a television monitor. The images (shadows) were obtained when a pulsed (30 times per second) UV-laser beam was directed through a spray scene onto a synchronized ultraviolet-sensitive vidicon camera/recorder. The narrow depth of field employed by this system is capable of recording shadows from 300 in focus droplets per second with a resolution down to approximately 0.3 microns in diameter.

The actual size measurements were taken from the stored videotaped data. Typically, droplets were observed up to 600 μ in diameter, with the major portion occurring in the 0-100 μ range. A count of the number of particles per size interval was made by grouping the data into one of sixteen size intervals. Histograms, number distributions, and number frequency distributions were generated from this information. Mean diameters, calculated according to the equations developed by Mugele and Evans[7], were also used to evaluate the nozzles. During this test program, we were able to vary the nozzle diameter, injection pressure, fluid surface tension, and location in the spray pattern where size measurements were recorded.

The data indicated that droplet size changes are primarily influenced by injection pressure and orifice size, while secondary changes can be attributed to fluid properties, orifice shape, and the nozzle's internal length/diameter ratio. This last point was not observed by Dombrowski and Wolfsohn[8] for more conventional swirl spray nozzles. Nevertheless, they present a useful correlation between Sauter mean diameter and operating conditions.

During an earlier test program, a limited number of observations were made on the maximum drop size generated by a commercial scale nozzle under conditions present in an ACR reactor. The tests were conducted at a production unit operated by Kureha. A non-destructive recording of the spray was obtained with the aid of a pulsed ruby laser holographic technique[9]. The resultant spray phenomena was reconstructed from holograms making it possible to estimate maximum particle size. This information was compared with data on maximum particle size for the same nozzle during ambient testing. From this comparison, we were able to translate the target Sauter mean diameter for scale-up to equivalent cold flow conditions.

Additional droplet size work under flow conditions was not undertaken. The empirical expressions provided by Ingebo and Foster[10] were developed under conditions sufficiently similar to those present in the ACR to justify their use as a first approximation. Their data was derived from the injection of sprays into a transverse subsonic gas flow. They obtained the following correlation between drop size parameters and force ratios using dimensional analysis.

$$\frac{D_{max}}{d_o} = 22.3\ (WeRe)^{-0.29} \qquad (5)$$

$$\frac{\bar{D}_{30}}{d_o} = 3.9\ (WeRe)^{-0.25} \qquad (6)$$

where, D_{max} = maximum droplet diameter

$\bar{D}_{30}$ = volume mean diameter

d_o = orifice diameter

We = Weber number, $\frac{d_o V_\infty^2 \rho_\infty}{\sigma}$

Re = Reynolds number, $\frac{d_o V_\infty}{\nu \ell}$

ρ_∞, V_∞ = free stream density and velocity

$\sigma, \nu\ell$ = liquid surface tension and kinematic viscosity

Oil Particle Trajectory

The initial path or trajectory (termed "penetration") which the injected oil particles make in the steam flow has been found to be significant in determining the distribution of the ACR gas product yields and thus effects the ACR process economics. Since the injected oil trajectory can be controlled by adjustment of operating variables (i.e., injection pressure, injector orifice diameter, and number of injectors), the ability to predict the oil trajectory as a function of these parameters is a significant step forward in the ACR development.

Exact analytical solutions to the governing equations which produce the penetration trajectory are extremely difficult to obtain. For this reason, empirical penetration equations based on experimental data correlations are most often presented in the literature. These best-fit equations contain the dominant parameters which have been experimentally determined to significantly affect the penetration. In order to detail the specific ACR penetration phenomena, a series of cold flow and hot test experiments was conducted.

Cold Flow Penetration Experiments

Flow visualization studies were first performed in a "plexiglas" mock-up of a small ACR. These studies revealed that the dynamic pressure ratio could significantly affect the liquid spray path. More importantly, it was discovered that large-scale testing would be necessary to examine ways to maintain kinematic similarity during scale-up. These initial conclusions were supported by previous work such as that carried out by Geery and Margetts[11] and Hojnacki[12] on the penetration of liquids into cross-flowing gases.

Partial reactor modeling was then employed to shed light on the factors controlling penetration in the ACR. A full-scale cold flow simulation of the reactor throat region was performed. The tests were conducted in a trisonic wind tunnel at the McDonnell-Douglas Aerophysics Laboratory[13].

Injector nozzles of interest were secured to a plate mounted in the plenum chamber of the wind tunnel. The plate was positioned so that the interaction between the spray and the free stream could be observed through windows on opposite sides of the tunnel. For each run, after steady-state liquid and gas flow had been confirmed, a spark of light was directed onto a parabolic mirror. The reflected parallel light was then passed through the spray scene via the viewing ports of the wind tunnel. A second parabolic mirror on the opposite side of the tunnel imaged the resulting spray shadow onto a film holder (Fig. 2). Penetration coordinates were taken from enlargements of negatives recorded with this back-lighted spark shadow photographic technique. The enlargements were scaled to actual size with the aid of a calibrated grid placed on the view window and recorded in each photograph.

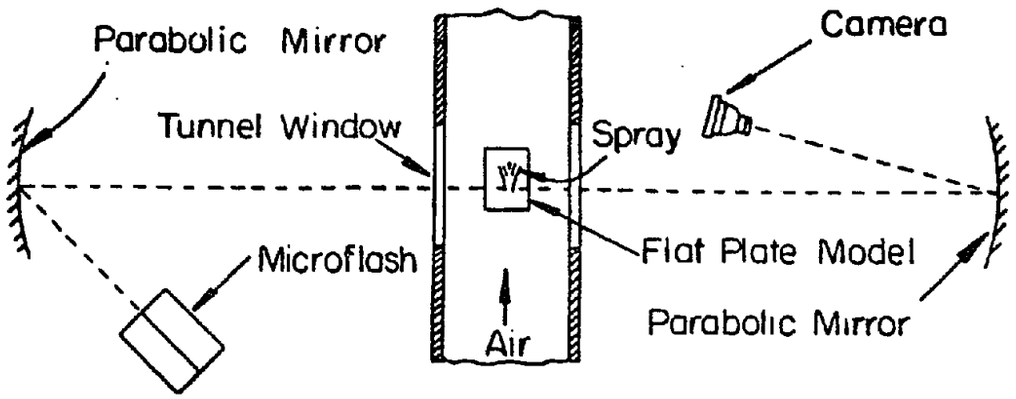

Fig. 2. Schematic optical setup for spark photographs.

The data collected during the test program consisted of the fluid injection and wind tunnel parameters corresponding to the spark shadow photographs. Water and air were used as the test fluids. Data was gathered for different sizes of injector nozzles at various levels of injection pressure and tunnel Mach number. Different injection angles were also examined.

Sets of penetration trajectory coordinates were extracted from each spark shadow photograph. A stepwise multiple linear regression was performed using coordinates associated with the maximum penetration depth (top curve in Fig. 3) and operating conditions. A generalized cold flow penetration trajectory equation was obtained in this manner having the following functional form:

$$X = f\ (Y,\ d_o,\ c_d,\ \alpha_e,\ \bar{q}) \qquad (7)$$

where X = axial distance from the injector
Y = radial penetration depth ("maximum")
d_o = orifice diameter
c_d = injector discharge coefficient
α_e = injection angle (free stream basis)
$\bar{q}$ = liquid-to-gas dynamic pressure ratio

The resulting equation is similar to the models given by Dobrzynski[14], in that X, rather than Y, was chosen as the dependent variable. This was preferred because Y is not a continuous function of X over the entire trajector path when the injection angle is greater than 90°. The rotated coordinate system proved to be a convenient way to handle upstream injection and avoid more cumbersome expressions.

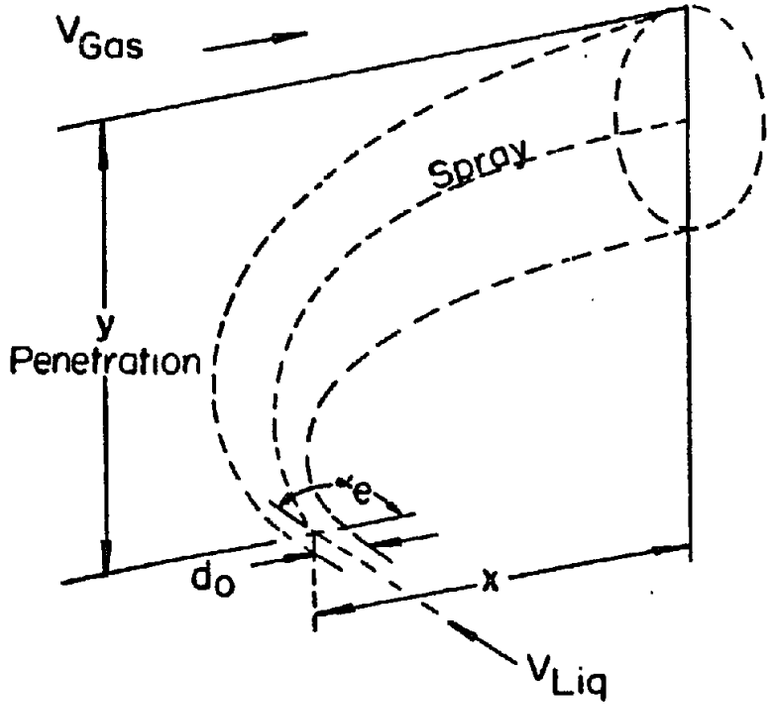

Fig. 3. Spray penetration trajectory coordinates.

The equation derived from cold flow simulation naturally cannot account account for deviations in penetration when the spray enters the high temperature and varied geometry ACR environment. However, the results permitted the design of an injection system suitable for the full-scale ACR high temperature flow tests which refined the cold flow penetration equation to assure kinematic similarity in a commercial ACR reactor.

Application of High Temperature-Short Duration Technology

The initial ACR experimental program proposed to test the scale-up criteria called for the construction of a 50 MM lb C_2H_4/year prototype reactor with its associated downstream gas processing facilities. This scale was originally thought to be the minimum size needed to assure the smooth start-up of a world scale olefin plant. When the technology and economics of this proposed ACR plant were examined, the cost of the total facility was found to be extremely high.

The problem was reconsidered and was divided into two distinct parts, (1) verifying the reactor design criteria at full scale, and (2) obtaining long term operating and ancillary scale-up data on the olefins process. It was estimated that the required operability data could be obtained from an intermediate scale unit. At the same time, a cost-effective breakthrough in the full scale reactor testing program was proposed. The combination of the test programs allowed the required information to be obtained at a relatively low cost.

The full-scale reactor tests were conducted with high temperature experimental technology originally developed by the aerospace industry and currently in use for testing NASA rocket engines[15,16,17]. These technologies make it possible to gather rocket engine data during test periods on the order of one second. A key factor in this technology is that fluid dynamic and chemical equilibrium can be achieved in small fractions of a second. The short duration of the tests allows for operation at temperatures above 2000°C in inexpensive equipment. As required, high temperature mixing of flows may be examined with non-destructive techniques and combustion product gases may be sampled.

Using this technology, it is possible to study the actual gas yields and fluid dynamics of a full-scale ACR at about two percent of the cost of a conventional chemical reactor prototype. One major factor contributing to this cost reduction is the use of standard construction materials (i.e., stainless steel rather than the high temperature ceramics), which must be used in a continuously operating ACR plant. In addition, the short test duration avoids the extensive supporting facilities and high utility costs associated with long tests at full scale.

Full Scale High Temperature Tests

Two full scale high temperature ACR experimental facilities were built at the Marquardt Company[18]. The first series of tests examined oil penetration in a two-dimensional version of the ACR operating at typical conditions. The experience gained from this facility was used to construct a second test facility which verified the full-scale ACR gas yields and confirmed the scale-up design methods. Both tests used similar equipment and experimental techniques.

The tests were run in multi-purpose rocket test cells. An overall schematic of the ACR gas yield test equipment is given in Fig. 4. The full-scale equipment was manufactured from uncooled 304 stainless steel. A water cooled burner was used to supply the cracking "steam" to the ACR test piece at commercial scale flow rates, pressures, and temperature. The burner was mated to the ACR venturi test piece through a choked orifice and a diameter transition section. The reactor venturi consisted of a converging region followed by the throat, diffuser and reactor cylinder sections. A variable area orifice at the end of the reactor was used to control the reactor pressure.

All of the experimental equipment was remotely controlled from inside a blockhouse. A bullet-proof window allowed the test equipment to be observed safely. During a test, the blockhouse was manned by several operators who controlled the flow and data systems. Flow data in the form of pressure and temperature readings from calibrated venturi flow systems were recorded automatically. Reactor and burner gas temperatures were measured with specially constructed thermocouples. The test piece was instrumentated with a series of pressure transducers throughout its length.

During a test, the following general sequence of events occurred as the operators followed their checklists.

- Cooling water flows were initiated in the burner.
- Igniter flows were brought up to a preset condition and the burner was ignited. This low combustion gas flow was allowed to preheat the piece.
- Main burner flows were slowly (5-15 seconds) brought up to the desired set point combustion conditions.
- After operators indicated all systems were "on condition", the data recording and oil injection systems were actuated.
- The data was recorded during the "on condition" time (5-20 seconds).
- The fuel, oxygen, and oil flows were then shut off with fast acting valves.

In the test hardware, there are rather large heat losses and corresponding combustion gas temperature drops which must be taken into account in order to generate the desired cracking temperatures at the oil injection location. For example, under typical ACR operating conditions, it is possible for the water cooled burner to lose on the order of 100°C in gas temperature. An additional 100°C in gas temperature is lost to the uncooled stainless steel transition ducting which connects to the test reactor. When running in the high temperature short duration mode, this significant heat loss is controlled by increasing the burner temperature while constraining the total mass flow near the cracking S/F level.

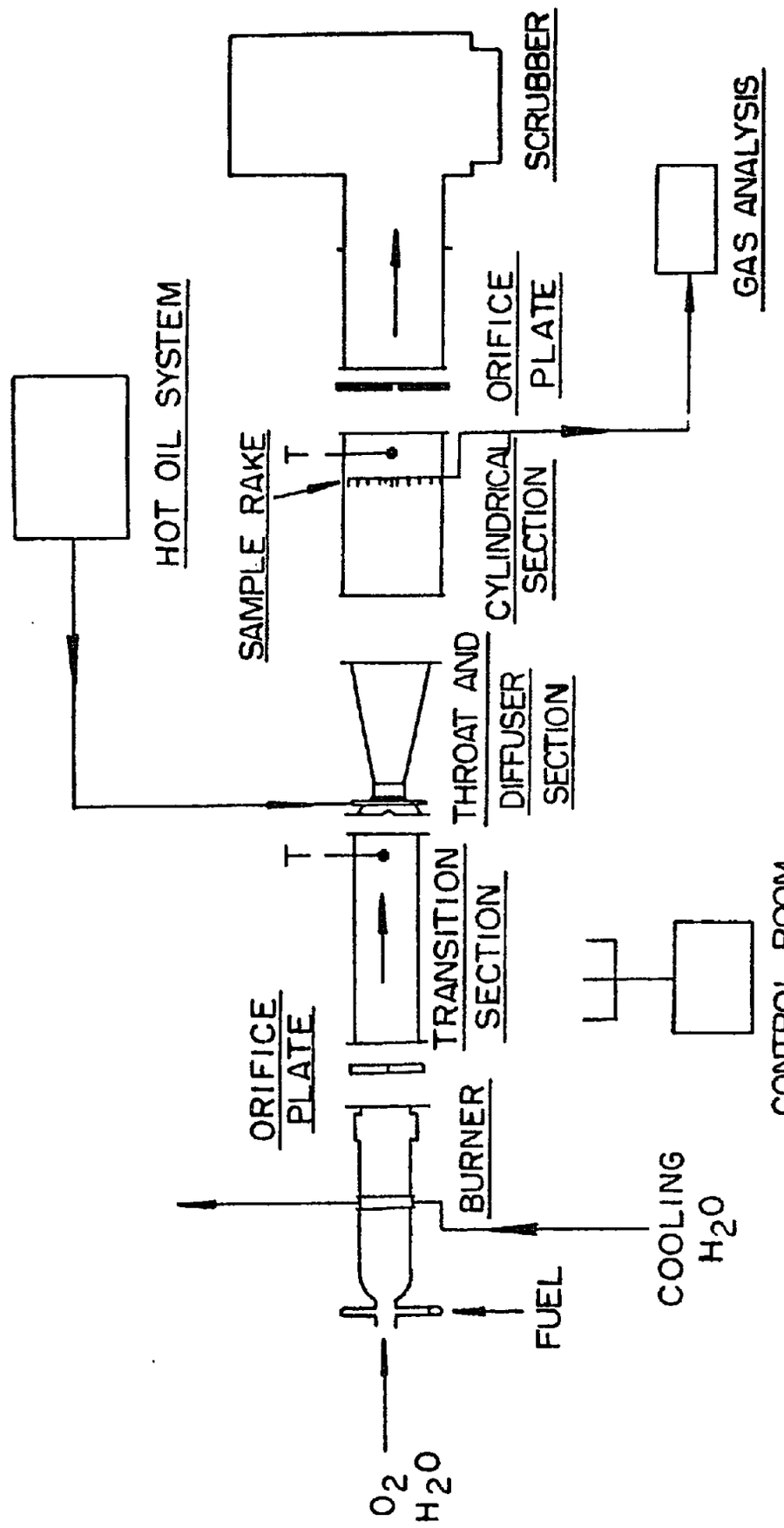

Fig. 4. Full scale ACR gas yield test equipment.

In order to predict the heat losses and operate the facility, a storage heat exchanges analysis paralleling that of Becker[19] was first performed for each desired ACR condition. The analysis included the simple cooling heat loss in the burner and the more complex time and position dependent transfer of heat to the walls of the transition section. Accounting for this type of heat storage is fundamental to high temperature-short duration operation, since it exists throughout the test assembly, including the reactor itself. For example, when the flows are at condition, the walls of the transition section near the burner exit are initially at a relatively low temperature (i.e., position = 0, time = 0, T_{wall} = 400°F). By the end of the test, the wall temperature has increased substantially (i.e., position = 0, time = 45 seconds, T_{wall} = 1500°F). This change in the transition section's average wall temperature is energy coupled with the gas temperature at the corresponding time and position.

During our short "on condition" test period, the heat loss associated with position rather than time is the dominating factor at the downstream oil injection location. The combustion gas temperature at this location is a prime process variable which was maintained nearly constant at the desired level. The temperature slightly upstream of the injection location was measured[20] at the 2000°C level and an experimental graph of the "steam" temperature-time profile taken during the gas yield test is shown in Fig. 5. This graph shows the burner ignition, operating changes in flows (ramps), and the constant level of "steam" temperature supplied during the "on condition" time.

Hot Flow Penetration Experiments

The full-scale ACR penetration test piece was equipped with large quartz windows in the throat region, which permitted the use of various laser-camera photographic techniques for recording the desired oil penetration and atomization data. In order to allow the windows to survive the typical 2000°C test conditions, a nitrogen film cooling technique was applied to the inner surface. The thin film of nitrogen was introduced into the combustion gas flow through a manifold and specially constructed knife edge slot positioned upstream from the windows in the test piece. Nitrogen film cooling was capable of protecting the entire exposed inner surface of the windows for up to 45 seconds.

The window design required the penetration test piece to be constructed with a rectangular cross-section rather than the typical circular ACR configuration. In order to duplicate expected ACR fluid flow parameters, the rectangular dimensions were sized to produce the area ratios and Mach numbers consistent with the originally proposed prototype ACR. A reactor cylinder was not required, since gas yields were not measured during this test.

In the test piece, the high temperature combustion gases converged into the venturi throat where oil was injected at high pressure from two opposing injectors located at the top and bottom. It was possible to observe the atomized oil vaporizing in the throat as it penetrates into the cracking gas stream. The resulting mixture then passes through the diffuser, exits into the atmosphere, undergoes combustion and finally passes into a high capacity vaccuum exhaust manifold.

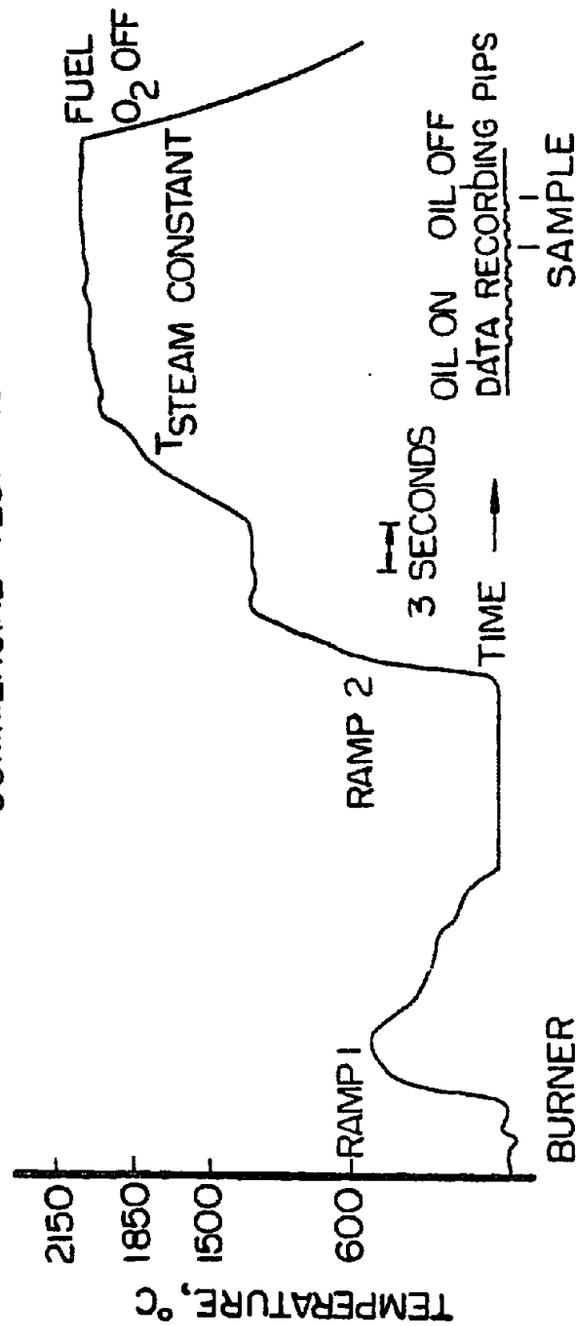

Fig. 5. Venturi inlet "steam" temperature-time profile.

The initial phase of the hot penetration experiments was conducted using TRW[9] optical techniques. These techniques were based on firing a high intensity ruby laser pulse (1/2 joule) through one of the test piece windows. The 5-50 nanosecond duration of the pulse effectively stopped the motion of the injected oil particles. The particle shadows were recorded with a lens-camera assembly (shadowgraphy) which was mounted on the far window. A similar experimental assembly was built to obtain "Gabor" holograms. Most of the test pictures were recorded on holographic plates, which were essentially grainless (∿3000 line pairs per milimeter). After the experimental program was completed, photomicrographic analyses were performed with a helium-neon laser interference reconstruction technique. Minimum oil particle sizes on the order of 10-50 microns could be detected in the test piece throat.

Double pulsing of the laser recorded two sets of bulk particle images on the same photographic plate. The measured particle distance travelled (∿1 cm) divided by the known time interval between pulses (20-400 u sec) was used to extimate the bulk particle velocity. The experimental velocities compare favorably with the theoretical velocities generated by the ACR computer model The computed droplet size and velocity histories in the ACR throat were generated from the cold flow test work droplet distributions. In the calculations, resistance to mass transfer from the droplet surface is assumed to be negligible. Thus, the rate of vaporization is controlled by the rate of heat transfer to the droplet surface which is at its boiling point. Also, it is assumed that the droplets are at a uniform temperature and they vaporize as in true boiling point distillation. The vaporizing drop phenomenon is then modeled by a film theory approach[21,22], in which the resistance to heat transfer is due to the film surrounding the droplet. The system conservation equations are then solved and the velocity of the vaporizing droplet is changed as momentum is transferred between the droplet and the gas by aerodynamic drag and by mass transfer.

During some of the penetration tests, a high-speed movie camera (16 mm Fastex) was used to record the time dependent spray stability in the ACR throat region. Film taken at 2,000 and 10,000 frames per second was then slowed down for data analysis. Also, conventional cameras (70 mm, Super 8) recorded the bulk oil spray by time integrating the overall oil penetration over relatively long exposure times (1/50 second). In this technique, the light from the oil-air combustion at the exit of the test piece diffuser illuminated the fine oil droplets in the throat. Color photographs showed the oil penetration as a well-defined light region. A reference grid on the window allowed the appropriate penetration coordinates to be taken from the photographs. The hot test penetration data was then compared to the cold test predictions.

The experimental data permitted the extension of cold flow work resulting in the desired high temperature oil penetration correlations. The additional information on particle sizes, velocities, and spray stability was used to confirm and revise our present understanding of the flashing/atomization/vaporization phenomena occurring in the ACR.

Full Scale Gas Yield Test

The full scale ACR gas yield test equipment is illustrated in Fig. 4. The appropriate ACR combustion gas temperature and mass flow rates (T ∿ 2000°C, W <25 lb/sec) were generated in a manner similar to the hot penetration investigation. A hot oil system injected preheated oil at commercial flow rates (5-15 lb/sec).

A typical reactor cylinder temperature-time profile taken during the test is shown in Fig. 6. This figure illustrates the general series of events controlled by a minicomputer. After the combustion gas temperature was brought "on condition", the oil was injected and the oil cracking rapidly lowered the reactor temperature. Constant flows were maintained and the reactor temperature remained approximately constant with a slight drift upwards. A number of vacuum, purge and sampling valves were actuated with the cracked gas sample being taken near the end of the oil injection period. Individual samples were simultaneously taken across the reactor cylinder diameter. Several hundred reactor volumes passed the sample probe during the sampling period. Pressure and temperature data were automatically recorded. The oil was then shut off, causing the reactor temperature rise due to the pure combustion gas flow condition.

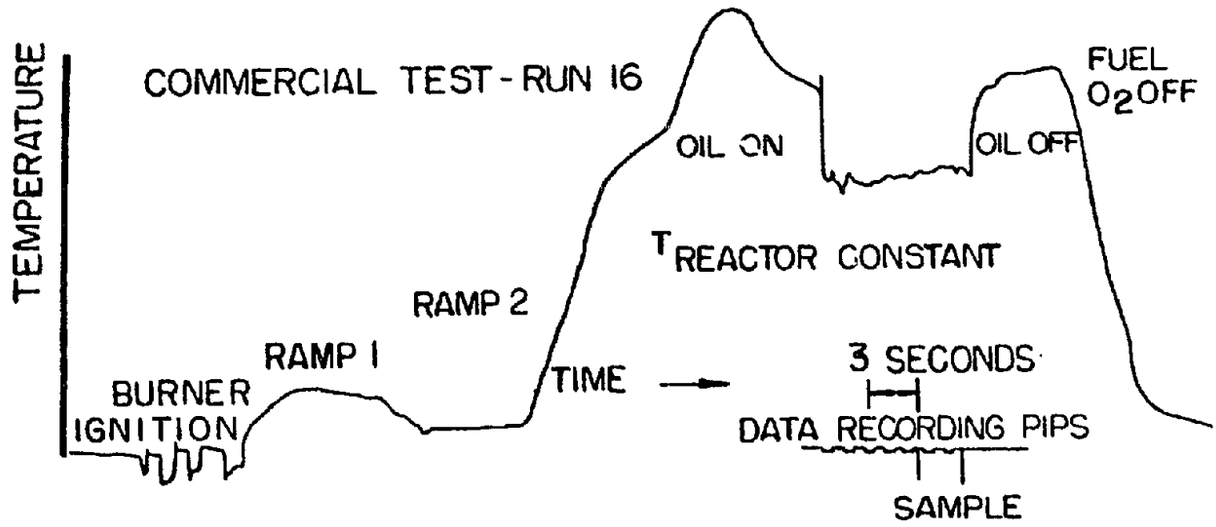

Fig. 6. Reactor exit temperature--time profile

The collected gas samples were analyzed batchwise with a gas chromatographic system. An Argon gas tracer technique was used to determine the actual gas yield concentrations in the reactor. This technique was based on introducing a small but extremely well-known flow of Argon into the burner.

The Argon in the reactor was measured and ratioed to the hydrocarbon reactor products. These ratios were multiplied by the known Argon mass flow to determine the absolute flow of reactor hydrocarbon products, which was then converted to a gas yield basis (lb/100 lb oil).

Computer data analysis was conducted on site. The yields were then best-fit regressed as a function of operating variables. Yield response contour maps around the base ACR operating case were also generated. This procedure was augmented by statistically designing the test around directly controllable operating variables. The general design allows one to obtain the maximum information from a minimum of data. This technique also avoids necessity of exactly matching all the process variables simultaneously. The inherent control problems of the short duration method are also minimized.

Since the described short duration technique was somewhat unique as a reactor gas yield test method, a reference test of a well known production oil cracking reactor was first run to calibrate the system. The reference reactor chosen was the crude oil cracker which is part of a production plant operated by one of our ACR partners, Kureha Chemical Ind., Ltd. The Kureha plant reactor operates at conditions approaching that of an ACR.

The reference test was conducted in a stainless steel reactor assembly which was sized to duplicate the Kureha reactor geometry. The experimental operating conditions compared favorable with the actual plant conditions. In particular, the steam temperature, S/F ratio, residence time, oil feed rate and heat input were matched very closely. However, the reactor exit temperature was somewhat lower than that of the operating plant. The experimental gas yields for ethylene, ethane, propylene, and propadiene agreed very well with the plant. There were slightly lower experimental values for hydrogen, methane, acetylene and total gas, which indicated a less severe crack.

In the reference test, the low reactor exit temperature at the constant plant energy input conditions indicates the expected higher heat losses in a short duration reactor. The corresponding lower overall temperature profile through the test reactor length reduces the process kinetic time-at-temperature. The associated gas phase chemical kinetics at the lower residence times are believed to be responsible for the slight discrepancies in the reference test gas yields. Also, the "true" enthalpy used for cracking is lower than that indicated by the measured reactor temperature.

The reference test work was used to calibrate and revise the operating procedures for the full scale ACR test. The additional reactor heat loss was accounted for by slightly increasing the process combustion gas flow location constant. This added energy made up for the reactor heat loss resulting in a reactor exit temperature which experimentally matched the pilot scale data. However, this technique actually corresponds to a slight increase in the overall temperature profile through the short duration reactor length. The temperature differential between the typical plant ACR case and the short duration reactor is greatest at the oil injection control volume. This is also the region of the highest process temperature, which tends to generate high C_2H_2 yields.

Based on the temperature profile, a kinetic analysis of this short duration heat loss adjustment technique predicts a slightly more severe cracking condition compared to the typical ACR operation. This effect is most pronounced near the oil injection region and decreases through the reactor length. The combined result is to slightly increase the C_2H_2 yield and correspondingly lower the C_2H_4 yield while keeping the total C_2's and total gas yield approximately constant. When the test is conducted without the heat loss adjustment technique, the initial process temperature at the oil injection control volume is equal in the short duration and continuous plant cases. However, as indicated by the Kureha reactor reference test, the final temperature at the reactor exit is too low. This tends to produce the same general quantities of C_2H_2 near the high temperature oil injection region while other yields fall off because of the lower overall temperature profile through the short duration reactor. Since the short duration test technique does not match both the oil injection region and the reactor exit temperatures simultaneously, combinations of the heat loss adjustment technique were run in the test design. The expected yield effects were observed experimentally and when they were accounted for, the full scale ACR yield distribution followed the pilot scale cracking pattern.

Thus, the ACR scale criteria has been verified under the extreme condition of directly scaling from a pilot to a full scale reactor. This allows the smaller scale ACR demonstration unit to be designed with confidence. As required, the data from the demonstration unit will be used to further refine the scaling techniques before the commercial ACR process design is finalized.

REFERENCES

1. Hosoi, T., and Keister, R. G., Chem. Eng. Prog., *71*, 63 (1975).

2. Ozaki, K., et al., Japan Patent Application Kokai (90302/1976), *Method of Recovering Heat from Hydrocarbon Thermal Cracking Products*, August 7, 1976. (See Chem. Wk. Sept. 28, 1977, p. 39).

3. Johnstone, R. E., and Thring, M. W., *Pilot Plants, Models and Scale-up Methods in Chemical Engineering*, McGraw-Hill, New York, 1957.

4. Walas, S. M., *Reaction Kinetics for Chemical Engineers*, Ch. 10, "Scaling Test Results", McGraw-Hill, New York, 1959.

5. Shapiro, A. H., *The Dynamics and Thermodynamics of Compressible Fluid Flow*, Ronald Press Co., New York, 1953.

6. Putnam, A. A., et al., *Injection and Combustion of Liquid Fuels*, Ch. 3, "Design of Atomizers", WADC Technical Report 56-344 (1957).

7. Mugele, R. A., and Evans, H. D., I and EC, *43*, 1317 (1951).

8. Dombrowski, N., and Wolfsohn, D. L., Trans. Instn. Chem. Engrs., *50*, 259 (1972).

9. TRW Defense and Space Systems Group, Redondo Beach, Calif.

10. Ingebo, R. D., and Foster, H. H., *Drop-Size Distribution for Cross-current Breakup of Liquid Jets in Airstreams*, NACA Technical Note 4087 (1957).

11. Geery, E. L., and Margetts, M. J., J. Spacecraft, *6*, 79 (1969).

12. Hojnacki, J. T., *Ramjet Engine Fuel Injection Studies*, AFAPL Technical Report 72-76 (1972).

13. McDonnell-Douglas Aerophysics Laboratory, El Segundo, Calif.

14. Dobrzynski, W., *Deutsch Luft-und Raumfahrt (German Aeronautics and Astronautics)*, Research Report 72-19 (1972).

15. *Main Engine Test Program Accelerates*, Aviation Wk. and Space Tech., 59, Nov. 8, 1976.

16. Wuerker, R. F., Matthews, B. J., and Briones, R. A., *Producing Holograms of Reacting Sprays in Liquid Propellant Rocket Engines*, JPL Contract No. 952023 (NAS 7-100), 1968.

17. George, D. J., and Spaid, F. W., *Holography as Applied to Jet Breakup and an Analytical Method for Reducing Holographic Droplet Data*, Tech. Report AFRPL-TR-72-72, 1972.

18. The Marquardt Company, Van Nuys, Calif.

19. Becker, J. R., *Analysis of Storage Type Heat Exchanger*, The Marquardt Co., October 15, 1956 from H. Leitinger, *Research on the Design of Hypersonic Nozzles and Diffusers at High Stagnation Temperatures*, Part 1, Appendix 4 (WADC 55-507).

20. *High Temperature Thermocouples*, Manual 48125, probe T-1105, Aero Research Instrument, American Standard.

21. Priem, R. J., and Heidmann, M. F., *Propellant Vaporization as a Design Criterion for Rocket-Engine Combustion Chambers*, Technical Report R-67, NASA, Lewis Research Center, Cleveland, Ohio, 1960.

22. Beer, J. M., and Chigier, N. A., *Combustion Aerodynamics*, Halstead Press, New York, 1972.

Comments and Replies on

"Development of Scaling Methods for a Crude Oil Cracking Reactor Using Short Duration Test Techniques"

Presented by G. R. Kamm

J. Bett: It's hard to imagine testing something close to a full-scale reactor in this time frame.

G. Kamm: We did it! I'll show you the graphs recording our test data. I will say that we didn't get quite as sophisticiated as NASA, running full-scale rocket engine tests in the one-second time frame. We took it slow. Running 10 second tests one can easily reach chemical and fluid dynamic equilibrium. Of course, this type of testing does not prove long term operability.

R. Edelman: What criteria were you using and what degree of scale-up were you trying to achieve. Were you really trying to duplicate something?

G. Kamm: The criteria we used is described in detail in the paper. We used dynamic and kinematic similarity concepts to scale. Chemical similarity or matching our reactor yields (small-scale vs. full-scale) was our measure of success.

It turns out that how you inject the oil feed is important from the standpoint of product distribution and making efficient use of energy. If you have a poor spray pattern, some of the oil feed is cracked very hard and makes a lot of acetylene. Acetylene is a useful chemical but it consumes a large amount of energy. You really don't want to make acetylene.

J. Young: Did you work on scaling injectors?

G. Kamm: We did a survey of the literature, gathering all the data on injector scaling. Then we designed and tested injectors that were of commercial interest to us, testing in both pilot and commercial scale and tuning them to our application. We also tuned the penetration and droplet size distribution correlations for our application.

R. Edelman: How did you measure droplet size?

G. Kamm: For the most part, we used laser shadow photography and laser holography. Droplet measurements are

easily done in low velocity non-combustion type environments. Laser holography will look through a high velocity luminous flame and still measure droplet size down to the theoretical optical limits of the system, about one micron. A nice piece of work was done by TRW under contract to RPL on this subject.

I. Osgerby: What is the function of that last orifice plate before the scrubber?

G. Kamm: The reactor runs at pressures significantly above those that are used in commercial tube cracking technology which is about 20 lbs. The orifice plate just creates back pressure.

R. Edelman: Can you set the range of the residence time in the reactor?

G. Kamm: Yes.

R. Edelman: Can you comment on the reproducibility of your fuel injector?

G. Kamm: We worked with the Marquardt Company who does quite a bit of ram jet work. They used to do very careful machining on each nozzle they used. What they do now is buy commercially available injectors, test each one, and use the ones that pass. We do careful machining and calibration on each nozzle that we use and we feel that they are reproducible.

R. Edelman: Did you run into any kind of instability problems?

G. Kamm: No chugging or screaming of any kind.

M. Zlotnick: It sounded like the main thing that you're doing in your scaling is you're making tests using less fuel. You're doing the test in ten seconds, and that's why it looks like a full-size rig, except you're running it for a shorter time.

G. Kamm: If we put the whole process package together to run a full-scale prototype reactor continuously, the difference in cost would be over two orders of magnitude higher.

M. Zlotnick: Why is it more?

G. Kamm: To build a full-scale facility to operate continuously (say hours), takes better than two years. You, in essence, are building a facility that's going to last ten years or more. You're going to be in a commercial plant. You are restricted by the safety requirements,

design criteria. You need ceramic lined vessels, big utility and feedstock supplies, and have strict health and pollution requirements. When you run ten seconds, you can avoid most costs associated with this type of operation.

A. Varma: I got a little confused. What was the size of your test facility?

G. Kamm: The reactor test facility was full commercial scale. We make about one hundred million pounds a year of ethylene per reactor. We use about ten pounds a second of feedstock.

A. Varma: In the penetration tests that you showed, were they, also, basically on full-scale?

G. Kamm: The throat section was full-scale as were the injectors.

R. Edelman: Was there any indication of the build-up of deposits?

G. Kamm: We are very sensitive to deposits both in our full-scale facility and in our small-scale facilities that run continuously. There is no residue build-up in them. We're building a sizeable, but less than full-scale demonstration unit. We will run it for about a year to prove long term operability.

I. Osgerby: Have you run any tests where the walls and everything else are hot for a long time?

G. Kamm: Yes. Typically, that's the way we run our small scale continuous systems. The walls are ceramic. They are hot.

I. Osgerby: You don't have any coking problems?

G. Kamm: Well, it depends on your feedstock. Our feedstock of choice is something like Arab light crude with the asphalt taken out. We go through a little refinery operation on the front end of the process, atmospheric and vacuum distillation. If you need asphalt or asphaltenes in significant quantity, they tend to deposit and plug the reactor.

K. Ushiba: When you say vacuum distillation -- that means you were just feeding vacuum gas oil?

G. Kamm: No. The feed depends on the crude used. If you have a nice, light north African or Pennsylvania crude, you can feed the whole barrel. We want to develop a process that will proliferate through the industry. We don't want a special situation process.

SMOKE AND FIXED NITROGEN SPECIES IN LABORATORY SCALE OIL FLAMES*

B. W. Gerhold, C. P. Fenimore, and P. K. Dederick
General Electric Company

Presented by B. W. Gerhold

INTRODUCTION

Previous studies (1) of two stage rich-lean combustion demonstrated that for both plain and N-doped oil, NO, HCN, and NH_3 were formed in the rich first stage flame. The latter species were essentially quantitatively oxidized into NO in the fuel lean second stage and for some conditions, were the major source of NO in the lean gas. The current experiments evaluated the effect of preheated air on the fixed nitrogen species and studied the effects of mixing and air preheat on smoke and hydrocarbon emissions from rich flames. This text presents an extended abstract of an oral presentation describing the apparatus, operating procedures and presenting the data. Additional discussion of fuel rich spray flame chemistry was published previously (1).

APPARATUS

Figure 1 is a schematic of the apparatus. First stage combustion air enters a plenum chamber at the base of the apparatus and is developed into a uniform flow concentric with an air atomized fuel nozzle (Delevan 30609-2).

A turbulent spray flame stabilized above the nozzle without a pilot and the burned gas was contained in a well insulated chimney. As shown in Figure 1, the chimney was constructed by insulating the inside of a 10 cm L.D. RA 26-1 tube with zirconia and insulating the outside with an alumina-silica tube.

The two air flow rates (atomizing air, first stage combustion air) were measured with calibrated critical flow orifices and are expressed as volume flow rates at atmospheric pressure and 25°C. Number 2 heating oil ($CH_{1.69}\ O_{.0043}$, LHV = 1.02×10^4 cal/gm) was fed to the fuel nozzle via a variable speed gear pump and the flow rate measured during the experiments by timing the draining of a buret. The equivalence ratio of the burner was verified by comparing the measured mole fraction CO_2 with that calculated from a carbon balance using the measured fuel air flow rates.

GAS ANALYSIS

The burned gases were sampled at the exit of the chimney where uniform profiles were verified. A water cooled (20°C water) stainless steel sampling probe was operated with a choked orifice at the tip. The sample

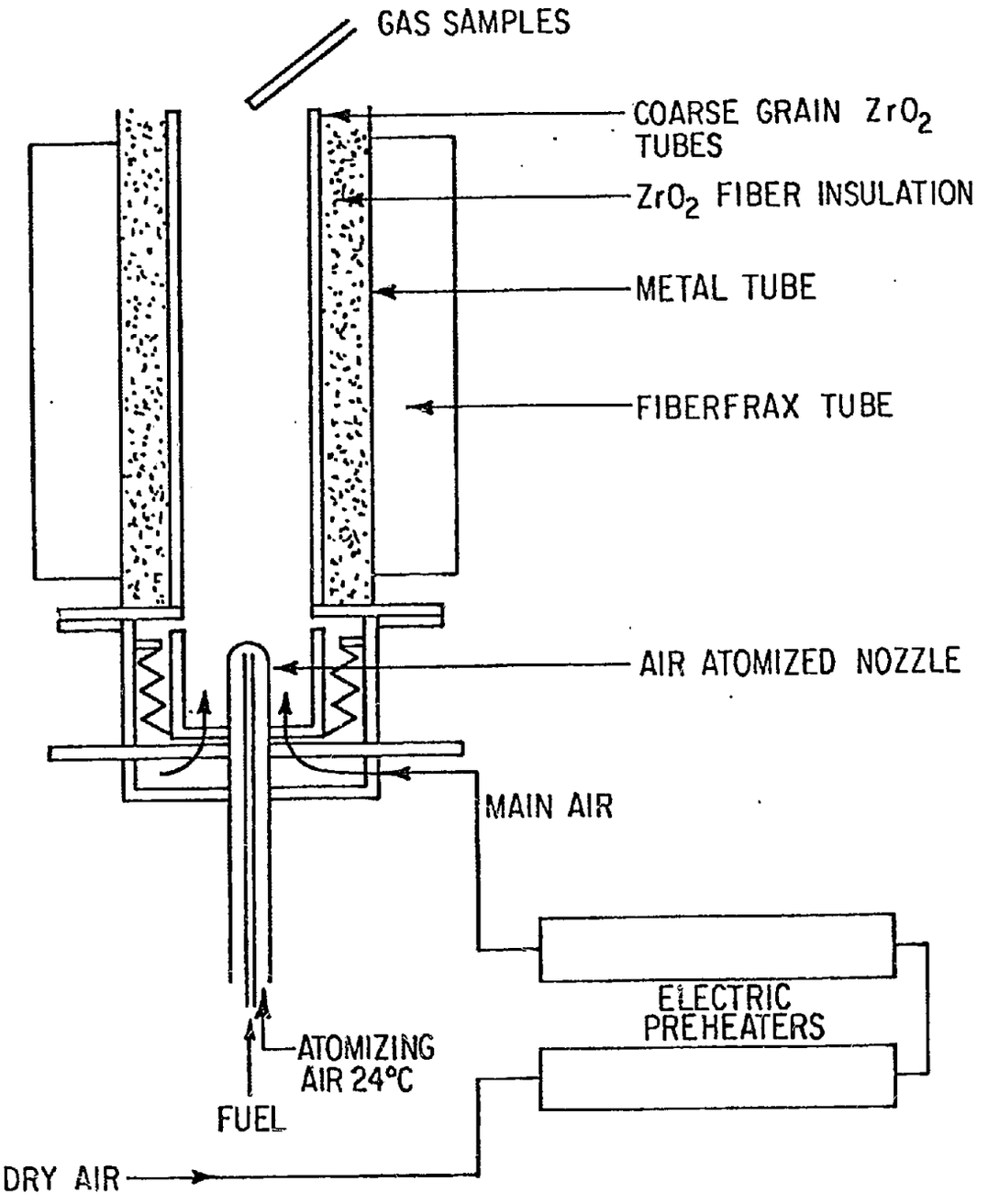

Fig. 1. Apparatus Schematic. The course grain ZrO_2 Tube with 6 cm I.D. with 3 cm walls and was insulated with 1.8 cm thick packed ZrO_2 fiber and a 15.25 cm O.D. Fiberfrax tube.

was dried in an ice bath condenser, filtered for soot, and analyzed for NO and CO_2 using Beckman NDIR analyzers. A Drierite canister was placed immediately upstream of the NO instrument to eliminate interference by water.

Unburned hydrocarbons were measured as ppm CH_4 using a Bendix 8402 total hydrocarbon flame ionization detector. These data are a lower limit to the total hydrocarbon mole fraction because the heavier hydrocarbons condensed when the sample was filtered and cooled.

Ammonia (2) and HCN (3) were measured via colormetric wet chemical techniques. Using the same probe, a measured volume gas sample was filtered and bubbled through .1 N H_2SO_4 to collect NH_3 or .1 N NaOH to collect HCN using a gas wash bottle (Corning 3170, 350 ml coarse frit). After a sample was collected, the sample probe, lines and filter were flushed with water which was added to the absorbing solution to include contributions dissolved in condensate remaining in the sampling system. Smoke was determined qualitatively by continuously passing a sample through a moving filter tape (75 cc sample/cm^2 tape) and measuring the reflectance of the smoke stain relative to the clean paper. The smoke sampling system (probe and lines) were heated to 60°C to prevent condensation.

OPERATING PROCEDURE AND DATA REDUCTION

The apparatus was operated for about 1 hour prior to an experiment to establish a steady state temperature of the metal tube (typically about 1400°K). The total air flow rate (atomizing air + main air) was held at 4.5 ℓ/sec and the overall equivalence ratio ([fuel/total air]/[stoichiometric fuel air ratio]) was varied by changing the fuel flow rate.

The NO emissions are reported as an emissions index

$$NO/C \equiv \frac{NO\ (ppm)}{(CO + CO_2)\ ppm} \qquad (1)$$

that were obtained from the measured NO and the calculated adiabatic equilibrium (CO + CO_2) based on the measured fuel and air flow rates.

The NO/C emissions index differs by a constant factor (2.17×10^3 for this fuel) from the more conventional index of g NO/kg fuel. However, for evaluating the total fixed nitrogen, the NO/C index was preferred because one can directly sum fixed nitrogen contributions from NO, HCN, and NH_3 if the latter two are similarly expressed as HCN/C and NH_3/C.

FIXED NITROGEN SPECIES

Figures 2 and 3 present the measured emissions indices for the fixed nitrogen species NO, NH_3 and HCN versus the overall equivalence ratio for inlet air temperatures of 298°K and 596°K. These data demonstrate the relative importance of the three fixed nitrogen species. HCN and NH_3 are fuel nitrogen species that will nearly quantitatively be converted into NO

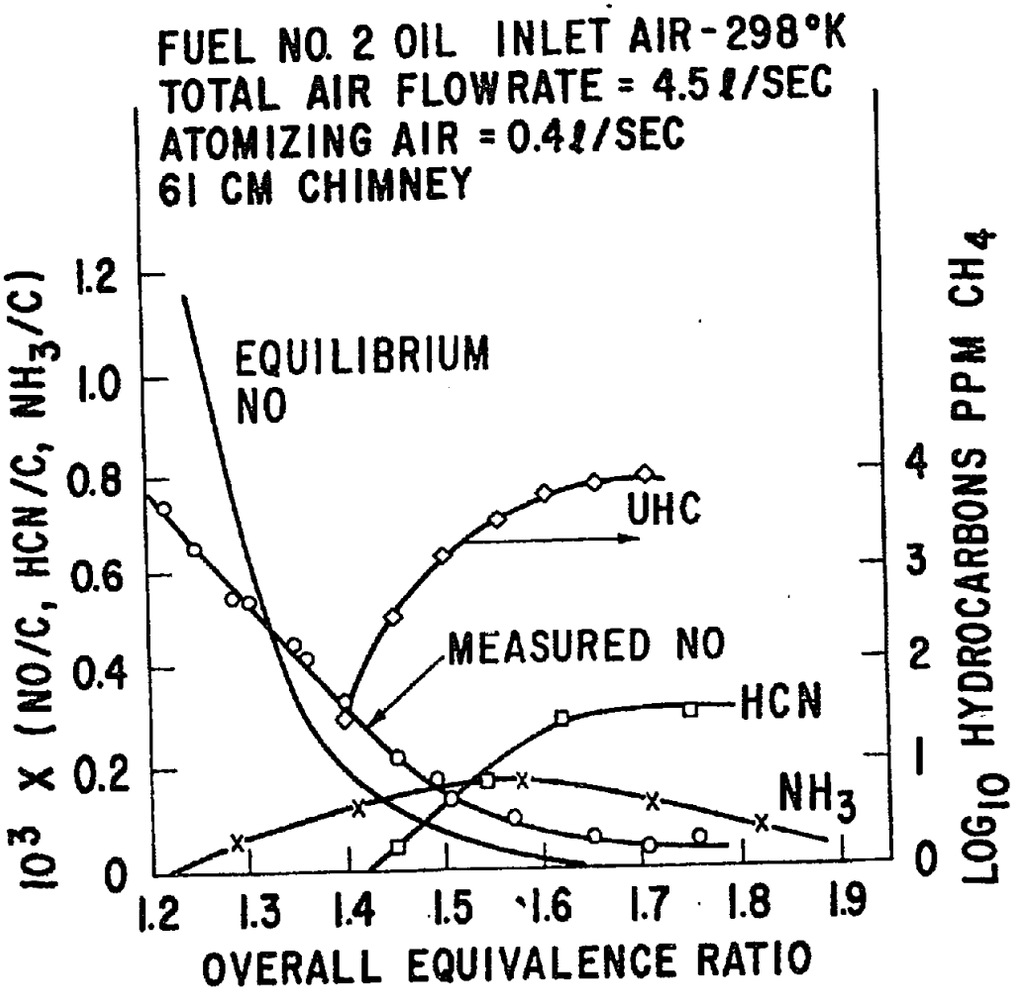

Fig. 2. Measured distribution of fixed nitrogen species, unburned hydrocarbons and equilibrium NO for fuel rich No. 2 oil/298°K air flames.

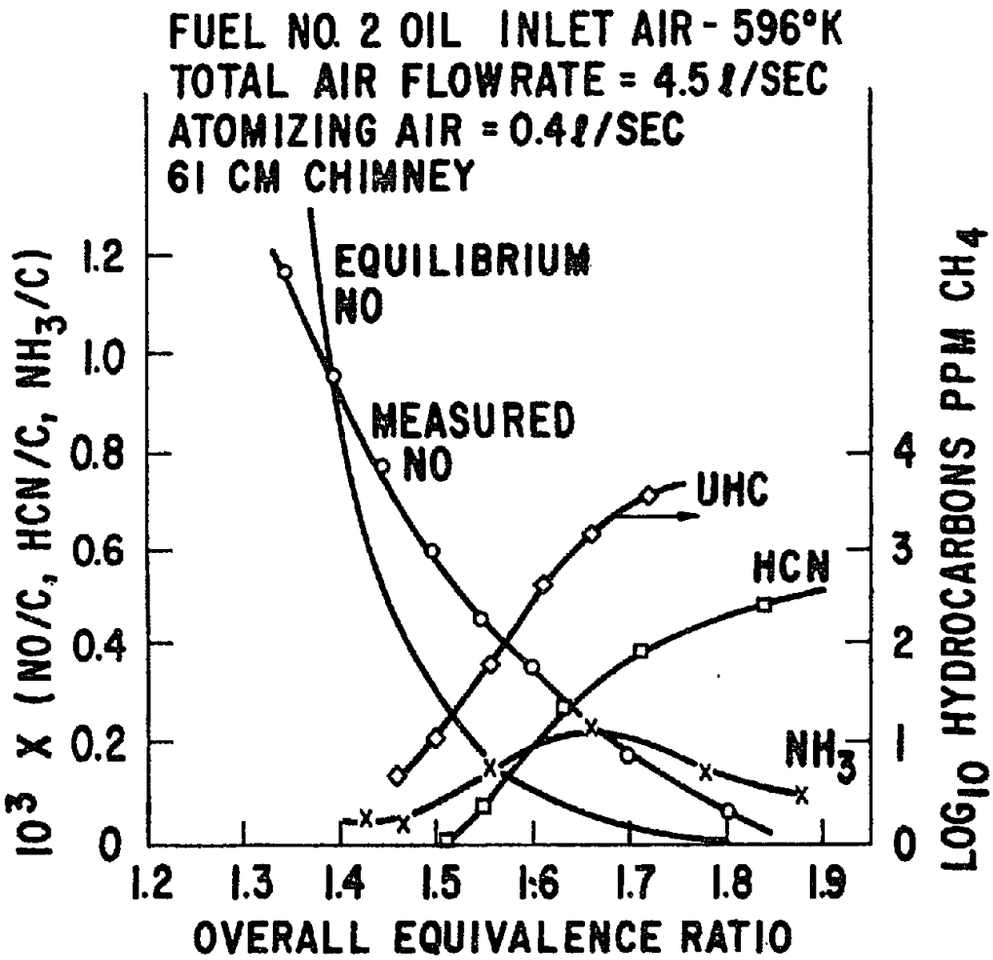

Fig. 3. Measured distribution of fixed nitrogen species, unburned hydrocarbons and equilibrium NO for fuel rich No. 2 oil/596°K air flames.

in an oxidizing environment. Consequently, if the HCN and NH_3 remain in the rich gas, the NO emissions index of the rich flame products is not representative of the total NO that would be generated by the system.

The equilibrium NO emissions index is also presented in Figure 2 and Figure 3. Note that HCN and NH were found only when $NO > NO_{eq}$ which has been interpreted (1) as one indication that HCN and NH_3 were formed from NO generated in locally stoichiometric flame zones.

Figure 4 presents the smoke number (100 = no smoke) versus the overall equivalence ratio for three atomizing air flow rates and inlet air temperatures of 298°K and 596°K. The smoke emissions were relatively insensitive to the inlet air temperature showing only a minimal decrease with preheated air. However, increasing the atomizing air flow rate, which both increases the mixing rate and improves atomization, is a very effective means for decreasing the smoke formation.

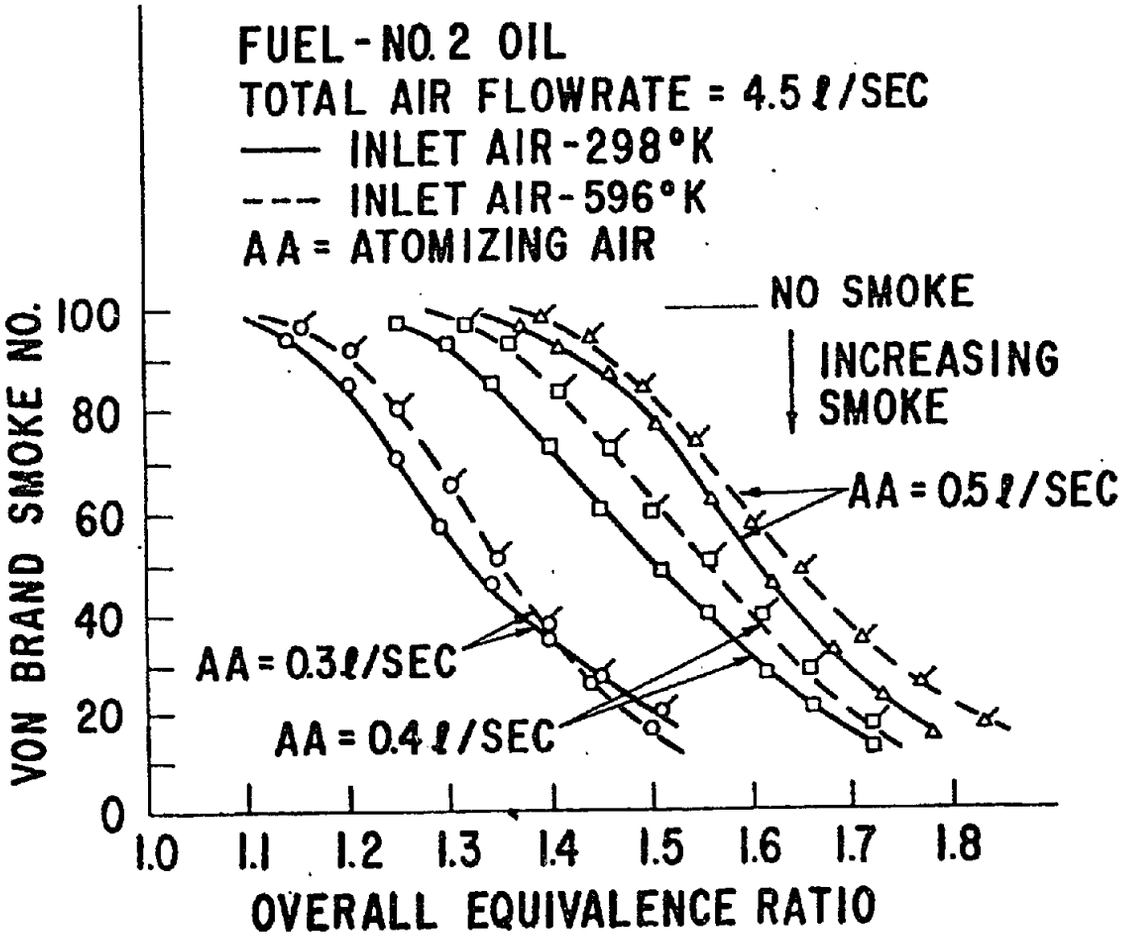

Fig. 4 Qualitative variation of smoke emissions versus the overall equivalence ratio. Data are shown for three atomizing air flow rates with both ambient (298°K) and preheated (596°K) inlet air. The flagged points represent the preheated air data.

The total unburned hydrocarbons were measured coincident with the smoke and these data are presented in Figure 5. Unlike the smoke data, the unburned hydrocarbons are not significantly effected by the atomizing air flow rate but are more dependent on the inlet air temperature. Therefore, the total UHC and smoke emissions do not appear to be related.

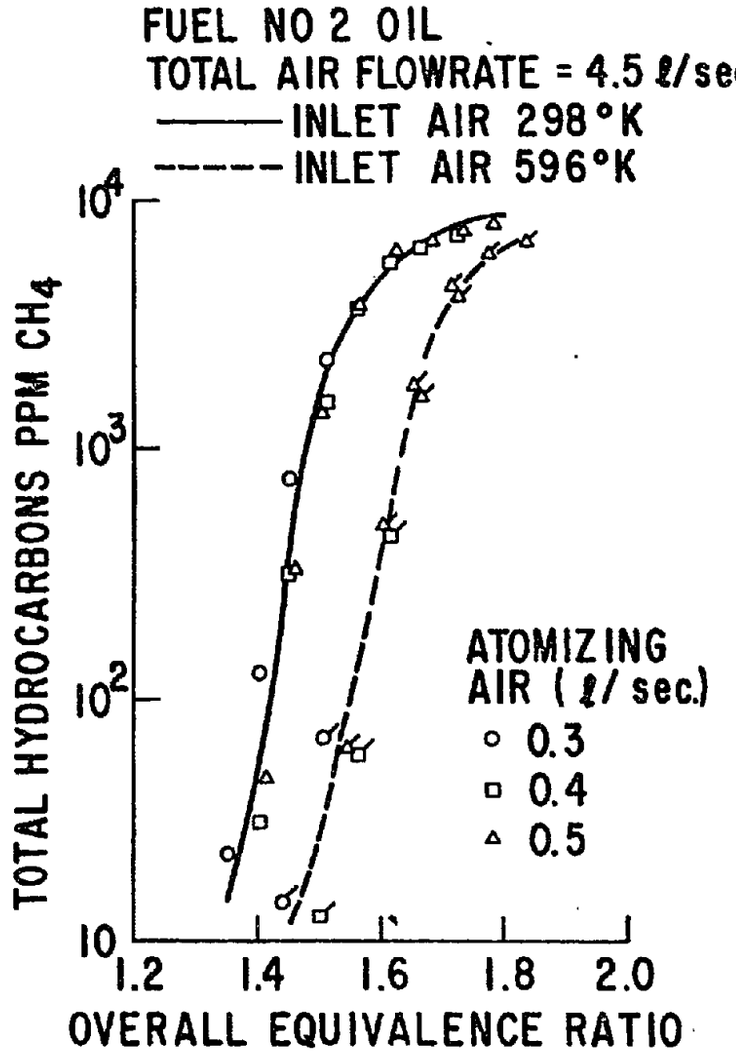

Fig. 5. Total hydrocarbon emissions measured as CH_4 versus the overall equivalence ratio for three atomizing air flow rates and both ambient (298°K) and preheated (596°K) inlet air. These data are a lower bound of the total hydrocarbons because the sample was dried to 0°C. The flagged points represent operation on preheated air.

CONCLUSIONS

Significant amounts of HCN and NH_3 are formed in rich flames and oxidation of these species in a fuel lean environment can increase NO emissions. Smoke and unburned hydrocarbon emissions do not appear to be related. Smoke is suppressed by improving mixing (higher atomizing air) while hydrocarbons were suppressed by preheated combustion air.

REFERENCES

1. Gerhold, B. W., Fenimore, C. P., and Dederick, P. K., *Two Stage Combustion of Plain and N-Doped Oil*, presented at Seventeenth Symposium (international) on Combustion, Leeds, England, August 1978.

2. *Standard Methods for the Examination of Water and Waste Water*, 14th Edition, American Public Health Association, Washington, DC, 400.

3. *Standard Methods for the Examination of Water and Waste Water*, 14th Edition, American Public Health Association, Washington, DC, 370.

ADIABATIC REFORMING OF DISTILLATE FUELS

J. A. S. Bett, R. R. Lesieur, D. R. McVay and H. J. Setzer
United Technologies Corporation
Power Systems Division

For dispersed fuel cell power plants both petroleum and coal liquid derived distillates are desired feedstocks for the fuel processor. The sulfur content of these fuels makes necessary high reactor temperatures in order to achieve suitable catalyst activity and fuel conversion at economic reactor space velocities. Thus, the rate constants for steam reforming on a nickel catalyst shown in Figure 1 indicate that reactor temperatures for reforming sulfur bearing fuels must be at least 600°F higher than those required to achieve the same conversion with low sulfur content fuels at comparable space velocities.

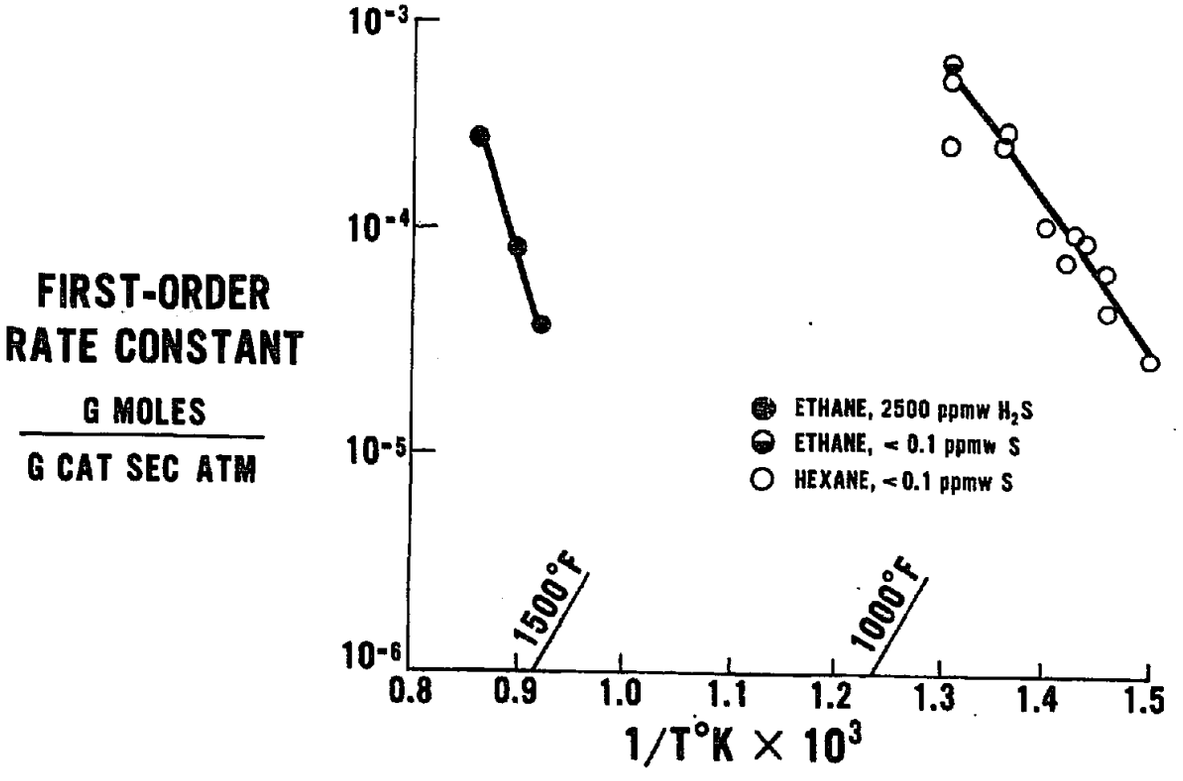

Fig. 1. Effect of Sulfur on Steam Reforming Activity of Supported Nickel Catalyst

The adiabatic reformer is being developed to process high sulfur and aromatic content fuels. In the adiabatic reformer high temperature is generated inside the reactor by combustion, eliminating the need for heat transfer through the reactor wall. Air is added to the reactor inlet in sufficient quantity so that the heat of combustion supplies the endothermic heat for reforming the remaining fuel. The thermal equivalence point, the point where the heats for combustion and reforming are equal, as in Figure 2,

occurs at an O_2/Fuel Carbon (O_2/C) molar ratio of about 0.27, varying slightly with fuel hydrogen content. Oxygen added in excess of this point, either to raise the reactor temperature to achieve catalyst activity, or as will be discussed later, to prevent the formation of carbon, will decrease the efficiency of the process for the fuel cell power plant, since product hydrogen is consumed. This relationship is illustrated in Figure 3. Design studies for the adiabatic reactor have used O_2/C = 0.36 as baseline. Operation of the reactor above this point incurs system cost or efficiency penalties from the baseline values.

$$(1 - x)\left[Cn\,Hm + 2n\,H_2O \rightarrow n\,CO_2 + \left(2n + \frac{m}{2}\right) H_2\right] \quad + \Delta H_1$$

$$x\left[Cn\,Hm + \left(n + \frac{m}{4}\right) O_2 \rightarrow n\,CO_2 + \frac{m}{2} H_2O\right] \quad - \Delta H_2$$

$$\Delta H_1 = \Delta H_2$$

Fig. 2. Adiabatic Reforming

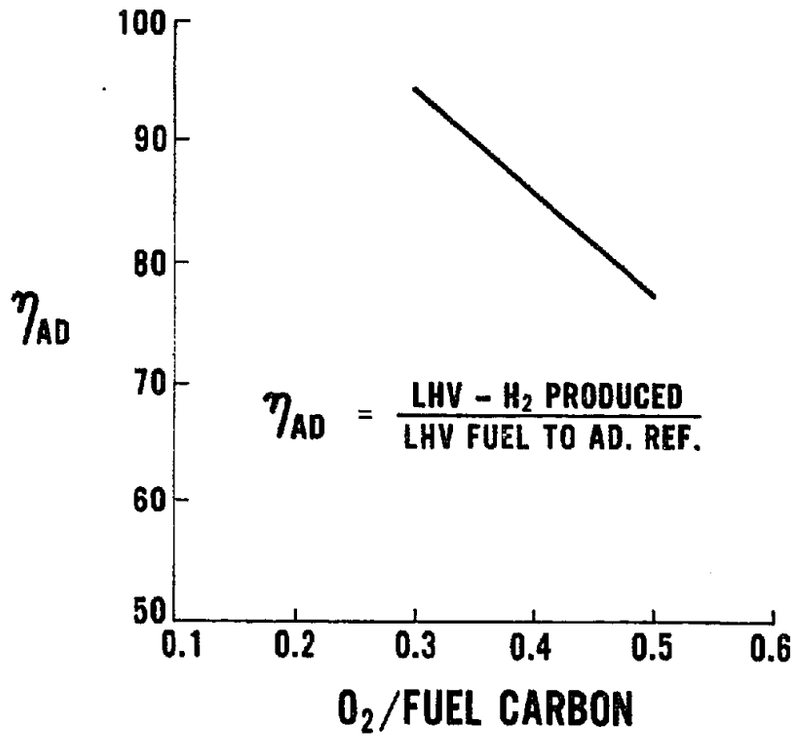

Fig. 3. Effect of O_2/Fuel Carbon Ratio on Adiabatic Reactor Efficiency

For development testing the adiabatic reactor was considered to have two elements: an entrance header section in which fuel was mixed with air and steam and in which combustion, cracking and some initial reforming occurred, and an exit section concerned principally with the catalytic reforming of methane. Justification for this division is found in Figure 4 which shows the rapid initial rise in temperature of the process stream, to approach the adiabatic flame temperature, followed by a gradual decrease as endothermic reforming of methane occurred. Hydrocarbon products exiting the combustion zone showed a product distribution typical of homogeneous cracking of reactant fuel. When carbon formed, it was found in the header section either on top of or a short distance into the catalyst bed. A 2-inch diameter (2 pph fuel) subscale reactor was used to study the effects of entrance header configuration and operating variables on O_2/C ratio required to prevent carbon formation. An idealized schematic of the entrance to the reactor is shown in Figure 5. Tests varied nozzle type, header shape, catalyst placement and process stream temperatures and compositions to achieve operation at minimum O_2/C ratios.

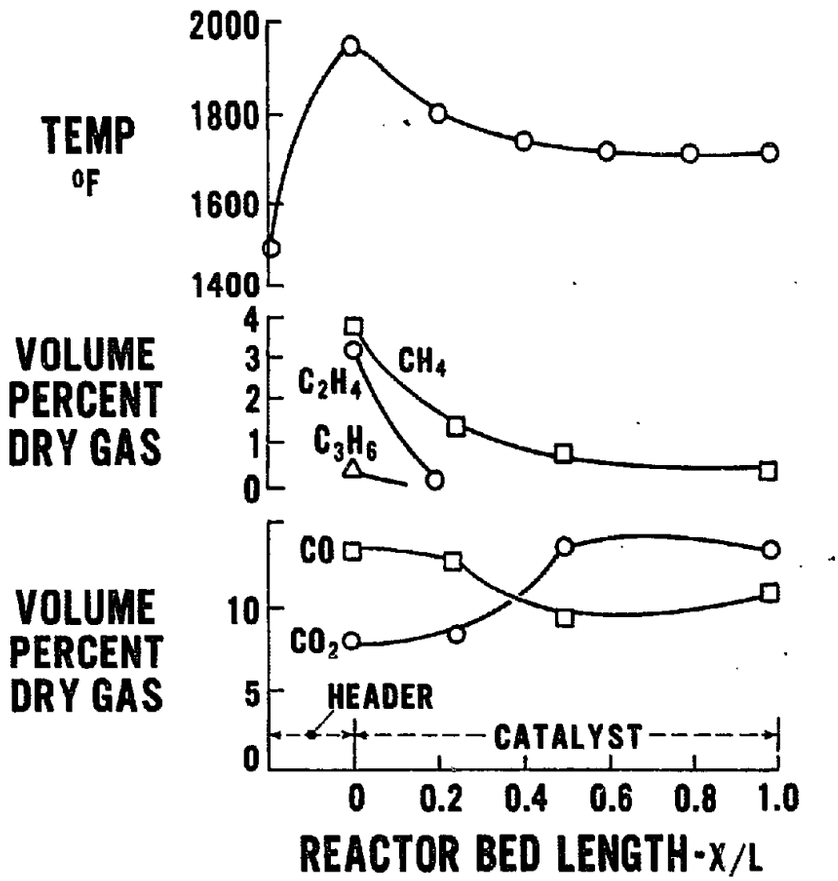

Fig. 4. Concentration-Temperature Profiles in the Adiabatic Test Reactor

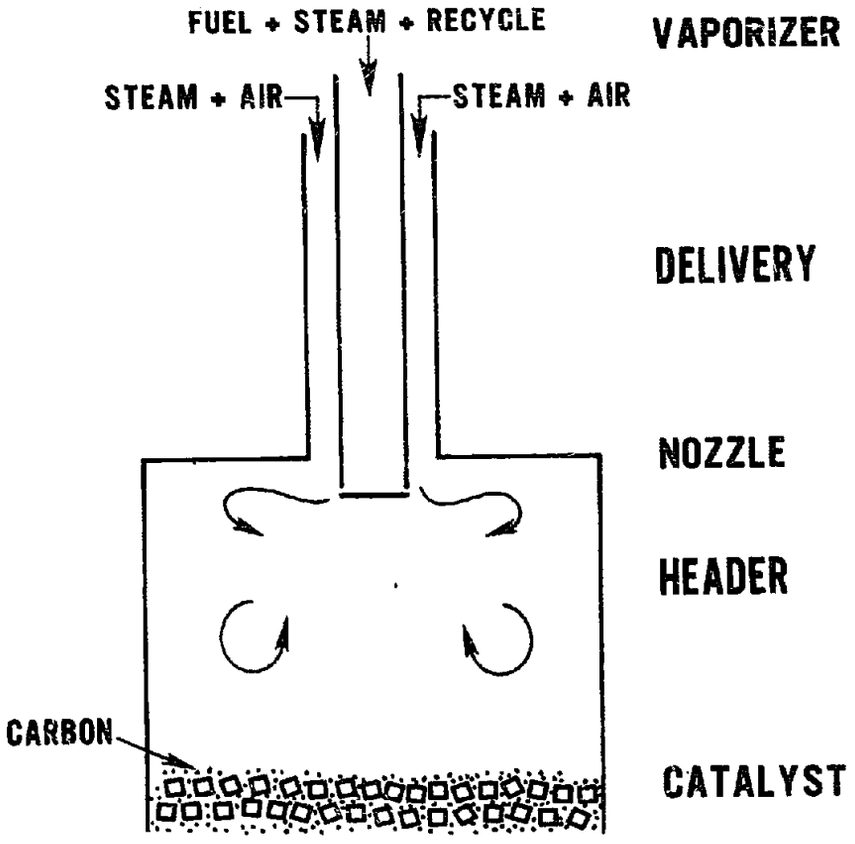

Fig. 5. Idealized Adiabatic Reactor

A 6-inch diameter (10 pph fuel) reactor was also used, to demonstrate scale-up of header deisgn, developed in the smaller reactor and to obtain data for conversion of residual methane. A schematic of the test rig is shown in Figure 6. Methane conversion was not a limiting factor in the performance of the reactors tested. Since the focus of the present workshop, mixing and scale-up, concerns the behavior of the header section, exit conversions are not considered further.

Characteristic behavior, typical of every header configuration tested is shown in Figure 7. At fixed pre-reaction temperature (temperature of the reactor mix prior to combustion) the reactor operated stably at high values of O_2/C. Air flow was reduced to a value for O_2/C where pressure drop across the reactor increased, indicating build-up of carbon in the reactor. Gradual increase of the O_2/C value from this point reduced the rate of pressure increase until an O_2/C value was determined at which pressure drop decreased and carbon burned off. By repeating this procedure at several pre-reaction temperatures a line of O_2/C values could be defined, above which the reactor would operate carbon free and below which it would rapidly plug with carbon (Figure 8). The operating line or carbon boundary was a characteristic of the configuration.

Some tests were halted after the reactor had operated in the carbon formation regime. Teardown of the reactor revealed a massive accretion of

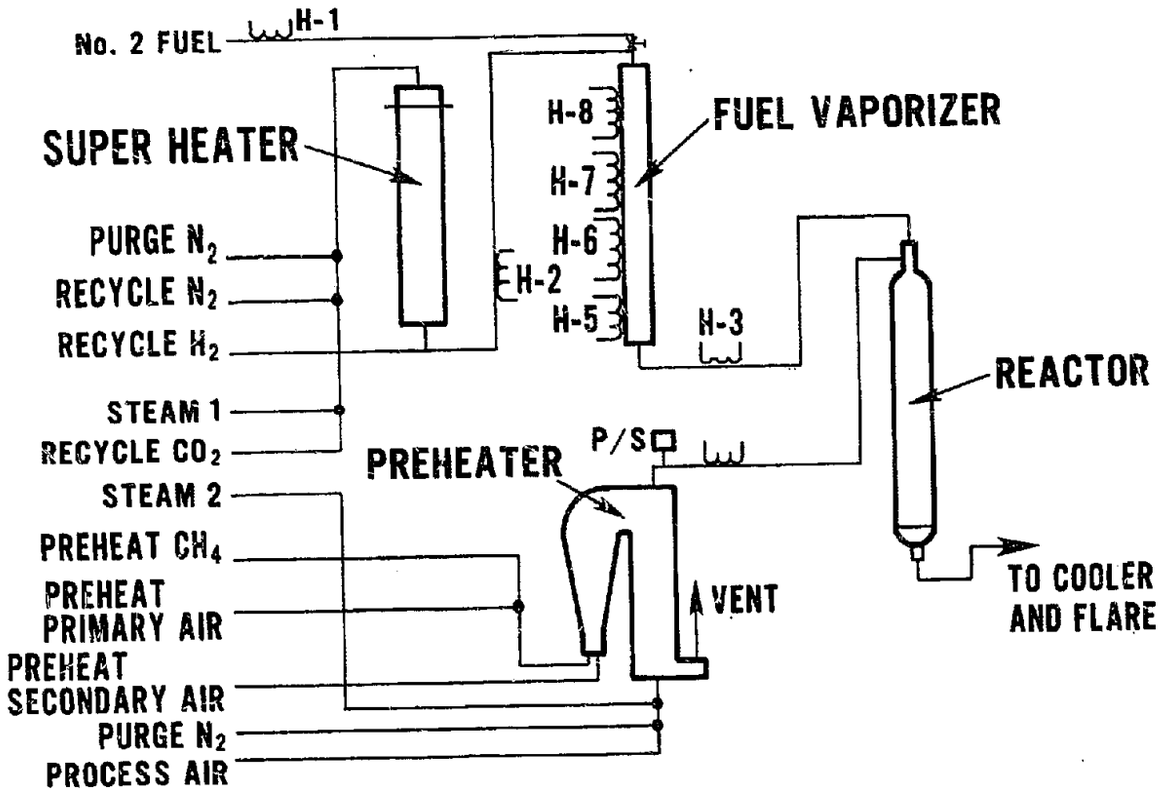

Fig. 6. 6-Inch Diameter Reactor Test Facility

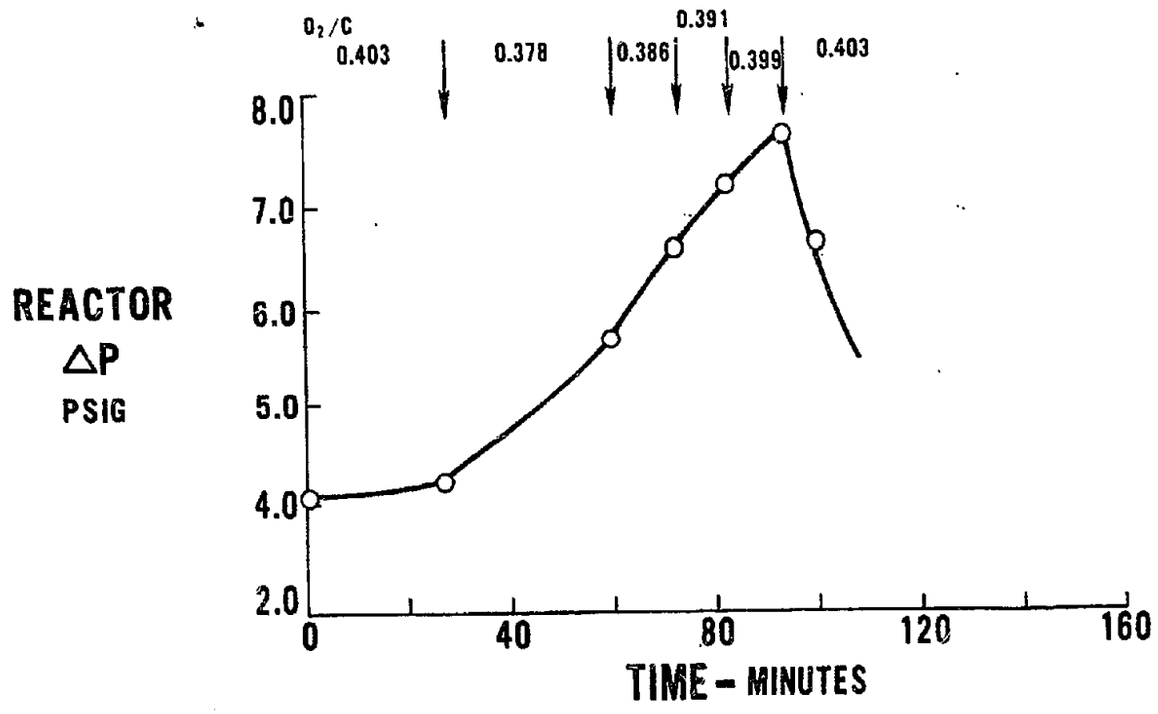

Fig. 7. Adiabatic Reformer Locating the Carbon Boundary

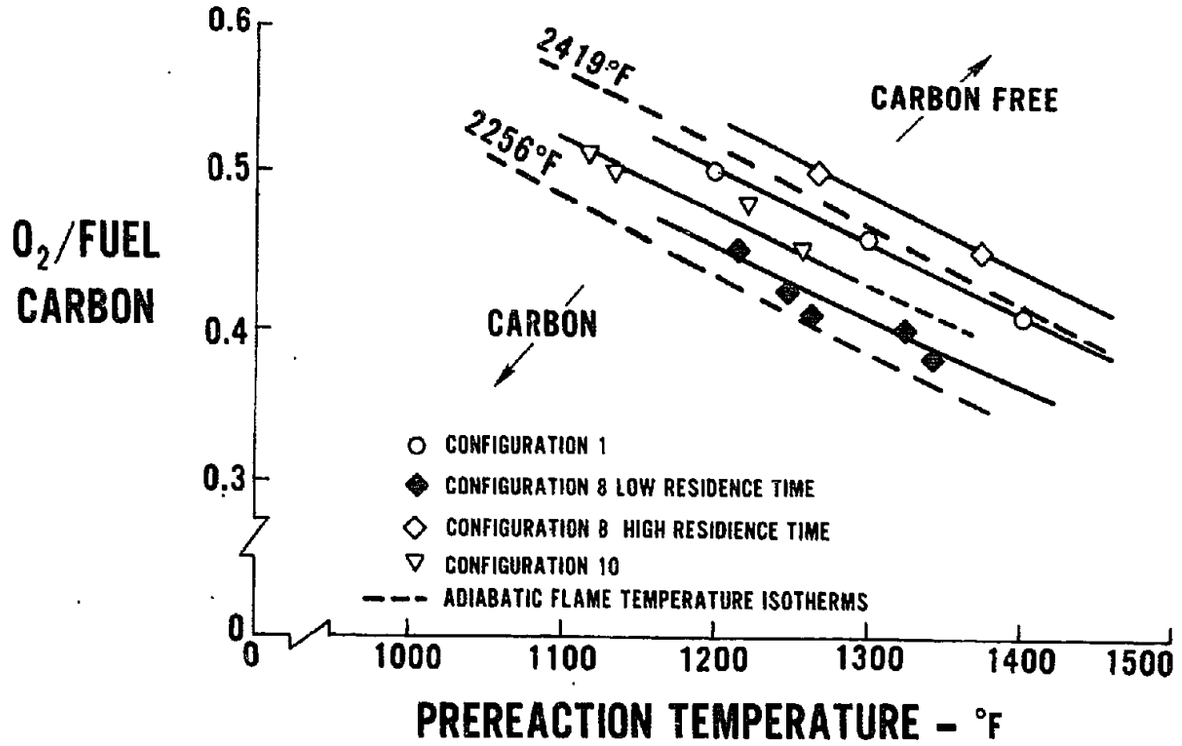

Fig. 8. Effect of Configuration and Residence Time on Carbon Boundary

carbon around and between catalyst pellets, close to the entrance to the catalyst bed (Figure 9). When pellets were split open the carbon was seen to be limited to the exterior. This evidence which suggested that the carbon had formed in the gas phase and deposited on the pellet was reinforced by scanning electron micrographs. The carbon plug contained spherical carbon particles with a wide range of diameters up to a micrometer in size, frequently forming strings and chains (Figure 10). Higher magnification revealed the presence of some carbon filaments with ordered cylindrical structures about 500 A° in diameter (Figure 11). These appeared similar in form to those frequently associated with growth from nickel crystallites. The overall carbon structure was similar to that described by Lahaye *et al* (2) to form during steam cracking of hydrocarbons. They suggested that the globular carbon mass grew by deposition of spherules formed in the gas phase and trapped on the surface by the underlying microfilaments.

Thermodynamic consdieration of the overall process stream composition did not predict the formation of carbon. Solution of equilibria for all of the

$$CH_4 + H_2O = CO_2 + 3H_2O \qquad (1)$$

$$H_2O + CO = CO_2 + H_2 \qquad (2)$$

$$CO + CO = 2C + CO_2 \qquad (3)$$

$$CH_4 = C + 2H_2 \qquad (4)$$

stable gaseous species present, equations 1-4, did not predict the existence of solid carbon at any point in the reactor at the temperatures measured. In addition, values for the experimentally determined reactant ratio for the Boudouard reaction, shown in Figure 12, lie far above the regime where carbon is predicted from thermodynamic equilibrium values. The formation of carbon in the reactor therefore appears to be kinetically controlled.

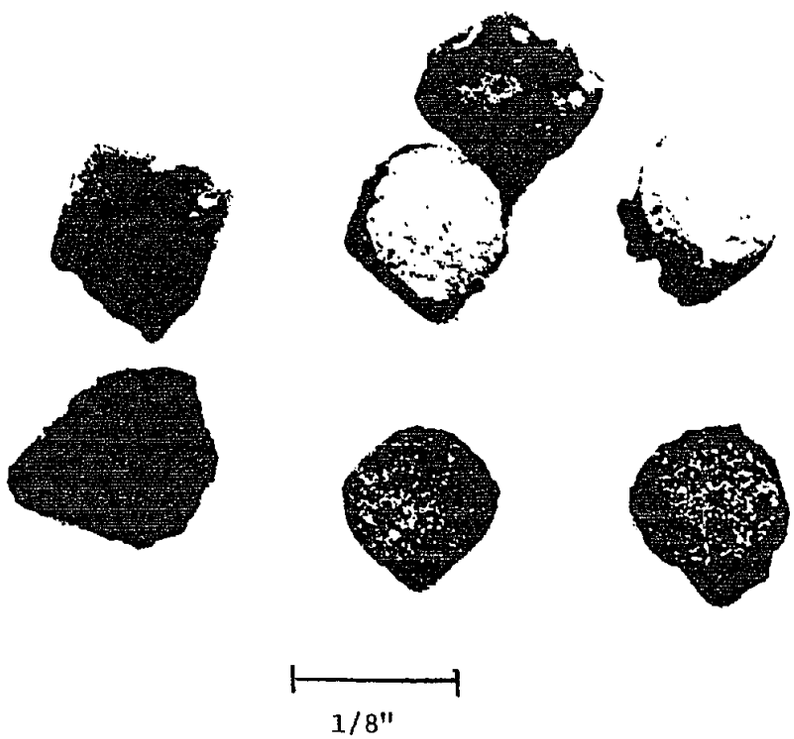

Fig. 9. Carbon Formation in Adiabatic Reactor

A mechanistic description of the processes occurring in the adiabatic reactor header section must predict the most notable feature of the experimentally defined carbon regime, *i.e.*, the constant value for the slope of the carbon boundary defined for each header configuration tested. This slope is close to that for the isotherm of the adiabatic flame temperature of the reactant gases. Decreasing heat of combustion with decreasing O_2/C ratio is compensated for by increased pre-reaction enthalpy to give the line indicated in Figure 8. The experimentally observed maximum temperatures were close to equal at each point on the carbon boundary, but the values measured were less than those calculated for the flame temperature due to some endothermic cracking and reforming in the combustion zone.

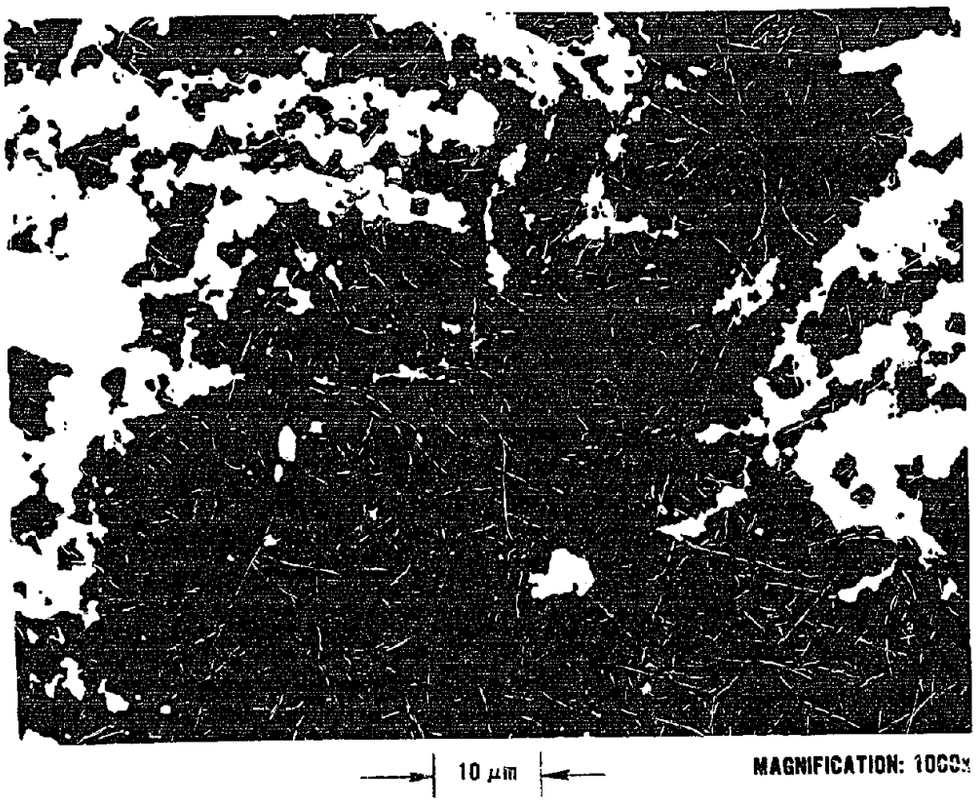

Fig. 10. Carbon From Adiabatic Reactor

Fig. 11. Carbon From Adiabatic Reactor

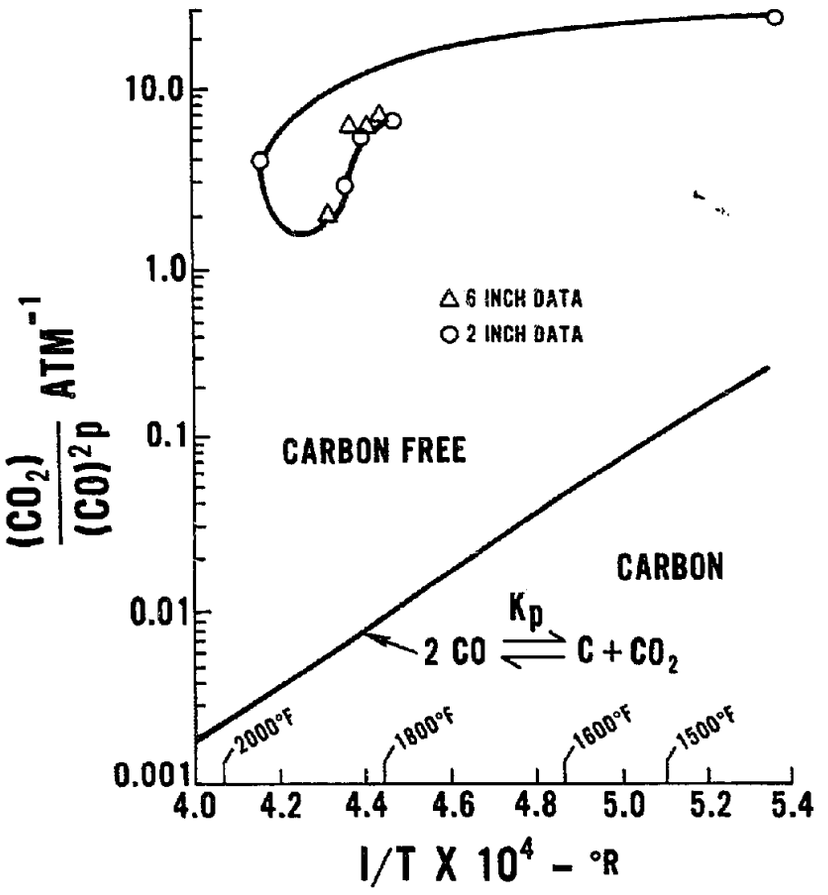

Fig. 12. Boudouard Reaction Ratios in 2-Inch and 6-Inch Reactors

The close correspondence between the experimentally observed slope of the carbon boundary and the adiabatic flame temperature isotherm suggests that the boundary defines a temperature at which the rates of carbon formation and removal are equal. With increase in reactor temperature beyond this point, by the addition of oxygen or increased reactant preheat, carbon removal exceeds formation and the reactor operates carbon free. This is represented as the intersection of the curves of rate versus temperature for the two processes in Figure 13.

If, at the position in the reactor where the carbon plug forms, the process stream is assumed to be in the pre-nucleation phase of soot formation, then the rate limiting step for carbon formation will be the addition to the carbon particle of free radical or unsaturated species resulting from cracking the fuel.

$$\text{Rate of carbon formation} = k_1 [P] [SA]_{carbon}$$

where [P] represents the steady state concentration of coke precusors and $[SA]_{carbon}$ the available surface area of carbon at the point $\frac{X}{L}$ in the reactor where the plug forms.

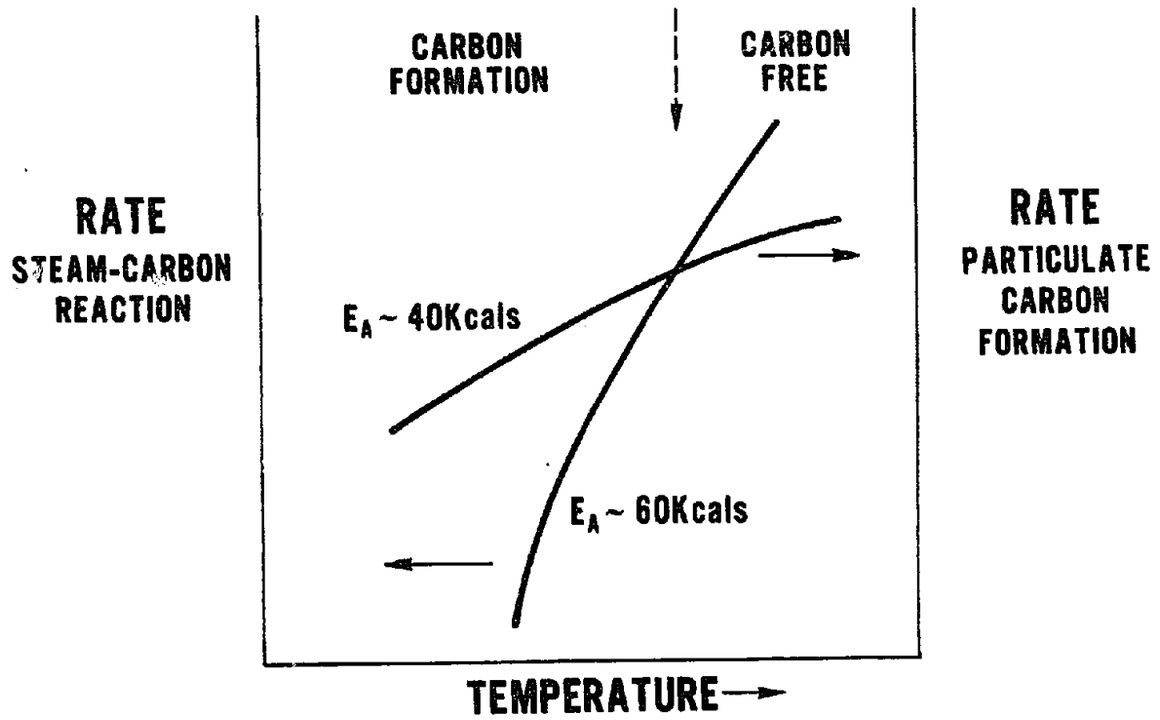

Fig. 13. Steady-State Rates of Carbon Formation and Burn-Off in the Adiabatic Reactor

Carbon removal may occur by reaction with the H_2O, CO_2 or O_2. Since H_2O is the major species present in the gas phase over the carbon plug, carbon removal is assumed to occur by the steam-carbon reaction.

$$\text{Rate of carbon removal} = k_2\ [H_2O]\ [SA]_{carbon}$$

At the carbon boundary the rates for the two processes are equal

$$k_1\ [P]\ [SA]_{carbon} = k_2\ [H_2O]\ [SA]_{carbon}$$

This equation can be solved to yield an expression for the temperature at the carbon boundary

$$T = A \ln B \frac{[P]}{[H_2O]}$$

where constant A contains the difference in activation energies for k_1 and k_2 and B is the ratio of the Arrhenius pre-exponential factors.

The concentration [P] of species contributing to carbon growth will be a function of critical fuel concentration and conversion in the cracking reactions. This will depend on the residence time and temperature profile

in the reactor. In steam cracking naphtha for ethylene production a first order rate constant is integrated through the reactor to give a kinetic severity function (KSF) to correlate conversion to cracking products.[3] By analogy [P] may be expressed as

$$[P] = [P]_{fuel}\ f\ (KSF)$$

and the temperature at the carbon boundary as

$$T = A \ln B\ \frac{[P]_{fuel}\ f\ (KSF)}{[H_2O]}$$

where $[P]_{fuel}$ is the initial concentration of fuel. Chambers and Potter[4] have correlated the accumulation of carbon stream cracked tube walls as a function of the KSF.

Since the KSF is a function of the temperature profile as well as time it is apparent that this treatment serves mainly to emphasize the complex dependency of the position of the carbon boundary on operating parameters. In particular the introduction of the severity function emphasizes the importance of processes occurring upstream of the position where carbon forms. Local inhomogeneities introduced by mixing will change the effective reactor severity function. Rapid and efficient mixing is required to minimize carbon formation.

The 2-inch subscale reactor has been used to investigate the effect of system variables on the carbon boundary. Included in Figure 8 are operating lines for three header configurations with different approaches to mixing the fuel oxidant streams. The variability in the value for the O_2/C intercept and hence for reactor efficiency illustrates the importance of mixing step. In addition for configuration 8 the residence time upstream of the catalyst was varied by changing the position of the catalyst bed. Reduction in residence time improved reactor performance.

Finally, the 6-inch diameter reactor (10 pph fuel) was operated to investigate effects of scale. A header configuration which had been tested in the 2-inch reactor was scaled to 6-inch size using the fluid dynamic mixing criteria developed in the smaller reactor. The close similarity in performance between the two reactors, shown in Figure 14, gave confidence in this approach.

The data for the 6-inch diameter reactor emphasize the well defined characteristic slope of the reactor carbon boundary. Present test efforts are focused on lowering the O_2/C intercept to improve reformer efficiency. A mechanistic understanding of the complex processes which determine the position and slope of the operating line would help greatly in reactor development.

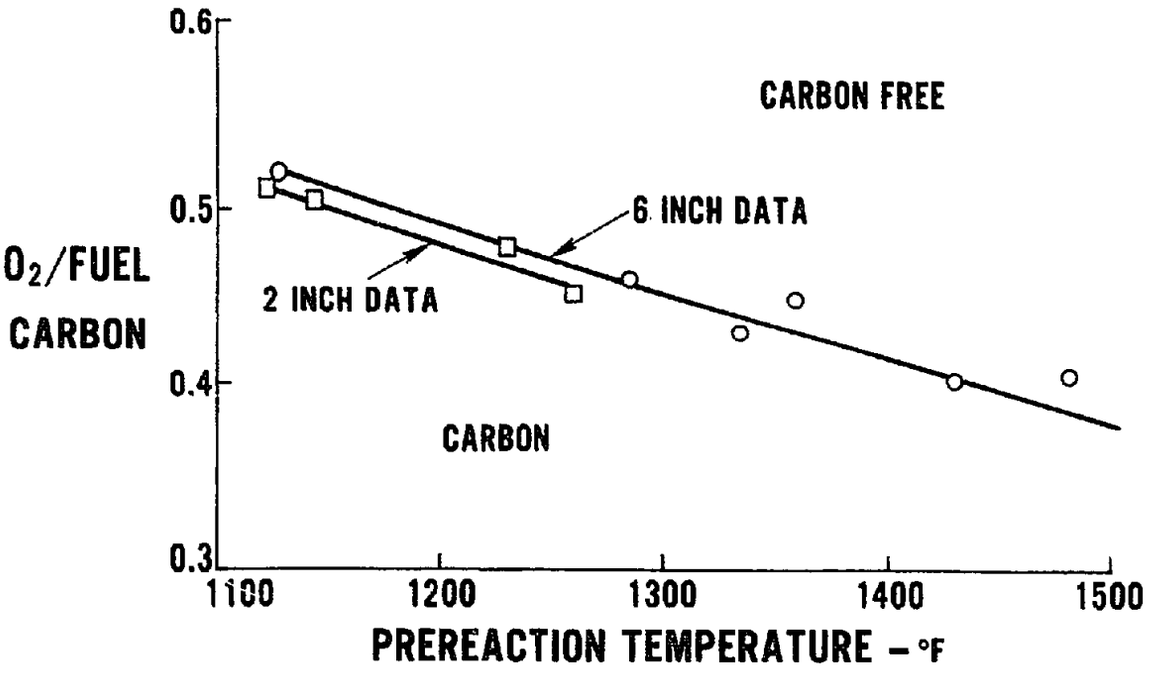

Fig. 14. Carbon Formation Boundary in 2-Inch and 6-Inch Reactors

REFERENCES

1. J. A. S. Bett, R. R. Lesieur, D. R. McVay and H. J. Setzer, *Adiabatic Reforming of Distillate Fuels*, National Fuel Cell Seminar, San Francisco, California, 1978.

2. J. Lahaye, P. Badie and J. Ducret, *Carbon*, 5, 87, 1977.

3. S. B. Zdonik, E. J. Green and L. P. Hallee, *Oil & Gas J*, p. 96, June 26, 1967.

4. L. E. Chambers and W. S. Potter, *Hydrocarbon Processing*, p. 121, January, 1974.

Comments and Replies on

ADIABATIC REFORMING OF DISTILLATE FUELS

Presented by J. A. S. Bett

K. Wray: Do the analyses of Fig. 4 correspond to a position just ahead of the catalyst bed or just into it?

J. Bett: In the case of Fig. 4, just ahead of the catalyst bed. Under other conditions the temperature maximum can appear several inches into the catalyst bed.

B. Gerhold: What was the steam-carbon mole ratio for these experiments?

J. Bett: The steam-carbon mole ratio in most experiments was 3.75.

I. Osgerby: What was the hydrogen concentration in Fig. 4?

J. Bett: At the exit of the reactor it was between 30 and 35 percent depending on temperature and space velocity. Both 2 and 10 inch reactors operated at relatively high space velocity and hydrogen product was not optimized.

G. Kamm: I should like to comment that photo micrographs of carbon found in ethylene cracker tubes are identical to the ones you have shown with agglomerated material and stringers. It also can be removed reversibly.

J. Bett: We used descriptions of behavior in ethylene tubes to interpret carbon formation in our reactors.

I. Osgerby: The steam carbon reaction which you propose as the carbon removal reaction occurs in the catalyst bed and not on the header, does it not?

J. Bett: We do not consider the header section to exclude some of the catalyst bed. A better division of the reactor might be between an upstream combustion zone and a downstream reforming zone. The steam carbon reaction proposed for carbon removal could be catalyzed since the carbon forms in the catalyst bed.

THERMAL GENERATION OF HYDROGEN BY RICH PARTIAL OXIDATION OF HYDROCARBON FUELS

David H. Lewis, Jr., Jet Propulsion Laboratory

ABSTRACT

The thermal generation of molecular soot-free hydrogen by rich partial oxidation has been studied experimentally. Four alkane fuels, n-heptane, n-octane, isooctane and n-nonane were burned on a flat flame burner. The hydrogen content of the product gases as a function of equivalence ratio as well as the sooting equivalence ratio was measured. For n-heptane, n-octane and n-nonane, hydrogen yields were typically 10 vol %, and showed only a weak dependence on equivalence ratio. In all cases, the observed hydrogen concentrations were less than the equilibrium hydrogen concentrations computed at the adiabatic flame temperature. Sooting equivalence ratios for the four fuels ranged from 1.94 to 2.17, clustering around 2.0. The utility of the flat flame burner compared to a turbulent burner as a prototype hydrogen generator is discussed. It is concluded that the turbulent burner shows more promise as a prototype hydrogen generator.

When hydrocarbon fuels are burned with air at equivalence ratios well beyond stoichiometric, equilibrium thermodynamics predicts the presence of substantial amounts of soot-free molecular hydrogen in the products of combustion. While novel, this method of hydrogen generation is not without application; one potential use is for precombustion staging in gas turbine combustion schemes designed for control of pollutant emissions, especially if broadened specification fuels are to be utilized. This application is attractive because, in principle, it effectively decouples the properties of the raw fuel from the combustion processes in the main combustion stage.

This work is a systematic experimental investigation of the rich burning properties of common hydrocarbon fuels. Of specific interest are the critical equivalence ratio, ϕ_c, which is the highest equivalence ratio for which the fuel/air mixture can be burned soot free, and the amount of hydrogen produced as a function of equivalence ratio. So far, the following paraffin hydrocarbons have been characterized: n-heptane, n-octane, n-nonane and isooctane with several alkylbenzenes scheduled for subsequent investigation.

A schematic of the experimental hardware is shown in Fig. 1. Metered flows of liquid fuel and air, which are thoroughly premixed and vaporized, are burned on a flat flame burner. The products of combustion, which contain hydrogen, pass up a glass chimney and exit to the atmosphere. The chimney prevents any secondary air entrainment and makes possible a precise determination of ϕ. The product gas composition is analyzed by an on-line gas chromatograph. In a typical data sequence, H_2 concentrations would be measured as a function of ϕ until sooting was observed. The highest value of ϕ, which burned soot free was recorded as ϕ_c, the critical equivalence ratio.

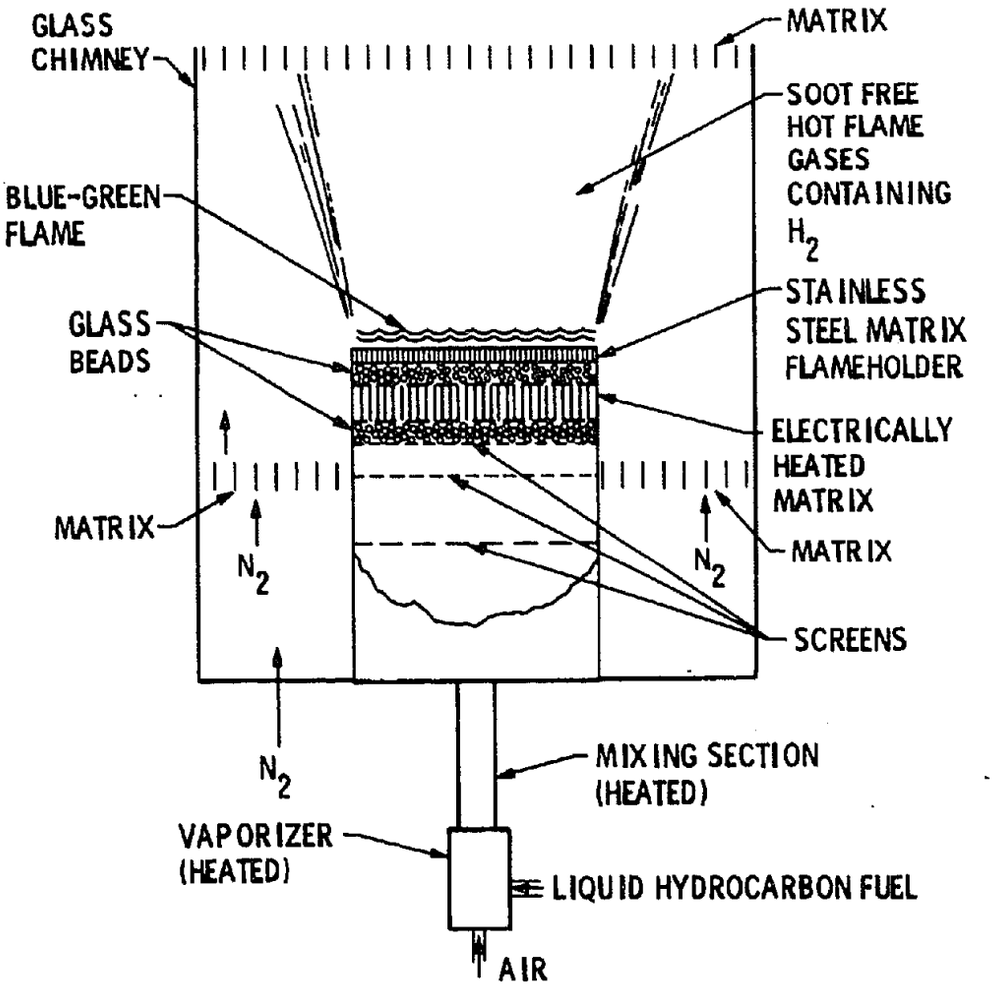

Fig. 1. Flat flame burner for rich, soot-free hydrocarbon flames.

Figures 2, 3 and 4 show data on hydrogen production as a function of equivalence ratio for n-heptane, n-octane, and n-nonane, respectively. Also shown on both figures are the equilibrium hydrogen concentration at the adiabatic flame temperature and the critical equivalence ratio ϕ_c.

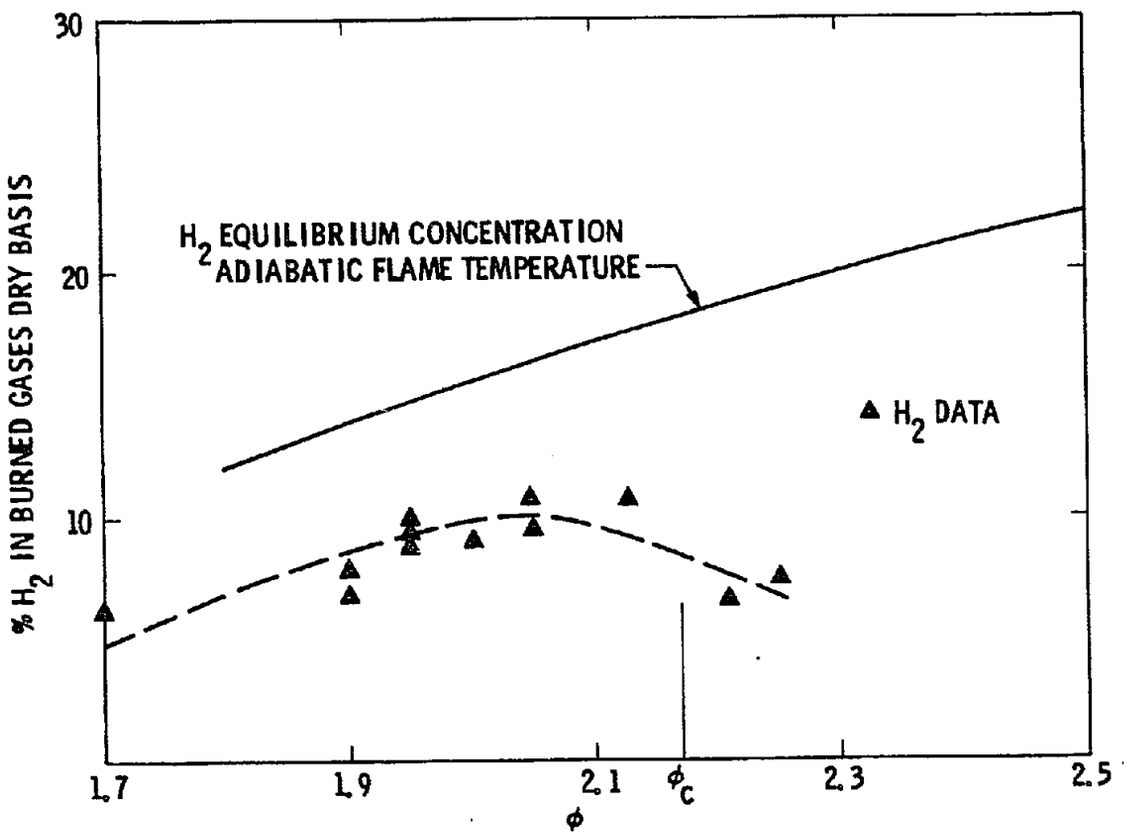

Fig. 2. Comparison of theoretical and observed hydrogen concentrations for n-heptane fuel.

Actual hydrogen yields were ∿10 vol % and showed only a weak dependence on ϕ. Computed equilibrium hydrogen concentrations were always greater than the measured values. For example, the predicted H_2 concentration for n-heptane is 16.9 vol % at ϕ = 2.1 compared to the observed 10%. The difference between the measured and predicted hydrogen concentrations is attributed to heat losses to the burner surface, which lowers flame temperature and subsequently lowers H_2 concentrations. The exact kinetics of fuel rich hydrogen production are unknown and have not been analyzed. Predicted equilibrium H_2 concentrations decrease as the fuel molecular weight increases; so, in one sense, the efficiency (defined as the observed H_2 concentration/equilibrium H_2 concentration) of this generation scheme appears to increase as the fuel molecular weight approaches the jet fuel range. It is emphasized that thorough premixing of the fuel/air mixture is essential to achieve these results.

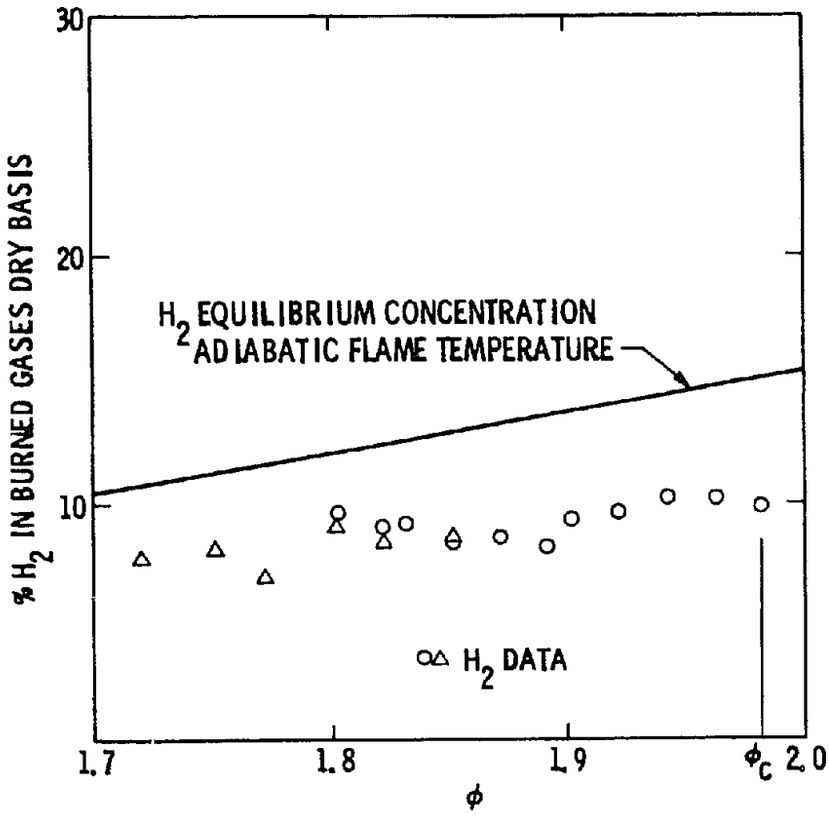

Fig. 3. Comparison of theoretical and observed hydrogen concentrations for n-octane fuel.

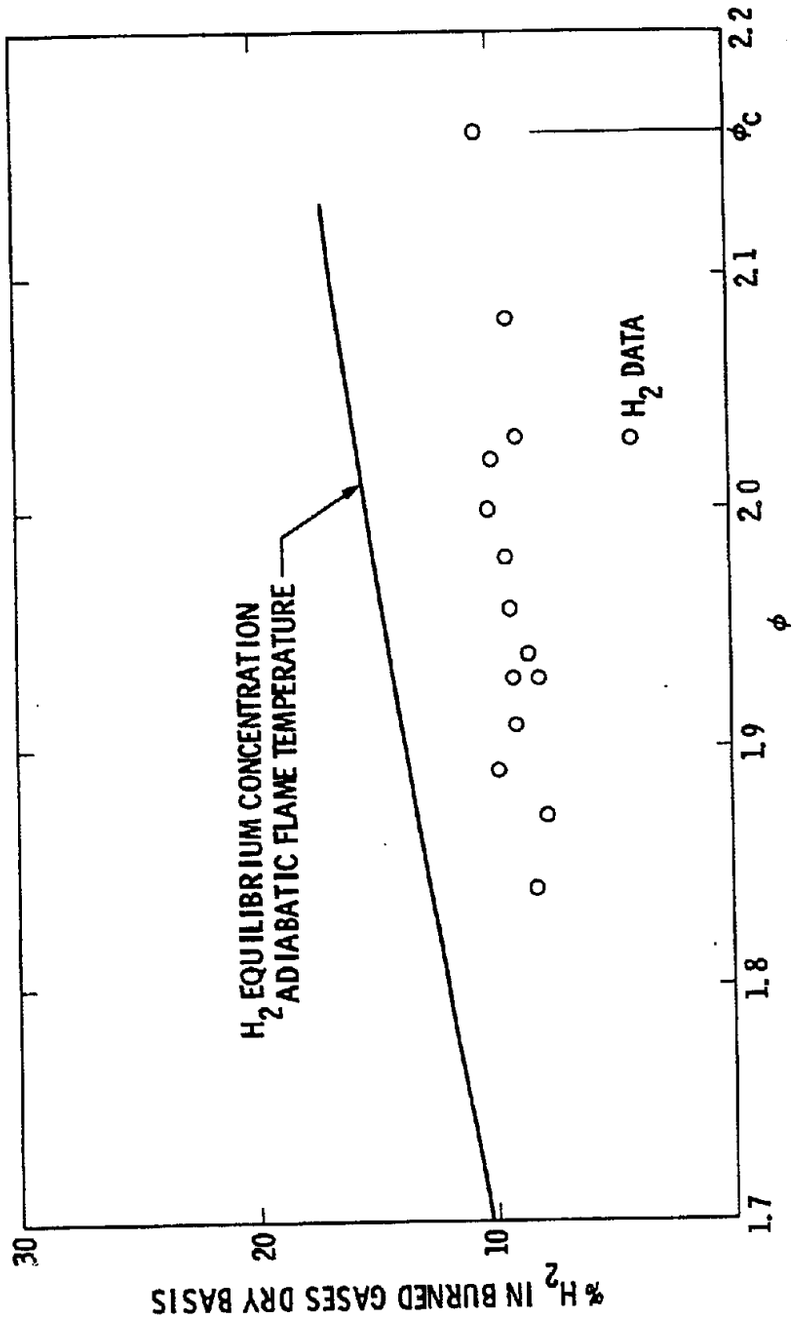

Fig. 4. Comparison of theoretical and observed hydrogen concentrations for n-nonane fuel.

A chart tabulating critical equivalence ratios for the paraffin fuels tested thus far is shown in Fig. 5. It is interesting to note there is only about a 10% change in ϕ_c for these fuels. This trend has not yet been verified for other fuel families (i.e., alkylbenzenes).

FUEL	FORMULA	ϕ_c
N-HEPTANE	C_7H_{16}	2.17
N-OCTANE	C_8H_{18}	1.98
ISO-OCTANE	C_8H_{18}	1.94
N-NONANE	C_9H_{20}	2.16

Fig. 5. Critical equivalence ratios for hydrocarbon fuels.

Although the flat flame burner is attractive for laminar flame studies, its utility as a prototype hydrogen generator is limited. This is due to the inherently low mass throughput associated with this type of burner. The only way to increase the mass throughput, while maintaining laminar flow, is to increase the burner size. Consequently, work is underway on a turbulent rich-burning hydrogen generator. This type of burner (shown schematically in Fig. 6) is capable of higher mass throughput, and may also yield higher values of ϕ_c and hydrogen concentrations. Presumably, the turbulence kinetic energy will suppress the thermal diffusion of the fuel and oxidant, which is observed at the onset of sooting, thus extending ϕ_c. Furthermore, if the flame is stabilized in free space (displaced from the flame holder) there is less heat loss to the burner, which presumably would produce higher hydrogen concentrations. The flat flame burner was useful in establishing the feasibility of the thermal hydrogen generation concept, but, in the near future at least, work will focus on the turbulent burning mode for thermal hydrogen generation.

REFERENCES

1. Ryason, R. R., *Combustion and Flame*, 29, 329-331, 1977.

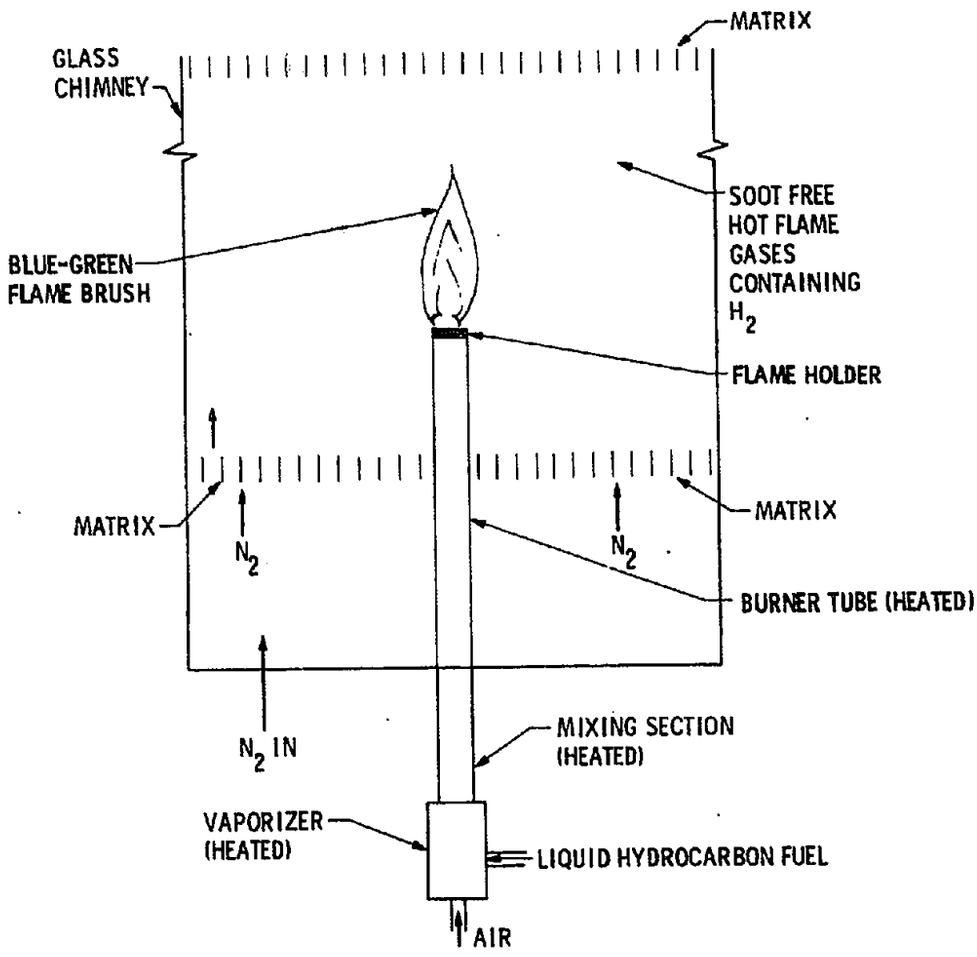

Fig. 6. Turbulent burner for rich, soot-free hydrocarbon flames.

Comments and Replies on

"Thermal Generation of Hydrogen by Rich Partial Oxidation of Hydrocarbon Fuels"

by D. H. Lewis

H. Palmer: Is your equivalence ratio defined in a standard way?

D. Lewis: The equivalence ratio is defined here as the actual fuel/oxygen ratio divided by the stiochiometric fuel/oxygen ratio.

H. Palmer: That, I think, is really a series of startling results, then, because I think the usual limits, if I made the calculations right, would give critical ratios defined that way around 1.4 to 1.6. You're probably accomplishing something very spectacular, and I'm wondering if you have made measurements on the light parafins -- propane or methane or something of that for, for comparison.

D. Lewis: No, I have not.

H. Palmer: When I convert this to the carbon-to-oxygen atomic ratio, it turns out to be quite different from those that have been recorded in some other studies.

WORKSHOP ON HYDROCARBON PROCESSING, MIXING AND SCALE-UP PROBLEMS
December 13-15, 1978
Washington, DC

Final Discussion*

Martin Zlotnick:

We want to tie together what has been going on the past three days and interpret what has been said in terms of what ought to be done next. I think we've gotten a number of answers, both in lunch time conversations and in John Bett's talk today. Let me try to summarize what I think those answers have been. If I haven't heard them right, I think it would be useful to have them restated and perhaps the answers could be amplified.

The first general answer I've heard is that it would be important to understand the basic chemical mechanisms--the reaction train--that leads to the formation of carbon in a generic way that is not dependent on the fluid mechanics. Just understand the chemistry, the reaction train and the kinetics and thermodynamics associated with it. That seems to be something that everyone is saying privately and in public. I think John Bett has offered some beginning of a train of thought for how that investigation might begin. The second conclusion has sort of evolved. We started from a situation where people were scratching their heads asking "what does the geometry look like?," and "how can you begin modeling without the geometry?", and "is fluid mechanics something that can be done in a relevant way without knowing exactly what's going on?", and "is modeling the flow a useful activity?" I think that the outcome of it (and this is not my own view, but my interpretation of the views of the other participants in the workshop), is that, yes, a certain amount of fluid mechanics modeling is worth doing of a generic sort. There is a reasonably constrained menu of injectors and mixers such that you can focus on, one or a couple classes of them, and then use them as a basis of a model for folding in the fundamental chemistry that is the other part of the picture. Now John Bett offered, by implication, a technical goal which is to try and match the slope of the oxygen/carbon ratio versus preheat temperature that seems characteristic of the measured phenomena. He did give us some insight, namely that this slope exists for a large variety of mixers.

John Houseman:

One point there, John, in particular, stressed that there's an interaction between what happens in the mixer and what might happen in the catalyst bed. I think so far we haven't stated that yet. You might

---

*Editors Note: All discussions were transcribed from a tape recording. In several instances the comments were not discernible. These are indicated by underlined blank spaces.

debate--for instance, if in the mixer you form some carbon and that carried over into the catalyst bed and that was the cause of carbon deposition within the bed. This issue we haven't discussed yet in talking about the mixer and the kinetics.

Raymond B. Edelman:

Are you considering recirculating flow in the mixer?

Martin Zlotnick:

No, he means carbon gets deposited in the bed, gets produced in the mixture and then gets eaten up in the bed. Homogeneously formed carbon. So the model will include the early part of the bed, perhaps, as well as the mixer. Is that what you're saying?

John Houseman:

Well, I'm saying we should consider--I don't know whether it's used or not.

I think we should mention. There's a second one I would like to add that is within the catalyst itself--within that space we could also have some carbon formation there, whether it be homogeneous or catalytic--they could be independent of what happens in the mixer. In other words, I'd like to stress what happens in the mixer to be treated separately from what happens in the catalyst bed. Maybe you can treat them the same way--I don't know. I guess that homogeneous carbon formation rate can be treated the same way. There could be a second different carbon formation rate on the catalyst surface. I'm not saying there is, but that there could be.

Martin Zlotnick:

That's something that could be looked into.

Gerald E. Voecks:

You can define that so that as long as the conditions used going into the catalyst are the same conditions that are being studied at the inlet conditions. There are the gas phase conditions, so that you get a point of reference.

John Houseman:

That's a complication, sorry to say.

Martin Zlotnick:

Well, I think one of the things to be considered is there's only a finite amount of time, funds, and brains, so it's a question of constraining the problem, and I don't know how anybody else feels about where the control surface for the problem should be going.

Bruce W. Gerhold:

What is the fuel type for the control surface? Western crude?

John A. Bett:

I think you would be talking about a fuel with very much aromatics--maybe if you could address the coal liquid problem. We're talking about what to do when you have a lot more aromatics.

Martin Zlotnick:

Yes, the fuel should be a parameter.

John Frankenfeld:

Absolutely.

Raymond B. Edelman:

Yes. I think you would want to start with a neat fuel such as an aliphatic type and then mix it with a pure aromatic like toluene. Such an approach will permit simulation of a wide variety of feedstocks.

Martin Zlotnick:

Yes, the model can't be very much good--it's limited to a single fuel I don't think. Well, I shouldn't say that, but its usefulness certainly would be limited.

Bruce W. Gerhold: But a fuel that you can prevaporize?

Gerard R. Kamm:

Don't you think eventually you're going to want to get into a heavier fuel than No. 1?

Martin Zlotnick:

Yes, but that might be a separate problem--you might go into a hydroprocessing pretreatment.

Raymond B. Edelman:

This leads to an important consideration in planning a program. I think we should consider vapor phase systems first then introduce the multiphase flow processes associated with direct liquid injection.

John Houseman:

That would simplify the problem to bypass the spray.

Ashok K. Varma:

I think the modeling can be much cleaner if you did not have to couple the spray and the mixing.

Martin Zlotnick:

I think it's certainly possible to have one set of problems where you start out with the vapor phase and deal with that and get results that would be useful. Gary, you had your hand up before.

Gary K. Patterson:

Yes. Well, what you just said was the first thing I was going to say--the rest of my comments are going to deal primarily with the prevaporized case, because the spray into the precombustion zone or wherever it happens to occur is a much more complicated case. But talking about the use of prevaporized fuel--one of the things that I feel has to be done if the modeling effort is going to be mounted to deal with the soot formation related to the hydrodynamic and chemical variables is to determine experimentally the levels of segregation that exist for the classes of mixers that are going to be used--say a couple of generic classes for those mixers which are going to be used for other experiments in the modeling. Cold flow experiments should be done to determine the effectiveness of mixing that exists from the basic standpoint and that is: what is the unmixedness or the segregation at various points in the mixing process?

Ashok K. Varma:

That could be part of the analysis. It would be useful to have data on that for validation of one phase of the model.

Gary K. Patterson:

It's necessary to have information on that for validation of any model.

Raymond B. Edelman:

It's important to keep in mind that cold flow may not be representative of the hot flow situation.

Gary K. Patterson:

You're talking about the next phase.

Raymond B. Edelman:

What I'm talking about is the necessity to keep cold flow experiments in perspective. If one were evaluating mixing techniques then cold flow simulation is a useful screening device. If it is the aerodynamic-chemical kinetic interaction one is interested in, then cold flow loses much of its relevance.

Gary K. Patterson:

The reason I brought that up is that I don't think we have enough confidence in our modeling ability yet for complex geometries which we might be involved in for getting the most out of mixing to just trust starting out with a modeling effort.

The next phase, then, is to try to devise experiments where we determine what these same mixing variables are in the hot flow case and it's much more difficult, but some effort should be made. Then also, the relationship of these segregational levels that exist in the hot flow case, whether we use the model extended to determine these or whether we successfully perform hot flow experiments to determine these, should be related experimentally to the levels of soot formation in order to validate the models that we formulate to make these calculations, particularly if unmixedness or efficiency of mixing, however you want to put it, is the primary variable which is going to be in the model that determines the selectivity to soot. To put it in chemical engineering terms, then, we're going to have to have a fair amount of good experimental data on at least one system to validate the model effort. And then, of course, the modeling effort is something that goes along with all of these.

Martin Zlotnick:

Gary, I didn't follow all the steps you talk about, but are there milestones in your view of where there would be results that would have engineering usefulness before you get to the very end?

Gary K. Patterson:

Yes. The first milestone is the first one which I'm interested in, and that's having defined segregation profiles for a couple classes of mixers

which are going to be useful. The second milestone would be to have this same kind of information in some kind of hot flow experiment whether that's with an actual flame or whatever, and a milestone which possibly should be 1A would be to have the hydrodynamic and scalar modeling to the point that it does a good job of representing the cold flow experiments. Then 2A would be the same thing for the hot flow experiments.

But that still doesn't predict how much soot is going to be formed. The third milestone would be to match up the combination of scalar and chemical modeling to the soot production process. Those are the five essential milestones which I identify off the cuff.

Adrian S. Wilk:

I just wanted to add one thing I think is important here, and I think everyone is saying it, but just to reiterate it, it's a communications problem and it's really since we're constrained to relatively simple geometries in our transport model, we just can't punch a button in the computer and get the right mixing configuration.

I think it's very easy to have conclusions buried in a forest of partial differential equations. So that it's important that there's a qualitative side and the people that can address the qualitative side from the analysis are the modelers, because they understand the implications of the mathematics that are going on. So, I think it's important that a lot of communication and clarification is addressed in any kind of modeling effort that deals with the simple geometry which is applicable to the real world development of a piece of hardware.

Martin Zlotnick:

I have the impression that there's at least one large school of thought in this group that says that almost the opposite of what you said, Gary--that it's not a practical approach to understand the details of the flow or the mechanisms of breakup of the species mixing to produce useful engineering results. I think that there are a substantial number of people who believe that.

Is there any way I can get a reading on that?

Raymond B. Edelman:

I think we should start by exploiting the state-of-the-art. This will help to establish the extent of the fundamental needs. After all, we have not as yet attempted analysis of this problem with state-of-the-art knowledge. It is easy to get fundamental. Is this what you have in mind?

Martin Zlotnick:

No. Well, I don't know. What should our objectives be?

Raymond B. Edelman:

That's what I'm getting at. If we take a situation where we want to look at kinetic effects then we want to look at the simplest possibly system that minimizes or eliminates the fluid dynamic effects. There are various configurations which are both of laboratory scale and computer model scale that exist now to do that. Then look at the fluid mechanics and there are turbulent mixing models that do characterize a lot of the effects of unmixedness and fine-scale mixing that can be used now to at least get the effect of the turbulence. We do want to take configurations that are relatively simple. If we get into complex configurations that may not be characteristic of fuel preparation mixing schemes, then we're not going to get any results in the near term. You don't have to look for the predictions to fall on top of the data. What you would want is all the trends to be predicted in the right direction. By the way, I believe that experiments are a necessary part of whatever is done on this problem.

Gary K. Patterson: What kind of experiments?

Raymond B. Edelman:

You already suggested cold flow and hot flow, and those are two categories of experiments. I have already expressed my reservation on cold flow experiments.

Gary K. Patterson:

Well, I said a couple of things to measure, too. So what would you measure?

Raymond B. Edelman:

Well, I think it's important to measure the concentrations, and if we select a simple diffusion-type flame (coaxial diffusion-type flame), you would want to measure property profiles, characterize the rate of mixing, but in particular, characterize the development of immediate species as mixing proceeds.

Ian T. Osgerby:

Which must be soot, to be relevant!

Raymond B. Edelman:

Which must include soot. Then one can control things like initial temperature levels, initial injection velocities, and geometry to a certain extent. Scale effects, for example, can be examined within the confines of a practical geometry.

Martin Zlotnick:

So you're saying, basically, that the detailed mechanisms of the mixing

is not the primary concern, but the effect of the mixing, whatever the mechanism is.

Raymond B. Edelman:

No. What I'm saying is that there are methods that exist now that do take into account some of the effects that have been discussed. We are far from being satisfied that all details are in hand with regard to the turbulence-chemistry interaction problem. But there are models that account for that effect, and in that sense, you can use those models to get some insight into the problem.

Ian T. Osgerby:

In terms of putting a perspective on this, I think it's profitable to sort of put the hardware picture together and march through the various parts of it and look at the problems that seem to exist in those particular parts, and take in the real environment as a frame of reference. So, at the front, you have to prepare a mixture of very hot air, very hot steam, and fuel. From what we're seeing, one would like to be in a range where you're not producing incipient soot actually in the fuel before you go in--why, I don't really understand where that temperature is, although some of the temperatures we've talked about are certainly in a range where that's important. Then one goes into the reactor--you may or may not have a high level of hydrogen recycled in this very hot steam, very hot air, and hot fuel. You want to mix this very rapidly. You don't want to produce soot, and yet you want to go into your reactor--the steam reforming part of the reactor--with a rather sudden temperature rise to the order of 1800°F, and this can happen out on the gas phase whether you like it or not. With some modeling, you perhaps could design around that, and maybe you'd want the first part of your catalyst bed to be a partial oxidation unit which is simply geared towards producing this temperature without soot. There are such games we play. Different kinds of .....do that. It seems to be one of the most critical things that I've heard, particularly from what John Bett was saying. Here we have producing soot, and it seems to be at the front end of the bed where plugging is a real problem on this ..... Where is this soot formed? Is it formed in the fuel? Is it formed in the mixing? Or is it formed in the bed? It seems to me that you're operating at such a level that it's produced ahead of the bed, so that the modeling work that would be of interest, as I see it, should be--what is the mechanism for soot production ahead of the bed? And then the mixing shouldn't be addressing or producing a mixing model at all, but what are the conditions that produce the soot ahead of the bed, and what do you do to get away from that? And then you have on the side from that some rather fundamental studies of the soot formation that don't have any fluid dynamics whatsoever, so that you can feed this in.

John A. Bett:

The modelers have discussed the eddy approach to modeling combustion and Professor Palmer mentioned a critical soot initiation period. Is there any feeling for the length of the critical soot initiation period relative to eddy lifetime?

X. B. Reed:

I think that's exactly the point that Gary was making. It's certainly true that one can write equations, chemical engineers can write equations with very bad models and show that certain concentrations went down, other concentrations went up with time or space or something, and trends were right. But you're not interested in a general trend that maybe there's a little bit less soot formed. You need to know whether it's formed and the only way you can understand that is if you sit and do the experiments and some mixing models, not simply plow ahead with a set of equations which are available. I suspect that the concentration equations are not yet at the stage where the momentum equations were.

Ian T. Osgerby:

If you want to pick a very complicated system geometry, that's true. But if you want to pick a system that's been well characterized and then look at the problems (the additional problems over...) the problem with the mixing model, the framework's already existing, as Ray says.

Martin Zlotnick:

I think the point is that you can identify parameters that define whether you are moving toward or away from soot. At that point in the modeling, perhaps you can make predictions beyond the range in which you made the experiments without actually knowing the details of the physics that's going on. That kind of approach is common in engineering.

Gary K. Patterson:

Well, I was just going to say that it is common in the chemical industry to do all kinds of things without knowledge of what's actually happening inside the vessel, and somehow engineers muddle through and get something that's of use for something. But generally, the excuse is given that, well, we couldn't do that because we don't understand how turbulence really works, and if it's a mixing problem we don't really understand how mixing works and, so, we have to go into it by using more general variables; looking at trends, and so on. But when we have a chance to look at the primary variable (and it isn't really too hard an experiment to do with some techniques recently developed), it seems to me to be extremely valuable to do that. But, it seems to me that using the approach of looking at the variable you think is the culprit is better than looking at all the other things and trying to bridge the gap just by thinking about it, and through the use of models which may or may not be exactly right, doesn't seem to be the right way to approach the problem. The other point that Rex is making is one that we should emphasize. That is that in this soot production problem, it isn't just trends that we are looking at. We are looking at a case where we need to know where the critical point is in beginning to form the soot, both chemically (which we heard a lot about this morning), and from the standpoint of "how bad can the mixing be before we're in trouble?" That's the thing that the present state of the modeling techniques can't give us an answer on,

because they are only good enough to give us trends and we don't know the absolute values. That's what we need experiments for.

Raymond B. Edelman:

I didn't quite say what you're implying.

Gary K. Patterson:

Well, maybe I misunderstood you.

Raymond B. Edelman:

Let me put it in a different way: we haven't determined that what we are able to do now is not, in fact, sufficient for the purposes of predicting the kind of information that we need now. Also, when I talk about trends, I'm talking about predicting and validating against controlled experiments.

John W. Frankenfeld:

Approaching this from an absolutely unbiased, naive idea of thinking about turbulency or mixing, from the chemistry standpoint, from what I've heard today and observed myself, I have a very strong feeling that this soot may well be formed before the bed, and it is going to be a strong function of the reacting unsaturated species and how long they are allowed to react before they get to the catalyst. First of all, that needs to be studied to find out what the characteristics of the soot is and how it's influenced by the composition of the fuel. Once you find that out, I think you can start choosing fuels.

Martin Zlotnick:

You mean the nuclei might be in the fuel?

John W. Frankenfeld:

That's one thing--that some fuels are going to form or are going to crack very readily and give you highly reactive (maybe even an acetylenic) species which we all know are going to produce carbon like crazy. And then the approach that Professor Palmer suggested, I think, is a great idea. You can add some hydrogen donors and they can be organic compounds that will burn. Tetralin is a good example. I think the point is try to avoid

production of these highly reactive, unsaturated species and, if you do produce them, don't let them lay around too long. I think that's an area of fruitful research. Not, by any means, superceding what all the other people have said, but in addition.

Ian T. Osgerby:

Isn't one of the most critical things that John Bett was saying is the system seems to be dominated by the air-carbon region of the soot, whereas the oxygen-carbon system says you are a long ways away from soot formation. Where can what happen? To me, that can happen out in the mixer. Not in the catalyst or homogeneously inside the catalyst. And that's quite difficult with a pebble bed where you set this huge surface-to-volume ratio. It seems to me that the only place that you have that could have the oxygen-carbon from air as the dominating factor is out in the gas phase ahead of the bed, because steam just doesn't react too well with fuel without a catalyst.

Ashok K. Varma:

I think that it's agreed upon, and in a way, what we started with--what we proposed to do. You have to couple the mixing analysis with the detailed knowledge of the soot formation analysis, what you started suggesting as the direct plan of attack. But there is a coupling between the mixing and the soot reactions to get the soot. It's not just a fuel decomposing by itself, and this is very intimately related to the mixing, and what I think what Ray is saying is that we have available now enough turbulence mixing models to do a relatively good job on coaxial mixing type problems. The soot chemistry has to be put into those kinds of models, and some interaction built in to reflect the turbulence interactions, and then you should be able to see how good those models do in predicting the soot limits.

Martin Zlotnick:

I think that what Frankenfeld said was that there is some study to be done, even before you start mixing, in characterizing the fuel that is being mixed.

Ashok K. Varma:

That is part of the chemistry mechanism that you would provide to the fluid mechanics modelers. That depends on the fuel.

Ian T. Osgerby:

One thing you can't do is select your fuel. The point is, it has to be oriented to the fuels that this is an application for, which is No. 2.

Ashok K. Varma:

If you know the chemistry for that, fine. You can work with the chemistry for any fuel that you want to use as long as you are given the kinetics information. If you don't know the chemistry....

Ian T. Osgerby:

I agree to separate the components. It must be addressed at the actual fuels being used.

Simon L. Goren:

When and how will this chemistry be obtained with the absence of carrying out a reaction in which the organic is mixed with the oxygen?

Raymond B. Edelman:

With premixing, you control the initial reactant composition. But we need to validate the chemistry for a wide range of conditions that would cover all possible local conditions within a turbulent mixing flow. No matter how the thing is structured out of this, the chemistry and the fuel effects are going to have to be identified and characterized.

Martin Zlotnick:

I think that what you are saying is that the actual real world path that the reactants go through has to be dealt with.

Raymond B. Edelman:

Yes. If you don't have the chemistry right, then any formalism, whether simple, complex, on turbulence and turbulence modeling becomes irrelevant.

Martin Zlotnick:

The way I pictured it, your focus is on the chemistry, which you are doing the best you can to determine what the concentrations are in the function of time and space.

John A. Bett:

What is the heat transfer mechanism and temperature of the eddy?

Raymond B. Edelman:

That's where the fluid mechanics come in. The transport of mass momentum and energy is dependent on the turbulent mixing process. But at any point in the flow, no matter how microscopic you get, like you are within an eddy. There is a local state which got there and better be consistent with what the instantaneous--if you are able to really follow in time rather than time average, what's fluctuating...you'd better be satisfying a local rate of production that is based on a local state. The local state is defined by the coupling of these transport processes to the chemical kinetics. If the chemistry is properly characterized, then the actual temperature-time history can be detailed with proper transport properties.

Ashok K. Varma:

There is going to be a local temperature, and temperature fluctuations in the eddy.

Ian T. Osgerby:

I don't think it's fruitful to design systems..... what we would like to learn is what is the mechanisms for soot and how to stop it and reoxidize or whatever, in the general framework.

John Houseman:

I'd like to separate the problem into two distinct problems. The first problem is where we have both mixing problems and, say, soot formation problems. You are going to have a soot formation rate. Our overall objective is we'd really like to run at the theoretical soot line, and not some distance away from it. We'd like to be able to minimize our oxygen input. We can do it. Somehow the soot formation stops suddenly.

Ian T. Osgerby:

But the total oxygen-to-carbon rather the air oxygen-to-carbon.

John Houseman:

We like to do all steam reforming and no particle oxidation. In practice, we find we have to put in air to stop the soot formation. So in this case where mixing affects the soot formation. Now, I can take the second case and say, "Let's assume we have perfect mixing." We still have a soot formation problem. Maybe that's the easiest one to deal with in terms of modeling. Let's assume a perfectly mixed system, and then throw the kinetics in there and just have a plug flow reactor. Let's not deal with the mixing problem. Let's do one thing at a time. Let's first attack the kinetics problem and see if we can see any way around this kinetics problem.

Of course, even if we solved the mixing problem, we will always be left with a kinetics problem. That, I think, should be the first priority, is to take a closer look at the chemical kinetics of the soot formation to see if there is anything inherent that will give us a clue as to how we can reduce the oxygen-to-carbon ratio; how we can avoid that soot formation.

Ashok K. Varma:

Along with that, I think very importantly, if we're ever going to use that information, is to also identify what is most important, and simplify them. Reaction schemes--you can keep building them until you have hundreds of reactions. But, if you are ever going to couple it with the fluid mechanics problem, somebody has to also simplify them by determining the importance of various reaction steps, so that maybe you have half a dozen reactions which are the main ones that you want to study with fluid mechanics.

Martin Zlotnick:

I'd like to have maybe two or three more speakers. I think that we ought to...

Colin R. Ferguson:

I was going to suggest, I think that if we were to do that, it might be one of these coalescence-dispersion models. In my opinion, that is the only way you are going to get a real turbulence chemistry interation model in any way. If you were to discover that the answer was sort of a weak function of whatever mixing parameter you had to put into the coalescence-dispersion model, you don't have to worry about the turbulence anymore. But, if you find it's a strong answer, then you have to figure out--use the turbulence modeling with simplified chemistry to give you that parameter that you need to introduce in the coalescence-dispersion model.

Gary K. Patterson:

This will be short. I would still like to challenge the idea that the scalar modeling with chemical reaction is adequate as it stands now, because my impression is that in doing this with analytical prototype techniques or PDD's or whatever, is really in its infancy. There is just a tremendous amount of work that has to be done before we can handle any kind of complex reaction very dependably. I'd like to echo what he says and that is the only dependable thing that I've seen so far on complex reactions are using the coalescence-dispersion method.

L. Marianowski, Inst. of Gas Technology, Chicago
A. P. Meyer, United Technologies Corp., South Windsor, Conn.
L. Nanis, Stanford Research Inst.
M. S. Ojalvo, National Science Foundation, Washington
I. T. Osgerby, Engelhard Industries, Edison, N. J.
H. B. Palmer, Pennsylvania State U.
G. K. Patterson, U. Missouri-Rolla
J. R. Peterson, General Electric Co., Schenectady
P. R. Ponzi, Exxon Research and Engineering Co., Florham Park, N. J.
X. B. Reed, Jr., U. Missouri-Rolla
A. W. Schnacke, General Electric Co., Schenectady
P. M. Sforza, Polytechnic Inst., Farmingdale
S. N. Simons, NASA Lewis Research Center
D. R. Stone, National Aeronautics and Space Administration
H. Tong, Acurex Corp., Mountain View, Calif.
K. K. Ushiba, Catalytica Associates, Inc., Santa Clara
A. K. Varma, Aeronautical Research Associates of Princeton, Inc.
G. E. Voecks, Jet Propulsion Lab.
G. Voelker, Office of Coal Utilization Systems, USDOE
C. W. von Rosenberg, Jr., AVCO Everett Research Labs, Inc., Everett, Mass.
R. D. Weaver, Stanford Research Inst.
A. S. Wilk, ESCOE, Washington, D.C.
K. Wray, Physical Sciences, Inc., Woburn, Mass.
M. Zlotnick, Office of Fossil Energy, USDOE

☆U.S. GOVERNMENT PRINTING OFFICE: 1980—681-118/24

Distribution for ANL-80-56

Internal:

W. E. Massey
J. P. Ackerman
L. Burris
F. A. Cafasso
A. V. Fraioli
J. D. Gabor
J. Harmon
J. E. Herceg
A. A. Jonke
A. Melton
P. A. Nelson
R. D. Pierce
J. J. Roberts
A. D. Tevebaugh
D. S. Webster
J. E. Young (50)
A. B. Krisciunas
ANL Contract File
ANL Libraries (3)
TIS Files (6)

External:

DOE-TIC, for distribution per UC-93 (160)
Manager, Chicago Operations and Regional Office, DOE
Chief, Office of Patent Counsel, DOE-CORO
V. H. Hummel, DOE-CORO
Argonne Universities Association:
President
C. B. Alcock, U. Toronto
T. Cole, Jet Propulsion Lab.
G. M. Rosenblatt, Pennsylvania State U.
W. L. Worrell, U. Pennsylvania
T. R. Beck, Electrochemical Technology Corp., Seattle
J. A. Bett, United Technologies, South Windsor, Conn.
T. R. Blake, Systems, Science and Software, La Jolla
E. Camara, Inst. Gas Technology, Chicago
D. Chatterji, General Electric Co., Schenectady
R. B. Edelman, Science Applications, Inc., Woodland Hills, Calif.
G. M. Faeth, Pennsylvania State U.
C. R. Ferguson, Purdue U.
L. M. Ferris, Oak Ridge National Lab.
A. P. Fickett, Electric Power Research Inst.
M. L. Finson, Physical Sciences, Inc., Woburn, Mass.
V. Fiore, Gas Research Inst., Chicago
J. W. Frankenfeld, Exxon Research and Engineering Co., Linden, N. J.
B. W. Gerhold, General Electric Co., Schenectady
E. Gillis, Electric Power Research Inst.
J. Giner, Giner, Inc., Waltham, Mass.
S. L. Goren, U. California, Berkeley
J. W. Harrison, General Electric Co., Wilmington, Mass.
L. C. Headley, Morgantown Energy Technology Center
J. Houseman, Jet Propulsion Laboratory
J. Huff, U. S. Army Mobility Equipment R&D Center
H. S. Hwang, Engelhard Industries, Newark, N. J.
G. R. Kamm, Union Carbide Corp., South Charleston, W. Va.
J. Kelly, Westinghouse R&D Center, Pittsburgh
J. M. King, United Technologies, Inc., South Windsor, Conn.
C. R. Krishna, Brookhaven National Lab.
D. H. Lewis, Jr., Jet Propulsion Lab.
M. N. Mansour, Office of Fossil Energy, USDOE